NuScale Power™

LO-0217-53029

2/15/2017

Docket: PROJ0769

U.S. Nuclear Regulatory Commission
ATTN: Document Control Desk
One White Flint North
11555 Rockville Pike
Rockville, MD 20852-2738

SUBJECT: NuScale Power, LLC Proprietary Marking Changes to "Subchannel Analysis Methodology" topical report, Revision 1 (NRC Project No. 0769)

REFERENCE: Letter from NuScale Power, LLC to U.S. Nuclear Regulatory Commission, "Subchannel Analysis Methodology," TR-0915-17564, Revision 0, dated October 31, 2016 (ML16305A445)

NuScale Power, LLC (NuScale) is submitting Revision 1 of the "Subchannel Analysis Methodology" topical report to include some changes to the proprietary and export controlled information (ECI) markings. These markings are being changed to reflect information released to the public in our recently submitted Design Certification Application and to correct some inconsistencies within the previously submitted Revision 0 (reference) of the topical report. There are no changes to the technical content of this topical report and the marking changes in all cases remove proprietary and ECI designations.

Enclosure 1 contains the proprietary version of the report entitled "Subchannel Analysis Methodology." NuScale requests that this enclosure be withheld from public disclosure pursuant to 10 CFR § 2.390. The enclosed affidavit (Enclosure 3) supports this request. Enclosure 1 has also been determined to contain Export Controlled Information. This information must be protected from disclosure per the requirements of 10 CFR § 810. Enclosure 2 contains the nonproprietary version of the report entitled "Subchannel Analysis Methodology."

This letter makes no regulatory commitments and no revisions to any existing regulatory commitments.

Please feel free to contact Jennie Wike at 541-360-0539 or at jwike@nuscalepower.com if you have any questions.

Sincerely,

Thomas A. Bergman
Vice President, Regulatory Affairs
NuScale Power, LLC

Distribution: Frank Akstulewicz, NRC, TWFN-6C20
Greg Cranston, NRC, TWFN-6E55
Rani Franovich, NRC, TWFN-6E55
Bruce Bavol, NRC, TWFN-6C20
Samuel Lee, NRC, TWFN-6C20

Enclosure 1: “Subchannel Analysis Methodology,” TR-0915-17564-P, Revision 1, proprietary version
Enclosure 2: “Subchannel Analysis Methodology,” TR-0915-17564-NP, Revision 1, nonproprietary version
Enclosure 3: Affidavit of Thomas A. Bergman, AF-0217-53030

Enclosure 1:

"Subchannel Analysis Methodology," TR-0915-17564-P, Revision 1, proprietary version

NuScale Power, LLC
1100 NE Circle Blvd., Suite 200 Corvallis, Oregon 97330 Office 541.360-0500 Fax 541.207.3928
www.nuscalepower.com

Enclosure 2:

"Subchannel Analysis Methodology," TR-0915-17564-NP, Revision 1, nonproprietary version

NuScale Power, LLC
1100 NE Circle Blvd., Suite 200 Corvallis, Oregon 97330 Office 541.360-0500 Fax 541.207.3928
www.nuscalepower.com

Subchannel Analysis Methodology

February 2017

Revision 1

Docket: PROJ0769

NuScale Power, LLC

1100 NE Circle Blvd., Suite 200

Corvallis, Oregon 97330

www.nuscalepower.com

COPYRIGHT NOTICE

Department of Energy Acknowledgement and Disclaimer

This material is based upon work supported by the Department of Energy under Award Number DE-NE0000633.

CONTENTS

TABLES

FIGURES

Abstract

This report documents the NuScale subchannel analysis methodology using the VIPRE-01 computer code. This methodology is used to calculate margin to fuel thermal limits, such as critical heat flux ratio and fuel centerline temperature.

This report discusses how NuScale meets the NRC requirements for use of VIPRE-01, the modeling methodology for performing steady-state and transient subchannel analyses, and the qualification of the code for application to the NuScale design. NuScale intends to use this methodology for thermal-hydraulic analysis in support of the NuScale Design Certification Application and for future design work.

NuScale requests NRC approval to utilize this methodology, with the noted limitations described herein, for the NuScale thermal-hydraulic design and supporting analysis.

Executive Summary

NuScale intends to use the NRC-approved VIPRE-01 computer code for steady-state and transient subchannel analysis and fuel temperature calculations for the Design Certification Application (DCA) and for future design analysis. The purpose of this report is to describe the methodology that NuScale intends to use for these analyses and to gain approval from the NRC. The specific elements of the requested approval are as follows:

- VIPRE-01 is applicable to the NuScale steady state and transient subchannel analysis utilizing the methodology presented.
- The NuScale methodology fulfills the NRC requirements in the VIPRE-01 MOD-01 and MOD-02 safety evaluation reports (SER).
- The methodology presented is independent of any specific critical heat flux (CHF) correlation and is used for NuScale applications if the methodology requirements are satisfied and the CHF correlation is approved by the NRC.
- The methodology for treatment of uncertainties in the NuScale subchannel methodology is appropriate.

VIPRE-01 is used throughout the industry for departure from nucleate boiling ratio (DNBR), critical power ratio (CPR), fuel and cladding temperatures, reactor coolant flow and temperature calculation during both normal and off-normal conditions. VIPRE-01 MOD-01 was generically approved by the NRC subject to five requirements, all of which are met by the NuScale methodology. The NRC generic safety evaluation report for the subsequent VIPRE-01 MOD-02 code includes four additional requirements for use of the code, all of which are met by the NuScale methodology. NuScale will use the latest MOD-02 version of the VIPRE-01 code, as approved, and will use its own NRC-approved CHF correlations. This report does not seek approval of the CHF correlations. The CHF correlations are submitted to the NRC in a separate topical report.

The NuScale subchannel methodology is deterministic and biases the key inputs, such as radial power distribution, axial power distribution, and inlet flow in a conservative direction. NuScale uses a 24-channel model for steady-state and transient analyses. Axial nodalization is established by performing sensitivity studies.

NuScale performed a detailed study of the uncertainties that could impact the subchannel analyses, including uncertainties in reactor power, inlet flow, core bypass flow, core exit pressure, core inlet temperature, core inlet flow distribution, radial power peaking factor, and fuel rod bowing impacts. These uncertainties are biased in the conservative direction in accordance with the deterministic subchannel methodology. For physics parameters, such as radial and axial peaking factors, conservative bounding values are used with the expectation that these values remain valid from cycle to cycle. Each cycle’s loading pattern and associated neutronics parameters are assessed against these bounding values.

One of the key purposes of subchannel analysis is the determination of the minimum critical heat flux ratio (MCHFR). A specific set of acceptance criteria is defined that must be satisfied for a valid CHF calculation:

- The local mass flux, equilibrium steam quality, and pressure at the location and time of MCHFR are within the CHF correlation applicability range.
- The MCHFR must occur in a channel geometry for which there is a valid CHF correlation.
- The MCHFR must not occur on a peripheral subchannel of an assembly.
- The hot channel must occur adjacent to the hot rod.
- The hot rod from the VIPRE-01 MCHFR calculation must be the rod with the highest radial power peaking factor.
- The VIPRE-01 calculation must satisfy all selected convergence criteria for the results to be considered valid.
- The MCHFR calculations must be performed using the VIPRE-01 RECIRC numerical solution.

Transient analyses use the 24-channel model and the biases established for the steady-state analysis. Special consideration is given to events that exhibit asymmetric power distribution. For some transients the radial power distribution is augmented, and an event-specific axial power distribution is used. The transient CHF calculations are performed using the steady-state CHF correlations. The CHF testing performed by NuScale and the industry supports the conservatism of using steady-state CHF correlations for transient CHF calculations. The methodology defines time steps depending on the nature of the transient.

Qualification of VIPRE-01 is based on code-to-code comparisons and comparisons to experiments performed as part of the original development of VIPRE. In addition, NuScale has performed its own code-to-code comparisons, comparisons against experiments, test simulations, phenomena examination, and sensitivity analyses. The comparisons provided in this report show good agreement over a wide range of conditions and provide reasonable results. The sensitivity analyses show that axial power shape, power of the hot rod, and mass flux are the most important parameters that influence MCHFR. Collectively, these analyses support the qualification of VIPRE-01 for subchannel analysis subject to the restrictions defined in this topical report.

NuScale did not make any code changes to the industry-maintained version of VIPRE-01 other than the addition of the NuScale-specific CHF correlation. In addition, the fundamental assumptions made in the development of VIPRE-01 remain valid for the NuScale design and operating conditions.

VIPRE-01 is used for design calculations in accordance with the NuScale quality assurance program description (Reference 8.2.41). An applicant or licensee that utilizes this subchannel methodology must implement the methodology in accordance with the restrictions and

conditions defined in the topical report. Additionally, subchannel calculations performed with VIPRE-01 should follow applicable software configuration control procedures, including requirements for error and warning documentation and error reporting. In addition, software and VIPRE-01 user procedures and processes provide direction on the applicability of models and correlations for each application, and proper usage of code inputs and outputs.

1.0 Introduction

1.1 Purpose

The purpose of this report is to define and justify the methodology for steady-state and transient subchannel analysis, including the qualification of VIPRE-01 for NuScale applications. This methodology will be utilized in future design applications, such as in Chapter 4 and 15 of the NuScale Final Safety Analysis Report (FSAR). NuScale requests NRC review and approval that the assumptions, codes, and methodologies presented in this report are technically acceptable and consistent with current regulations. This report provides the methodology for performing subchannel analyses, but the analysis results presented are for demonstration of the analytical methodology and approval of these results are not sought as part of this report.

The specific elements of the requested approval are:

- VIPRE-01 is applicable to the NuScale steady state and transient subchannel analysis utilizing the methodology presented.
- The NuScale methodology fulfills the NRC requirements in VIPRE-01 MOD-01 and MOD-02 SERs.
- The methodology presented is independent of any specific critical heat flux (CHF) correlation and is used for NuScale applications when the methodology requirements are satisfied and the CHF correlation is approved by the NRC.
- The methodology for treatment of uncertainties in the NuScale subchannel methodology is appropriate.

1.2 Scope

This report describes the assumptions, codes, and methodologies utilized to perform steady-state and transient subchannel analysis for design-basis accidents. This topical report focuses on the NuScale subchannel methodology and is not intended to provide final detailed reactor core design or final values of any other associated accident evaluations. Subchannel analysis results and comparisons to applicable specified acceptable fuel design limits (SAFDLs) are provided for illustration purposes to aid the understanding of the context of the application of these methodologies.

1.3 Abbreviations

Table 1-1. Abbreviations

Term	Definition
AO	axial offset
AOO	anticipated operational occurrence
ARO	all rods out
BWR	boiling water reactor
BOC	beginning-of-cycle
CFR	Code of Federal Regulations
CHF	critical heat flux
CHFR	critical heat flux ratio
COLR	core operating limits report
CPR	critical power ratio
DBE	design basis event
DNBR	departure from nucleate boiling ratio
DSRS	Design-Specific Review Standard
EOC	end-of-cycle
EPRI	Electric Power Research Institute
$F_{\Delta H}$	enthalpy rise hot channel factor
F_Q	total peaking factor, also referred to as the heat flux hot channel factor
F_Z	rod axial peaking factor
FCM	fuel centerline melt
HFP	hot full power
HZP	hot zero power
IBDCF	Inter-Bundle Diversion Cross Flow
IE	infrequent events
LHGR	linear heat generation rate
MCHFR	minimum critical heat flux ratio
MSLB	main steam line break
NRC	Nuclear Regulatory Commission (United States)
NRELAP5	NuScale-specific system analysis code that is used for system hydraulic response to reactor transient events.
NSSS	nuclear steam supply system
PDIL	power-dependent insertion limit
PLHGR	peak linear heat generation rate
PWR	pressurized water reactor
RCS	reactor coolant system
RSS	root sum of squares
SAFDL	specified acceptable fuel design limit
SER	safety evaluation report
SRP	standard review plan
UCBW	uncontrolled bank withdrawal
UCBWS	uncontrolled bank withdrawal at subcritical
95/95	95-percent probability at the 95-percent confidence level

Table 1-2. Definitions

Term	Definition
Aspect ratio	Ratio of key adjacent node size along an axis. As an example, an axial level of 2 inches above a level of 0.5 inches would have an aspect ratio of 4.
Basemodel	A reference to the 24-channel model that has been built using an assumed axial and radial power distribution. This is the licensing model used for code validation as well as steady-state and transient calculations.
Critical heat flux (CHF) point	A unit for the arithmetic difference of two CHF ratios (CHFRs) multiplied by a factor of 100. For example, a change from a CHFR of 1.00 to 1.01 results in an increase of 1 CHF point.
Courant number	A stability criterion for numerical analysis that is calculated by: $u \cdot \Delta t / \Delta x$, where u is the axial velocity, Δt is the time step size, and Δx is the axial node size. It is a dimensionless number used as a necessary condition for convergence of numerical solutions of certain sets of partial differential equations.
Design-basis accident	A postulated accident that a nuclear facility must be designed and built to withstand without loss to the systems, structures, and components necessary to ensure public health and safety.
Deterministic methodology	The uncertainty associated with each parameter is applied in the conservative direction without regard for the combination nature of uncertainties.
Statistical methodology	The uncertainties associated with each parameter are considered random and are statistically combined to increase the minimum CHFR design limit.
Specified acceptable fuel design limit (SAFDL)	If this limit is met, the fuel rods do not fail and that fuel design dimensions remain within tolerances so that the cooling functionality is maintained.
Undamaged fuel	Fuel cladding is not breached, fuel system dimensions remain within operational tolerances, and functional capabilities are not reduced below those assumed in the safety analysis.

2.0 Background

The regulatory basis for subchannel analysis is fundamentally derived from General Design Criterion 10 of 10 CFR 50, Appendix A, which states that a design include *"…appropriate margin to assure that specified acceptable fuel design limits are not exceeded during any condition of normal operation, including the effects of anticipated operational occurrences."* Standard Review Plan (SRP)[1] Section 4.2 provides further guidance on interpreting this design criterion by defining SAFDLs and acceptance criteria that, when met, satisfy the intent of the general design criteria. Specifically, this SRP section states that *"…the SAFDLs are established to ensure that the fuel is not damaged*," where "*'not damaged' means that the fuel rods do not fail, fuel system dimensions remain within operational tolerances, and functional capabilities are not reduced below those assumed in the safety analysis."* This section goes on to explicitly define the known mechanisms for fuel rod failures: overheating of cladding and fuel pellets, pellet-clad interaction, hydriding, cladding collapse, excessive fuel enthalpy rise, bursting, and mechanical fracturing.

A primary goal of subchannel analyses is to determine the thermal margin to the failure mechanism of cladding overheating. As stated in SRP Section 4.2, *"traditional practice assumes that failures will not occur if the thermal margin criteria (DNBR for PWRs and CPR for BWRs) are satisfied."* A reference to Section 4.4 of the SRP is then provided as the description for defining and analyzing with thermal margin criteria. In short, violation of the thermal margin criteria is not permitted for normal operation and anticipated operational occurrences (AOOs). For infrequent events (IE) and design-basis accidents, the total number of fuel rods that exceed the criteria are assumed to fail and used as input for radiological dose calculation purposes.

In a traditional subchannel analysis, measuring margin to departure from nucleate boiling ratio (DNBR) or critical power ratio (CPR) is not absolutely required. Section 4.2 of the SRP makes the point that exceeding the thermal margin criterion is itself not a failure; rather, it is used as a conservative indicator. The regulations allow for other mechanistic methods to be proven for acceptability; however, there is little experience with other approaches. NuScale uses the standard thermal margin approach as outlined in Sections 4.2 and 4.4 of the SRP. Section 4.4 of the SRP provides two options for demonstrating compliance with the SAFDLs via thermal margin:

- There should be a 95 percent probability at a 95 percent confidence level (95/95) that the hot rod in the core does not experience a critical heat flux condition.

[1] Within the context of this report, reference to the SRP is also meant to account for NuScale Design-Specific Review Standards (DSRSs).

- The limiting (minimum) value of CHF ratio (MCHFR) for CHF correlations is to be established such that at least 99.9 percent of the fuel rods in the core will not experience a CHF condition.

Traditionally, pressurized water reactors (PWRs) have used the 95/95 option, while boiling water reactors (BWRs) have used MCHFR for the thermal design criteria. In either approach, a definition of the SAFDLs and sufficient technical justification for their limits is required. Explicit values in measurable units are not specified in Section 4.2 of the SRP, but they are left to the applicant to define following the appropriate regulatory guidance. Because the SAFDLs span multiple disciplines, only the SAFDLs CHF and fuel centerline melt (FCM) are calculated by subchannel analysis.

The two approaches to meet the 95/95 acceptance criteria use deterministic or statistical methods to account for uncertainties. These methods are described in further detail below.

- **Deterministic:** Uncertainties associated with the CHF correlation are statistically treated in order to determine a 95/95 correlation limit above the predicted-to-measured average. For a subchannel calculation, the uncertainties associated with inputs (system conditions, power distributions, design tolerances, etc.) are biased independently in the limiting direction within the subchannel analysis. Thus, uncertainties in the analysis are accounted for as biases on the inputs without regard for the random nature of uncertainties.
- **Statistical:** Uncertainties associated with the CHF correlation are statistically treated in order to determine a 95/95 correlation limit. Additionally, uncertainties that are considered random are statistically combined to increase the MCHFR design limit. For a subchannel calculation, the initial conditions are input without bias into VIPRE-01. Thus, uncertainties in the analysis and correlation are accounted for in the MCHFR design limit.

Generally, PWRs have used the term DNB for all thermal margin analysis, while BWRs have used the term CPR. Terms such as CHF, boiling crisis, and boiling transition are generic terms for the phenomenon of degraded coolant heat removal. For consistency in modeling the range of NuScale-specific phenomena, NuScale uses the generic term CHF due to the observation of multiple mechanisms occurring during the NuScale CHF testing.

2.1 VIPRE-01

The VIPRE-01 analysis software was developed primarily based on the COBRA family of codes by Battelle Pacific Northwest Laboratories for the Electric Power Research Institute (EPRI). The intended use was to evaluate nuclear reactor parameters, including minimum DNBR, CPR, fuel and cladding temperatures, and reactor coolant state, in normal and off-normal conditions (Reference 8.2.1).

As described in Reference 8.2.3, the three-dimensional velocity, pressure, and thermal energy fields and radial fuel rod temperature profiles for single and two-phase flow in reactor cores are predicted by VIPRE-01. These predictions are made by solving the field equations for mass, energy and momentum using the finite differences method for an interconnected array of channels assuming incompressible thermally expandable flow. The equations are solved with no channel size restrictions for numerical stability, with consideration of lateral scaling for key parameters in lumped channels. Although the formulation is based on the fluid being homogeneous, non-mechanistic empirical models are included for subcooled boiling non-equilibrium and vapor/liquid phase slip in two-phase flow.

Like most other core thermal-hydraulic codes, the VIPRE-01 modeling structure is based on subchannel analysis. The core or section of symmetry is defined as an array of parallel flow channels with lateral connections between adjacent channels. These channels characterize the dominant, longitudinal flow (vertical) by nodalization with various models and correlations predicting thermal-hydraulic phenomena that contribute to inter-channel exchange of mass, enthalpy, and momentum. These channels can represent all or fractions of the coolant channel bordered by adjacent fuel rods (hence "subchannel") in rod bundles. The axial variation in channel geometry may also be modeled with VIPRE-01. Channels may represent closed tubes as well as larger flow areas consisting of several combined (lumped) subchannels or rod bundles. These channels communicate laterally by diversion crossflow and turbulent mixing. A representative diagram of a subchannel and an individual control volume within the context of a fuel assembly and entire reactor core is provided in Figure 2-1.

The original VIPRE-01 version (MOD-01) was submitted to the NRC in 1985 for use in PWR and BWR licensing applications. An SER by the NRC was issued the following year (Reference 8.2.42). The NRC accepted VIPRE-01 MOD-01 with several specific restrictions and qualifications, limiting its use to PWR licensing applications for heat transfer regimes up to the point of CHF. This approval was contingent on: (1) the CHF correlation and its limit used in the application is approved by the NRC and (2) each organization using VIPRE for licensing calculations must submit separate documentation justifying their input selection and modeling assumptions. In 1990, the MOD-02 version of VIPRE-01 was submitted to the NRC to review an improved and updated version, and included changes and corrections from the MOD-01 version. This version was approved with an SER issued in 1993 with the same requirements and qualifications as in the MOD-01 SER (Reference 8.2.1) and some additional requirements. All of the SER requirements from Reference 8.2.1 are met by the NuScale methodology. Unless otherwise stated, a reference to VIPRE-01 in the remainder of this document is referring to the MOD-02 version.

VIPRE-01 has been used throughout the industry for subchannel analyses. The contents of this report were informed by other similar VIPRE-01 applications in References 8.2.13 through 8.2.16.

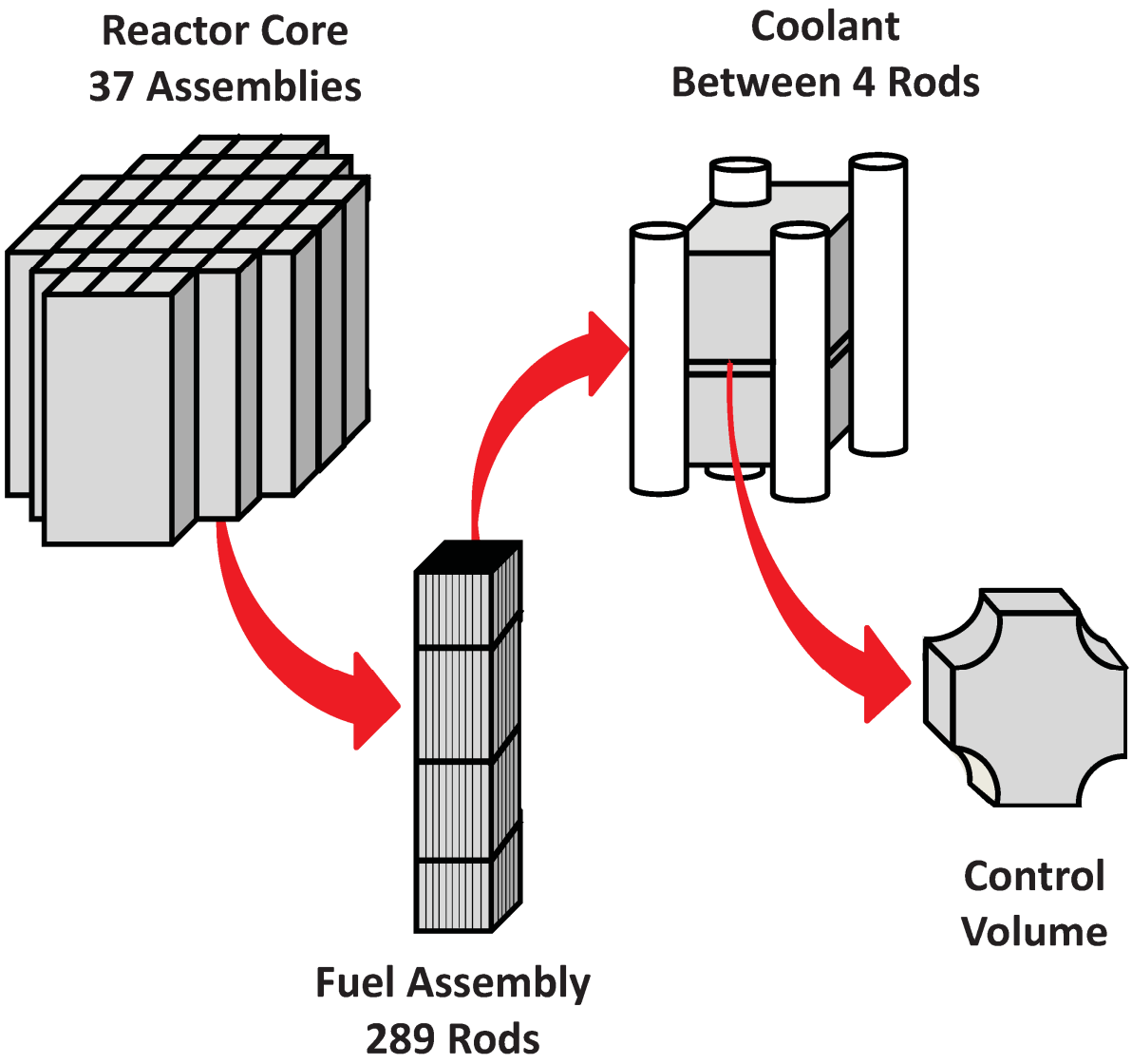

Figure 2-1. Schematic of subchannel analysis nodalization

2.2 As-Approved Use

NuScale use of VIPRE-01 is “As-Approved” because there are no modifications to the NRC-approved constitutive models and algorithms in VIPRE-01 and the computational philosophy remains unchanged. Therefore, the VIPRE-01 qualification is fully applicable to the NuScale implementation.

The only enhancement made to VIPRE-01 for NuScale use is the addition of NuScale-specific CHF correlations to the existing suite of VIPRE-01 CHF correlations. These CHF correlations are being submitted to the NRC for approval in a separate topical report

(Reference 8.2.7). Additional CHF correlations may be used with the code in the future. Each one of these correlations is qualified or verified in its own report, and submitted for NRC review and approval, prior to licensing use.

Modeling, testing, and benchmarking of VIPRE-01 is presented in this report. The VIPRE-01 User's Manual (Reference 8.2.3) is fully applicable, but it has been augmented to clarify the option of NuScale-specific CHF correlations.

CHF correlations are empirical fits to limiting local thermal-hydraulic parameters obtained by simulating CHF tests. CHF test simulations are performed using the same thermal-hydraulic code that the resulting CHF correlation is to be used with. Reduction of CHF test data to obtain limiting local thermal-hydraulic conditions is performed using the same thermal-hydraulic code options, such that the CHF correlation serves as a final closure relation. Using a CHF correlation with the same thermal-hydraulic code that was used for its development ensures that code predictions are not affected by differences in modeling. The use of user-defined CHF correlations is facilitated through dynamic link library (DLL), which precludes the need to open or recompile VIPRE-01, such that the approved state of the code remains intact even while permitting the use of user defined CHF correlations.

2.3 VIPRE-01 Safety Evaluation Report Requirements

The generic VIPRE-01 SER (Reference 8.2.1) provides specific restrictions and qualifications. For NuScale applications, each of these restrictions is addressed in this topical report. The five requirements are repeated from the SER, and a summary of the NuScale fulfillment of each requirement is provided below and in the conclusion of this report (Section 7.1).

1. *The application of VIPRE-01 is limited to PWR licensing calculations with heat transfer regime up to CHF. Any use of VIPRE-01 in BWR calculations or post-CHF calculations will require prior NRC review and approval.*

   The methodology in this report does not seek approval for use of VIPRE-01 for post-CHF calculations.

2. *Use of a steady state CHF correlation with VIPRE-01 is acceptable for reactor transient analysis provided that the CHF correlation and its DNBR limit have been reviewed and approved by NRC and that the application is within the range of applicability of the correlation including fuel assembly geometry, spacer grid design, pressure, coolant mass velocity, quality, etc. Use of any CHF correlation that has not been approved will require the submittal of a separate topical report for staff review and approval. The use of a CHF correlation that has been previously approved for application in connection with another thermal hydraulic code other than VIPRE-01 will require an analysis showing that, given the correlation data base, VIPRE-01 gives the same or a conservative safety limit, or a new higher DNBR limit must be used, based on the analysis results.*

NuScale CHF correlation(s) are demonstrated to be valid for design-specific experimental data. The test bundles represent the fuel geometry and spacer grid design, and the test points adequately cover the parameter ranges, such as pressure, coolant mass velocity, and quality, that characterize the reactor operation. VIPRE-01 is used to reduce the experimental CHF data to obtain local thermal-hydraulic conditions. The CHF correlation is used with VIPRE-01 for the calculation of event-specific CHFR values and limits. The CHF correlation that will be used is submitted in a separate topical report for NRC review and approval.

3. *Each organization using VIPRE-01 for licensing calculations should submit separate documentation describing how they intend to use VIPRE-01 and providing justifications for their specific modeling assumptions, choice of particular two-phase flow models and correlations, heat transfer correlations, CHF correlation and DNBR limit, input values of plant specific data such as turbulent mixing coefficient, slip ratio, and grid loss coefficient, etc., including defaults.*

This topical report is the separate documentation describing NuScale's intended use of VIPRE-01 and the justification for specific modeling assumptions, choice of particular two-phase models and correlations, heat transfer correlations, CHF correlation and limits, and input values of plant specific data.

4. *If a profile fit subcooled boiling model (such as Levy and EPRI models), which was developed based on steady state data is used in boiling transients, care should be taken in the time step size used for transient analysis to avoid the Courant number being less than 1*.

The VIPRE-01 user must check that the transient time step, axial nodalization, and coolant velocity utilized ensure satisfaction of the Courant number requirement. Section 4.3 addresses this requirement.

5. *The VIPRE-01 user should abide by the quality assurance procedures described in [the SER].*

VIPRE-01 is used for design calculations in accordance with NuScale quality assurance program description. The approved subchannel methodology follows the restrictions and conditions defined in the topical report (see Section 7.2). Additionally, subchannel calculations performed with VIPRE-01 follow applicable software configuration and usage procedures that include requirements for error and warning documentation, error reporting, applicability of models and correlations for each application, and usage of code inputs and outputs.

Additionally, the NRC generic SER for VIPRE-01 MOD-02 includes four additional conditions for use of the code. These conditions are defined in Reference 8.2.1 as:

1. *The use of [VIPRE-01] for BWR licensing applications is contingent upon full qualification of the [(1) water tube channel modeling (2) leakage flow path*

connection (3) drift-flux model] described in [Technical Evaluation Report] TER Section 3.2.2.

Water tube channel modeling and leakage flow path connections are specific to BWR applications. Bypass flow (including guide tube flow) is modeled in a similar manner to conventional PWR applications and described in Section 3.8.4. An evaluation of drift-flux modeling is described in Section 5.10, in which a negligible effect on NuScale applications was observed.

2. *The GEXL correlation is the only correlation currently having NRC approval for use in CPR calculations of a core containing GE fuels. However, use of the GEXL correlation for other vendors' fuels or any other correlation requires a separate submittal for NRC review and approval.*

NuScale does not perform CPR calculations for BWR fuel with VIPRE-01.

3. *Section 2.2 of Volume 5 of the submittal [Reference 8.2.6] identifies a spectrum of limitations of the code. Each user should ensure that the code is not being used in violations of these limitations.*

Section 2.2 of Reference 8.2.6 describes several two-phase flow conditions, local pressure phenomena, and a free-field not dominated by wall friction that are not applicable to NuScale applications. Section 6.3 and Figure 6-12 demonstrate that the NuScale design is similar to conventional PWRs, for which VIPRE-01 was designed, with respect to equilibrium qualities and flow regime.

With regard to the applicable range of constitutive correlations, closure relationships used in CHF analyses are the same that were used in deriving the CHF correlation from the testing database as stated in Section 7.2.2. As NuScale utilizes the CHF testing database for the applicable range of the given closure relationships, not based on the ranges of the derived empirical closure models (i.e., subcooled boiling, bulk boiling, two-phase friction), this condition is satisfied.

4. *By acceptance of this code version, [the NRC does] not necessarily endorse procedures and uses of this code described in Volume 5 as appropriate for licensing applications. As the code developer stated in Reference 5, the materials were provided by the code developers as their non-binding advice on efficient use of the code. Each user is advised to note that values of input recommended by the code developers are for best-estimate use only and do not necessarily incorporate the conservatism appropriate for licensing type analysis. Therefore, the user is expected to justify or qualify input selections for licensing applications.*

The input and modeling options and corresponding justification presented in this report meet this requirement and are summarized in Table 7-1. The quality assurance procedures required for usage with VIPRE-01 are described in MOD-01 SER Requirement number 5 (above).

2.4 Regulatory Requirements

The following regulatory requirements and guidance documents are relevant to the subchannel analysis evaluations described in this report:

- 10 CFR 50, Appendix A, General Design Criterion 10, *Reactor Design*
- NuScale DSRS, Section 4.4, “Thermal and Hydraulic Design,” June 2016
- NUREG-0800, Section 4.2, “Fuel System Design,” Revision 3, March 2007
- NUREG-0800, Section 4.4, “Thermal and Hydraulic Design,” Revision 2, March 2007

3.0 General Application Methodology

This section provides an overview of the thermal design analysis methodology for NuScale subchannel analysis. Both the basis for the subchannel model development and its application are discussed. The thermal hydraulics of the reactor core are modeled with a one-pass approach, meaning all the characteristics of the hot channel are captured, including inter-channel feedback. A one-pass approach allows the use of a fully-detailed pin-by-pin model as well as lumped channels to resolve the desired enthalpy and flow field. The core is analyzed using one-eighth core symmetry. Analyzed core designs may not necessarily be one-eighth core symmetric but must be quarter-core symmetric at a minimum; however, the conservatisms used in the model account for the insignificant non-symmetries in the core design, as further described in Section 3.10.

3.1 Nuclear Safety Engineering Disciplines

The full scope of a design-basis safety analysis evaluation for a nuclear reactor core is inherently multi-disciplinary in nature. An overview of the key functional groups and the information flow between these functional groups is discussed below. These functional groups are generic and do not necessarily correspond to NuScale organization titles.

1. **Nuclear analysis:** Develops the loading pattern for each cycle that meets cycle design requirements and performs a set of steady-state simulations of the proposed core design that defines the neutronics characteristics of the reactor core. This includes power distribution, moderator temperature coefficient, Doppler coefficient, control rod worth, effective delayed neutron fraction, and prompt neutron lifetime. The primary nuclear analysis parameters used in the subchannel analysis are the radial and axial power distributions. Nuclear analysis also performs transient-specific neutronic calculations for input to subchannel and transient analyses. The nuclear analysis methods are described in Reference 8.2.8.
2. **Fuels:** Performs calculations to define the initial conditions of the fuel, specifically the thermal conductivity of the fuel pellet, the conductance of the fuel pellet-to-clad gap, and the conductivity of the fuel clad itself. These calculations are used to calibrate VIPRE-01 so that it can be used for calculation of fuel centerline temperatures. The applicability of AREVA fuel analysis methods to the NuScale design is described in Reference 8.2.9.
3. **Transient analysis:** Performs calculations to evaluate the neutronic and thermal-hydraulic response of the reactor coolant system (RCS) following anticipated operational occurrences or postulated design-basis events as defined in the NuScale FSAR Chapter 15. The key parameters used by transient analysis are the moderator and Doppler temperature coefficients, control rod worth, effective delayed neutron fraction, prompt neutron lifetime, and initial power distribution. The transient analysis methods are described in Reference 8.2.10.

4. **Thermal hydraulics**: Performs subchannel calculations to determine the thermal-hydraulic safety limits of the core and thermal margin for MCHFR and SAFDLs during normal operation, AOOs, and postulated events. A bounding radial and axial power distribution is used for these analyses.
5. **Accident Radiological Analysis:** Performs calculations to determine the radiological consequences (on-site and off-site) following postulated design-basis events for verification of the SAFDL related to dose. It is assumed that if a fuel rod exceeds its SAFDL, the fuel rod fails, and all of the contents of the fuel rod gap are released. The radiological methods are described in Reference 8.2.12.

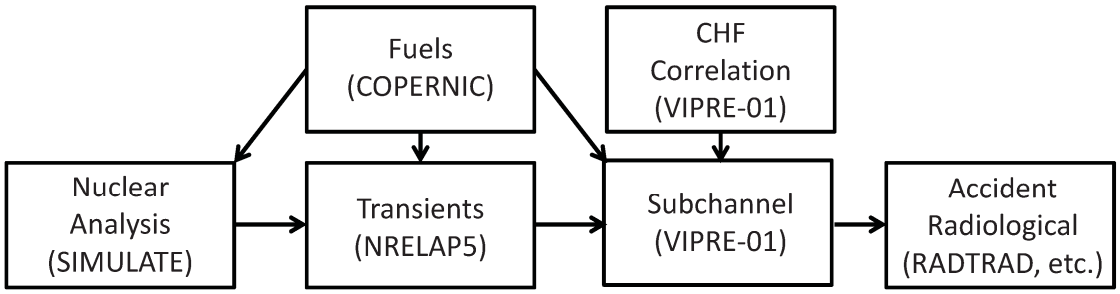

Figure 3-1. Discipline flow with example software utilized

This report focuses on the interfaces of thermal-hydraulics subchannel analysis with other functional groups. Additionally, Section 7.2 provides a summary of the interfaces and corresponding restrictions in order to explicitly define the subchannel analysis scope presented in this report.

3.2 Core Design Limits

The subchannel analysis basemodel is developed in a conservative manner such that it does not represent a cycle-specific core. The basemodel is constructed to preserve the limiting core conditions along with the operational envelope specified in the core operating limits report (COLR). It is established using the design peaking factors in combination with the limiting RCS global parameters. With this method, a one-eighth core subchannel analysis model is appropriate because the methodology ensures the limiting conditions of the cycle-specific core are captured by the basemodel.

The radial power peaking parameter is defined to be the enthalpy rise hot channel factor ($F_{\Delta H}$). This parameter is the ratio of the maximum integrated rod power within the core to the average rod power. Therefore, $F_{\Delta H}$ is a measure of the maximum total power produced in a fuel rod. The $F_{\Delta H}$ limit is representative of the hot fuel rod and the subchannel connected to this rod is required by the thermal margin acceptance criteria to have the limiting MCHFR.

The COLR will impose a limitation on the peak value of $F_{\Delta H}$, and therefore the highest value for any fuel rod at hot full power (HFP) will be limited to 1.5, as an example. The

$F_{\Delta H}$ peaking design limit, also known as the core operating limit peaking factor, is relaxed for lower power levels, allowing a linear increase to a hot zero power (HZP) value of 1.65, as an example.

The total peaking factor (F_Q) is also referred to as the heat flux hot channel factor. This parameter is the ratio of maximum local heat flux on the surface of a fuel rod to the average fuel rod heat flux. The maximum F_Q value is used to calculate the peak linear heat generation rate (LHGR). The design F_Q acceptance criterion is defined to be 2.0 at hot full power, as an example.

In the COLR, there will be no limit on axial peaking because (i) the other limits of F_Q and $F_{\Delta H}$ enforce a sufficiently flat power distribution, and (ii) axial peaking is treated in a multi-step approach involving operational restrictions and analysis that will be subsequently described. A rod (not core average) axial peaking factor (F_z) is defined as the maximum relative power at any axial point for a unique rod divided by the average power throughout the fuel rod. For any rod, the relationship between total, radial, and axial peaking factor is given by:

$$F_Q = F_{\Delta H} \times F_z \qquad \text{Eq. 3-1}$$

The axial peaking factors used more often than the rod peak in subchannel analysis are that of the core average axial peaking factor (F_z^{Core}) and an assembly average axial peaking factor (F_z^{Assm}), because when used in combination with the $F_{\Delta H}$ value it is generally conservative. Similarly, another key axial power parameter is the axial offset (AO), which is a measure of the difference in power generated in the top and bottom halves of the core.

$$AO(\%) = \frac{Power_{Top} - Power_{Bottom}}{Power_{Total}} \times 100 \qquad \text{Eq. 3-2}$$

Axial offset alone is not enough of an indicator for the axial power shape. Two axial power shapes with different peak F_z^{Core} values and peak locations can have the same AO percentage as long as each half of the core produces the same power. Therefore, the MCHFR for two axial power profiles with the same AO can be quite different. This difference is addressed in Section 3.10.8.

3.3 Critical Heat Flux Correlation

The CHF correlation is an empirical fit to test data for a particular fuel design that determines the heat flux beyond which heat transfer is degraded. The CHF correlation uses calculated local conditions from VIPRE-01 at {{

}}[2(a),(c)]. From this information, a correlation is developed based on the condition ranges simulated with the tests. A 95/95 design limit for MCHFR is also determined as the acceptance criterion for meeting the CHF SAFDL in SRP Section 4.4.

The subchannel methodology presented in this report is not dependent on a specific CHF correlation as long as the CHF correlation satisfies the following applicability criteria. The CHF correlation may only be used for design analysis that implements this subchannel methodology if:

- The application must explicitly state that an approved CHF correlation is used.
- The CHF correlation is used within its applicable parameter ranges.
- Local conditions are simulated with VIPRE-01 to predict the CHF test data.
- The same two-phase flow model options are used for local condition simulations.
- The CHF correlation is applicable to the fuel design (including spacer grids) being analyzed.

A CHF correlation for NuScale, referred to as NSP2, is presented in Reference 8.2.7. The CHF 95/95 limit is the design limit on MCHFR which meets the acceptance criterion and is used for all thermal margin calculations. The 95/95 correlation limit for the NSP2 CHF correlation is 1.17. The correlation limit takes into account the uncertainties associated with the correlation development. For conservatism a design limit of 1.19 is used in subchannel analyses. In order for CHF correlations to be used within their applicable parameter ranges, they are developed to be valid for an extended range of parameters. For example, the EPRI CHF correlation is valid up to 70 percent quality and a lower pressure limit of 600 psia. Parameter ranges applicable to the NSP2 CHF correlation are even wider and are presented in Table 3-1. These parameter ranges are much wider than the limiting local conditions of the reactor to ensure that the CHF correlation remains valid for a wide range of off-normal conditions. For example, the NSP2 correlation remains valid down to a system pressure of 300 psia and up to 95 percent local equilibrium quality, while the NuScale core is not expected to operate at more than 20 percent quality. Example NuScale operational ranges are provided in Table 3-1 for comparison.

Table 3-1. Parameter ranges for example (NSP2) CHF correlation

Parameter	Lower Limit	Upper Limit	Example NuScale Range (Normal / Off-Normal)
pressure, psia	300	2300	1,700 – 2,200
local mass flux, Mlbm/hr-ft^2	0.110	0.700	0.1 – 0.5
local equilibrium quality, %	-	95%	< 20%

The effect of increasing pressure resulting in a reduced CHFR is discussed in more detail in the CHF topical report (Reference 8.2.7).

3.4 Thermal Margin Results Reporting

The key results for subchannel analyses are CHF margin and MCHFR; the latter is a direct output from VIPRE-01 calculated for all modeled fuel rods and channels. The MCHFR is the limiting ratio calculated for any rod or channel in the core. For transients, MCHFR is calculated for each time step. CHF margin is reported as a percentage or CHF points above the CHF analysis limit as indicated below:

$$\text{CHF margin (\%)} = \frac{\text{MCHFR}_{\text{VIPRE}} - \text{CHF}_{\text{Analysis Limit}}}{\text{CHF}_{\text{Analysis Limit}}} * 100$$

$$\text{CHF margin (CHF points)} = (\text{MCHFR}_{\text{VIPRE}} - \text{CHF}_{\text{Analysis Limit}}) * 100 \qquad \text{Eq. 3-3}$$

where

$\text{MCHFR}_{\text{VIPRE}}$ = minimum CHFR from VIPRE-01 calculation

$\text{CHF}_{\text{Analysis Limit}}$ = CHF limit incorporating margin applied to the design limit

The incorporation of uncertainties or biases to produce a conservative subchannel methodology is performed in two places: (i) within VIPRE-01 inputs prior to MCHFR calculation, and (ii) outside the VIPRE-01 calculations, but as an increase on the MCHFR design limit. The derivation of the penalties and conservative bias determine whether the penalty is applied within the VIPRE-01 input model or external to the calculation as an increase in the correlation limit. The biases and penalties are presented throughout Section 3.0 of this report and are summarized in Section 3.13. When an external penalty is needed (e.g., rod bowing, F_Q^E, etc.), the following equation is used to modify the 95/95 CHF design limit (e.g., 1.17 from Section 3.3) for margin reporting:

$$\text{CHF}_{\text{Analysis Limit}} = \text{CHF}_{95/95\text{ Limit}} \cdot (1+\gamma_a) \cdot (1+\gamma_b) \cdot \ldots \cdot (1+\gamma_i) \qquad \text{Eq. 3-4}$$

where

$\text{CHF}_{95/95\text{ Limit}}$ = 95/95 CHF design limit (NSP2 = 1.17)

γ_i = penalty, fraction

Figure 3-2 shows the MCHFR limits and the example margins in the MCHFR calculation.

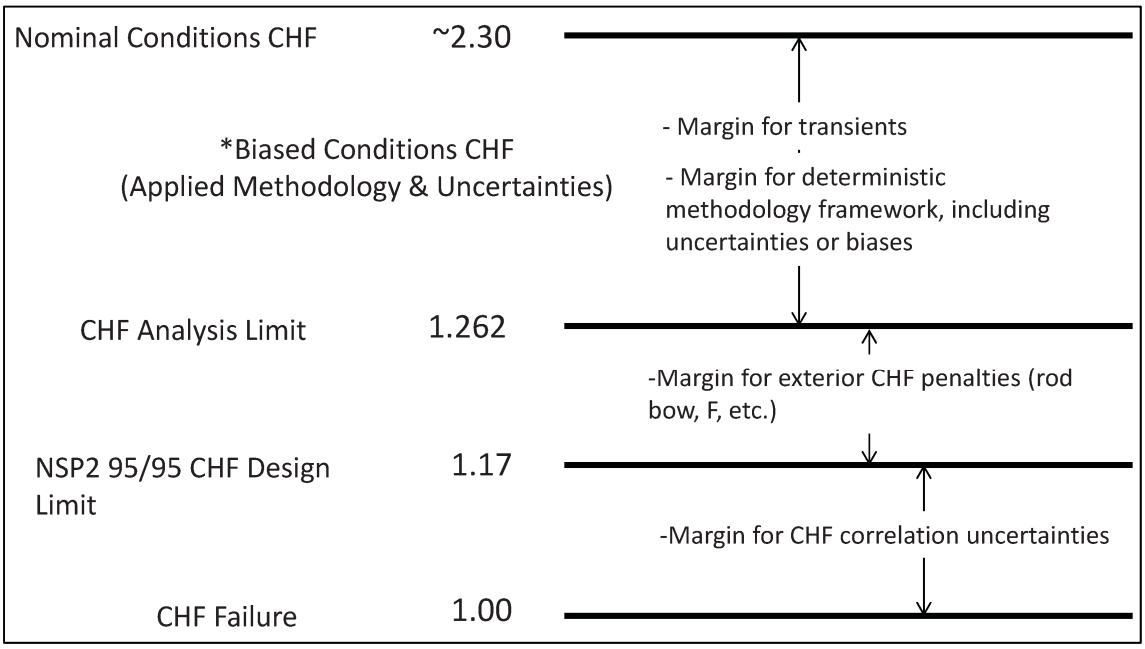

Figure 3-2. Example thermal margin pictorial

3.5 Geometry Design Input

The geometry for the radial and axial dimensions must be defined to develop the inputs for the subchannel basemodel. Geometry may be input for ‘cold’ conditions, meaning the dimensions are the measured values at room temperature (approximately 70 degrees F), or for ‘hot’ conditions, which are traditionally the dimensions that are thermally expanded using a material-specific equation evaluated at the core average temperature.

The NuScale subchannel analyses use ‘cold’ geometry conditions. This assumption allows the use of dimensions directly from the reference fuel design document and maintains consistency with the pressure drop information. The grid spacer form loss and bare rod friction losses are evaluated with flow areas consistent with ‘cold’ conditions. To remove any conversions required for the inputs based on the bare rod flow areas, the inputs are simplified to assume ‘cold’ conditions. The thermal expansion for fuel and spacer materials are nearly identical; thus the change in flow area, and wetted and heated perimeters for the ‘hot’ conditions, is negligible. Additionally, axial geometry changes in the active fuel occur with exposure; however, hot channel factors discussed later in this report account for pellet densification among other variations.

3.6 Fuel Design-Specific Inputs

Fuel design-specific information is required as input into the subchannel basemodel. Spacer grid loss coefficients and friction factor are derived from pressure drop tests. The correlations for the turbulent friction factor value and grid form loss coefficient are input

as a Blasius-type relation in VIPRE-01 (Reference 8.2.3). The correlations derived from the test data are used for both laminar and turbulent conditions. The grid spacer form loss coefficients may be identified for each channel. When the pressure-drop tests are performed, the pressure difference is measured across the entire spacer grid, and the loss coefficient is simply derived. This pressure loss is associated with the entire flow area of the grid; however, each type of subchannel contributes to the losses in different magnitudes. For example, the outer edge and corner subchannels have a large loss coefficient due to the presence of the outer grid straps within that subchannel part of the model; however, the flow area is much smaller than that of unit or guide tube subchannels. The generation of the loss coefficients on a subchannel-specific basis requires assumptions based on the impact that the size and volume of strap and grid material that is within the flow area. Because the entire grid spacer loss coefficient is derived from the actual test data, NuScale uses assembly-wide (flow area based) losses for the spacer grids. This “smeared” approach of applying the same loss coefficient to each subchannel is acceptable as long as the predicted-to-measured ratio is preserved, which implies that the CHF correlation is derived with the correct local losses. A single value for the loss coefficient is used and is applied to each subchannel type (specifically, typical unit cell and guide tube cell).

This modeling method is justified by a parametric sensitivity analysis in Section 6.3 which demonstrates that the impact of the grid loss coefficients applied globally is negligible. Increasing or decreasing the grid loss coefficients has no impact on the MCHFR results as long as the same losses are used globally throughout the model. The overall pressure drop will increase or decrease accordingly, but the flow field distribution is not significantly perturbed. Applying different loss coefficients for grids in assemblies impacts the flow field results and, therefore, the calculated MCHFR. The NuScale core is simulated with the actual grid spacer loss coefficient for each assembly at its appropriate location. VIPRE-01 is able to resolve the hot channel flow conditions while modeling the applicable grid loss coefficients for each assembly. Total core pressure drop varies with loss coefficient input, yet results in a global effect on the core.

The axial dimensions of the model include the full length of the fuel rod. This dimension is chosen as the reference plane for the model because it allows proper accounting of friction losses for the fuel rod and guide tube. The losses for the upper and lower core plates are accounted for within the boundary conditions being used for input and, therefore, are not considered in the VIPRE-01 subchannel model.

Due to the axial reference plane being used, the axial hydraulic losses are applied in the model referenced to the centerline elevation of the spacer grid. The losses for the bottom nozzle and lower end grid are lumped together and applied at the centerline of the lower end grid elevation. The local losses for the intermediate spacer grids are placed at their respective centerline elevations, while the top nozzle pressure drop is lumped with the upper end grid and placed at the upper end grid centerline elevation. The lumping of the nozzles with the closest spacer grid has no impact on the CHF results because the region of MCHFR interest is accurately depicted.

3.7 Basemodel

The NuScale core design contains 37 assemblies as shown in Figure 3-3. The subchannel analysis basemodel uses one-eighth core nodalization even though core designs may exhibit a quarter-core symmetric or one-eighth core symmetric shuffle pattern. As noted previously, the basemodel is developed in a conservative manner and it does not represent a cycle-specific core. Rather, it is established based on the design peaking factors in combination with the limiting RCS global parameters. With this method, a one-eighth core subchannel analysis model is appropriate, because the methodology ensures the limiting conditions of the cycle-specific core are captured by the basemodel.

The methodology for subchannel analysis utilizes a 24-channel model for all steady-state analyses. For the purposes of subchannel methodology, the 24-channel model is called the “basemodel” as it is the model used for licensing calculations.

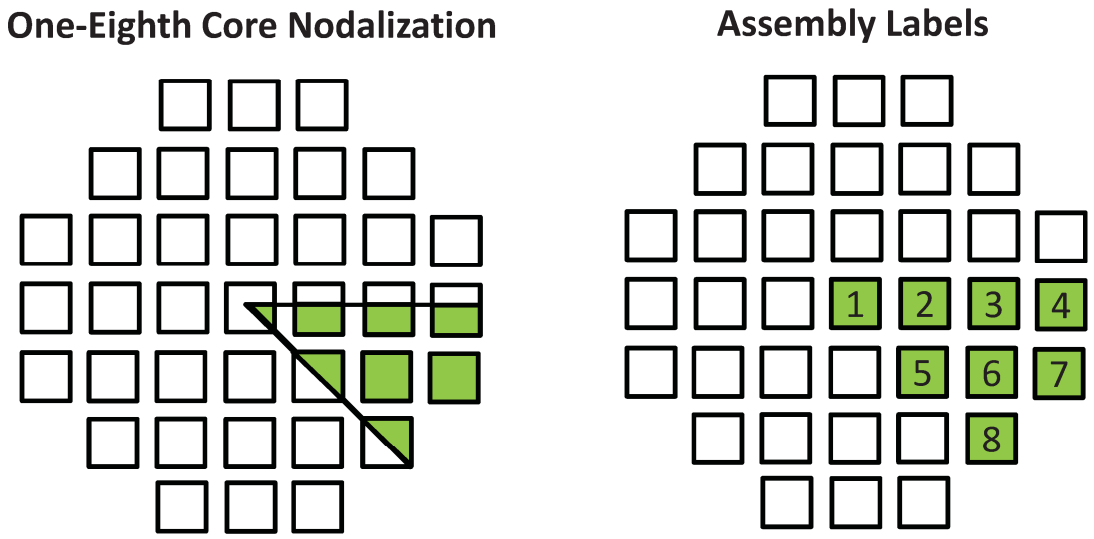

Figure 3-3. One-eighth core nodalization template

3.7.1 Radial Nodalization

The radial nodalization for the subchannel VIPRE-01 model allows for flexibility in representing the one-eighth core. VIPRE-01 defines channels based on flow area, wetted perimeters, and heated perimeters, with subchannel communication modeled through gap size and centroid distance. The heat input for VIPRE-01 is defined such that the fraction of power from each rod deposited to each channel area is provided as an input.

Based on the features available in VIPRE-01 and the application usage of determining a conservative MCHFR SAFDL, the one-eighth core for the NuScale core was modeled

with 24 subchannels and 52 rods. This model utilizes 'lumped channels' to combine several subchannels into one channel. The methodology ensures that the limiting subchannel local conditions are not perturbed resulting in a non-conservative MCHFR. This modeling approach is used for all steady-state calculations and most transients. However, some transients result in significant changes to the generic power distribution, resulting in the need to use a more detailed model with each subchannel and fuel rod or guide tube explicitly modeled (using symmetry). A fully detailed one-eighth core model includes 1388 subchannels and 1388 rods. Another intermediate model with 51 channels was developed to study the adequacy of the basemodel for preserving the hot subchannel local conditions. The intermediate model is not used for design or licensing calculations.

The NuScale core basemodel is depicted in Figure 3-4, while the 51-channel intermediate model is in Figure 3-5. In both figures, the channel numbers are indicated in white and the rod numbers are indicated in red. All subchannels in the one-eighth core are explicitly treated in the fully-detailed model, thus a diagram is not provided. In the figures, the smaller circles are the fuel rods and the larger circles are the guide and instrument tubes.

{{

}}2(a),(c)

Figure 3-4. Diagram of 24-channel basemodel

{{

}}2(a),(c)

Figure 3-5. Diagram of 51-channel (lump51) model

The 24-channel basemodel must calculate a conservative MCHFR for all radial nodalization configurations to satisfy the constraints of the methodology. This modeling method is further justified from parametric sensitivity analysis in Section 6.4 in which radial geometry nodalization is confirmed to accurately maintain the hot channel flow field (void fraction, mass flux, and crossflow profiles vs. elevation) and results in a conservative MCHFR. Benchmarking was performed for high pressure, low pressure, low power and flow, high power and flow, and high radial peaking augmentation.

Additionally, it is confirmed in Section 6.4 with the MCHFR results and hot subchannel local conditions that combining channels more than a few rod rows from the hot channel has a negligible impact on the flow field and the MCHFR.

In summary, there are three radial nodalization models that are used and are referred to in the remainder of this report. These all model one-eighth of the full core and are listed below:

- Basemodel (24-channel licensing model)
- Lump51 (51-channel intermediate model)
- Detailed (all 1388 subchannels in the one-eighth core are modeled in full detail)

The 24-channel basemodel is used for most steady-state and transient licensing calculations. The fully detailed model is used for some transient calculations. The 51-channel intermediate model is used for studies and sensitivity analyses performed in this topical report.

3.7.2 Axial Nodalization

The axial nodalization for the subchannel model is critical to capturing the variation of the flow field throughout the height of the fuel assembly. Axial node size directly impacts the calculated MCHFR. Axial node size is selected to capture the flow field accurately without unnecessarily complicating the calculation.

The leading edge and downstream edges of the spacer grids are explicitly modeled, allowing the pressure drop for the spacer grid to be modeled within a single axial level. As a result of the spacer grid being modeled as a single axial level, an elevation discrepancy between the cell center and grid location is not possible. Limiting MCHFR values typically occur between the fourth and fifth spacer grid because the enthalpy of the water and the clad surface heat flux are both near maximum values. Using this experience, the region of CHF interest is modeled with smaller axial nodes.

This modeling method is justified based on a parametric sensitivity analysis in Section 6.4 in which different axial node sizes within the “CHF region” are assessed. This sensitivity analysis demonstrates that the nodalization increments are sufficiently small to calculate the flow field and the MCHFR. The “CHF region” of interest is between the fourth spacer grid and the end of the active fuel length. MCHFR is of no concern above the top of the active fuel. The other levels within the active fuel region are split into equal increments between the edges of the defined spacer grids. Smaller axial nodes are used at the inlet of the model and exit of the model to allow proper resolution of the flow field prior to or just after a pressure drop. A reasonable aspect ratio of less than three is maintained, which is utilized to ensure that axial flow remains dominant in the subchannel analysis. Figure 3-6 shows the axial nodalization scheme for all models.

{{

}}2(a),(c)

Figure 3-6. Axial nodalization diagram for subchannel basemodel (not to scale)

3.8 Boundary Conditions

In VIPRE-01, the boundary conditions define the conditions of a problem for a steady-state subchannel analysis, and also provide the starting condition requirements for a transient subchannel analysis. The boundary and operating conditions required by VIPRE-01 for NuScale applications are:

- inlet flow rate (mass flux)
- inlet enthalpy or temperature
- system pressure
- bypass flow
- power
- exit pressure (assumed uniform if not specified)
- inlet and exit crossflows (assumed zero if not specified)

The core boundary conditions for VIPRE-01 are consistent with the methodology described in References 8.2.2 through 8.2.6 and discussed below. As defined in Reference 8.2.10, the boundary conditions input into VIPRE-01 are based on a once-through linear process (i.e., no iteration or coupling of codes).

3.8.1 Inlet Flow

The NuScale RCS loop is a single-phase natural circulation loop designed to minimize flow resistances. At operating power conditions (>15 percent RTP), the Reynolds number in the core of the RCS is well within the forced convection turbulent flow range, making correlations like Dittus-Boelter appropriate for approximating the surface heat transfer coefficient. One of the primary inputs to subchannel analysis is RCS flow. The NRELAP5 code is used to perform this calculation. NRELAP5 was used to predict flow as a function of power during the NuScale integral effects scaled RCS loop. This assessment confirms the ability of NRELAP to accurately calculate the buoyancy-driven flow rates due to the lower density in the riser compared to higher density in the downcomer. The pressure head, caused by the height of the higher density water column, is ultimately balanced by the loop hydraulic flow losses, primarily through the steam generator and core, creating a unique steady-state flow condition at each power level. NRELAP5 is appropriate for calculating natural circulation flow as input into subchannel analysis (Reference 8.2.10).

The mass flux boundary condition is input as the core inlet flow, meaning all bypass mechanisms are already accounted for. The subchannel methodology accounts for all forms of bypass flow before input into VIPRE-01. The flow boundary condition is the system flow from a transient analysis simulation (Reference 8.2.10). The primary system

flow for the NuScale design accounts for the total amount of flow that circulates through the nuclear steam supply system (NSSS). With the natural circulation design of the NuScale reactor, the flow rate is dependent upon the pressure drop from the steam generator and reactor core.

VIPRE-01 is used with the RECIRC numerical solution option even though positive flow (upward flow) is maintained within the core when applying this methodology. Although the core pressure drop and the exit enthalpy can be input in place of the inlet mass flow rate boundary condition, this is not a requirement or necessarily the optimum technique for VIPRE-01 simulation of the NuScale core. Using the inlet flow rate boundary condition provides a more direct way of accounting for bypass flow and the treatment of flow imbalance-related uncertainties.

3.8.2 Inlet Enthalpy

The inlet enthalpy may be uniform or prescribed for each channel separately. If the inlet flow is subcooled or superheated, the inlet temperature may be specified in lieu of enthalpy, and may be either uniform or specified for each channel. As a PWR, the NuScale design has subcooled inlet flow; therefore, inlet temperature (uniform) is utilized. The exit enthalpy is not needed unless the exit (top of the bundle) flow reverses.

3.8.3 System Pressure

The system pressure is used to define saturation conditions uniformly throughout the core. VIPRE-01 assumes the flow is incompressible and that the momentum pressure drop is small compared to the system pressure. The pressure drop for the NuScale fuel assembly is on the order of {{ }}$^{2(a),(c),ECI}$ psid, with a nominal system pressure of 1850 psia. As defined in Table 3-1, an example CHF correlation minimum valid pressure is 300 psia.

Therefore, even at the minimum values of the applicable pressure ranges, a change in pressure as a result of the fuel pressure drop would have negligible impact on the fluid properties. As a result, the treatment of system pressure as uniform is valid for NuScale conditions. In the event future CHF correlations use significantly different pressure ranges, a restriction of this methodology defined in Section 7.2.1 is that the fuel pressure drop must be significantly less (by a factor of 10) than the minimum system pressure evaluated with the uniform pressure option or the local pressure drop option must be used in VIPRE-01.

3.8.4 Bypass Flow

For subchannel calculations, the maximum bypass is conservative because this results in less coolant flow in the reactor core available for heat transfer. The following bypass flow paths for bypass are considered:

- reflector block cooling channels (for the purpose of cooling the heavy reflector)

- gap between the heavy reflector block and the core barrel
- fuel assembly guide and instrument tubes

3.8.4.1 Reflector Cooling Channel Bypass

The heavy reflector surrounding the core has several cooling channels that allow flow to pass through the reflector. A conservative calculation results in a recommended example value of 4.5 percent for the reflector cooling channel bypass fraction for steady-state and transients.

3.8.4.2 Flow Leakage between the Heavy Reflector and Core Barrel

It is permissible for flow to occur between the heavy reflector and the core barrel to bypass the core. This region is expected to decrease in area due to thermal expansion from the reflector cooling block. Because the flow in this region is relatively stagnant and there are conservative assumptions in the other bypass fractions, this bypass flow path is treated as negligible.

3.8.4.3 Guide Tube and Instrument Tube Bypass

The maximum amount of bypass flow fraction for the guide tubes and instrument tube for the fuel assemblies is an input into subchannel analysis. An example value for this report is a maximum bypass flow of 4 percent, which includes a 1 percent uncertainty. NRELAP5 uses core bypass flow as an initial condition for Non-LOCA analyses as discussed in Reference 8.2.10.

3.8.4.4 Total Bypass

The total bypass flow assumed in the subchannel analysis is 8.5 percent of total system flow at full power conditions. This is considered to be a maximum value and conservative with respect to MCHFR.

3.8.5 Inlet Flow Distribution

In general, the core inlet flow distribution is dependent on the geometry of the RCS loop, including the lower core plate and bypass flow paths. The bypass flow paths for the NuScale design are discussed in Section 3.8.4. There are flow inlets for each of the 37 assemblies in the core, similar in nature to the current fleet of PWRs. However, the natural circulation design of the NuScale reactor is unique in that the flow distribution is dependent on the buoyancy-driven flow rate and unique vessel design in which flow in the lower plenum changes direction. The core inlet flow distribution is not constant and changes based on power level, axial and radial power distribution, and core average temperature. An example value for this report is a 5 percent inlet flow maldistribution applied to the fuel assembly that contains the hot rod.

The modeling technique used for the inlet flow distribution is justified from a parametric sensitivity analysis provided in Section 6.4.4, which shows that the 5 percent lower inlet flow for the assembly containing the hot channel results in a conservative MCHFR. Additionally, it is shown that if the inlet flow fractions surrounding the hot channel are also reduced by 5 percent, a conservative MCHFR results. This is because the reduced flow in channels around the hot subchannel lessens the turbulent mixing effects in a conservative manner. The parametric study included a flow maldistribution that penalized the hottest fuel assembly up to 15 percent, which showed that the resulting effect on MCHFR is negligible.

3.8.6 Inlet Temperature Distribution

The core inlet temperature distribution is an important boundary condition for steady-state and transient subchannel analysis that is dependent on NSSS design geometry. The NuScale design is unique in that the integral steam generator has the primary flow on the shell side and the secondary flow through the tubes. The helical tube columns for both steam generator hot legs encircle the entire reactor core barrel. This means that azimuthally around the entire core barrel, the primary fluid will see heat transfer from both steam generator tube sets. This design feature removes any asymmetric steam generator influences for the coolant through the downcomer into the core inlet.

A calculation for the RCS loop was performed on the core inlet temperature distribution for several power levels and power distributions in the NuScale NSSS design. This showed that the largest deviation in core inlet temperature for any case was approximately 0.24 degrees Fahrenheit from the average inlet temperature. The impact of this slight inlet temperature non-uniformity on MCHFR is negligible. The fluid on the inner surface of the core barrel is heated from the core and reflector resulting in the peripheral assemblies seeing slightly higher inlet temperatures.

For this reason, it is acceptable that the core inlet temperature distribution is evaluated with a uniform inlet temperature distribution for all AOOs, infrequent events, design-basis accidents, and special events.

3.9 Turbulent Mixing

The turbulent mixing model within VIPRE-01 accounts for the exchange of enthalpy and momentum between adjacent subchannels due to turbulent flow. The coefficient for turbulent mixing and the turbulent momentum factor are the two inputs needed for this model. This mixing model is incorporated into the energy and momentum equation, which is dependent on the amount of turbulent crossflow per unit length. The turbulent crossflow, *w′* is calculated as:

$$\mathrm{w}' = \mathrm{ABETA} \cdot \mathrm{S} \cdot \overline{\mathrm{G}} \qquad \text{Eq. 3-5}$$

where

ABETA = turbulent mixing coefficient

S = Flow gap width

$\overline{G}$ = Average axial mass flux velocities among adjacent subchannels

The value of ABETA is determined from thermal mixing tests in Reference 8.2.7. An example value for NuScale is {{ }}$^{2(a),(b),(c),ECI}$. This value is fuel-design specific; however, this is a conservatively low value representative of non-mixing vane grid fuel assemblies. This modeling value is further justified from parametric sensitivity analysis in Section 6.4.

The turbulent enthalpy mixing parameter used in VIPRE-01 is derived for subchannels. Lumped channels, as used in the VIPRE-01 basemodel (Section 3.7), require a reduction in the mixing coefficient ABETA. The mixing coefficient ABETA is reduced by dividing the standard subchannel value, {{ }}$^{2(a),(b),(c),ECI}$, by the ratio of the centroid distance to the fuel rod pitch. This equates to non-lumped subchannel gaps having the {{ }}$^{2(a),(b),(c),ECI}$ mixing coefficient while the lumped channels are reduced in proportion to the centroid distance differences for each gap. The effect from reducing the turbulent mixing coefficient has negligible impact in the lumped basemodel because the value of ABETA is small already.

The value for the turbulent momentum parameter is not measured and is justified based on parametric sensitivity analysis in Section 6.4. The sensitivity study results demonstrate that NuScale basemodel is not sensitive to this value and {{ }}$^{2(a),(c),ECI}$ is suitable.

3.10 Radial Power Distribution

The radial power distribution for the core is characterized by $F_{\Delta H}$, which is the enthalpy rise hot channel factor describing the integrated rod power for a particular rod. This peaking parameter is variable depending on the cycle design as the exposure, fuel composition, burnable poison loading, operational history, and thermal-hydraulic conditions all affect the power distribution. As a result, the location of the peak $F_{\Delta H}$ fuel rod changes throughout an operating cycle.

A one-eighth core basemodel is used in the subchannel analysis as discussed in Section 3.7. To decouple the use of a cycle-specific, or time-in-life, dependent radial power distribution, a conservative power distribution for a NuScale core that accounts for the worst radial power distribution during the cycle is used. The expectation is that this limiting radial power distribution will be bounding for all fuel cycles, although the analysis for each cycle loading pattern will confirm this.

The radial power distribution for use in steady-state analyses and most transients is the conservatively determined artificial distribution, using lumped rods in the 24-channel, 52-rod basemodel described in Section 3.7. The radial power distribution will remain constant throughout the transient for subchannel analysis.

3.10.1 Static Standard Review Plan Section 15.4 Analyses

Standard Review Plan Section 15.4 addresses events that are caused by reactivity and power distribution anomalies. The radial power distribution for static nuclear analysis control rod calculations will remain the same as that derived for the basemodel with one slight modification. An $F_{\Delta H}$ augmentation peaking factor for asymmetric radial peaking is applied to all the rods within the central limiting assembly, which preserves the peak-to-average value. The assembly furthest from the central limiting distribution is reduced by a factor to maintain normalization of power. The equations for increasing and lowering the radial power in the central limiting and renormalized assemblies are shown below.

$$F_{\Delta H}^{CENTER} = F_{\Delta H} * F_{aug} \quad \text{Eq. 3-6}$$

$$F_{\Delta H}^{OUTER} = F_{\Delta H} - 0.1875 * (F_{aug} - 1) \quad \text{Eq. 3-7}$$

The augmentation factor is determined by nuclear analysis as the ratio of the change in $F_{\Delta H}$ from post-event to the initial condition. The relative increase in $F_{\Delta H}$ captures the peaking increase from control rod motion and is applied to the basemodel limiting central assembly as a multiplicative factor.

3.10.2 Time-Dependent Standard Review Plan Section 15.4 Analyses

The fully-detailed basemodel is used for transients where the power distribution changes over time and is severely skewed from that determined in Section 3.10.6. The radial power distribution used in the subchannel analysis is that *at the time of peak core power* as determined from an event-specific nuclear analysis. Using the power distribution at the time of peak power is conservative because it is used throughout the entire transient with the transient fluid boundary conditions.

3.10.3 Enthalpy Rise Hot Channel Factor

The core design has imposed a design limitation on the peak value of $F_{\Delta H}$, and therefore the highest value for any fuel rod at hot full power has been limited to 1.50, for example. The core operating limit peaking factor is increased for lower power levels, allowing a linear increase to a HZP value of 1.65, for example.

$$F_{\Delta H}^{OL} = 1.5 + [0.15 * (1 - P)] \quad \text{Eq. 3-8}$$

where P = % rated thermal power/100

The subchannel methodology bounds any radial power distribution that occurs in the core prior to any AOO, infrequent event, or accident. By using the 95/95 acceptance criterion on the hot rod, the hot rod for the radial power distribution is set to the core operating limit peaking factor (or design limit) dependent upon the initial condition.

Uncertainties associated with $F_{\Delta H}$ are accounted for in the subchannel analysis as an increase on the core operating limit value. The uncertainties accounted for are measurement uncertainty related to the instrumentation used for monitoring, which is detailed in Section 3.12.2, and engineering hot channel uncertainty, which is detailed in Section 3.12.4. Increases in $F_{\Delta H}$ peaking for rodded configurations are also included as detailed in Section 3.10.5.

For cases evaluated at partial power levels, the $F_{\Delta H}$ distribution in the central assembly is increased by a factor that is the ratio of the partial power core operating limit value divided by the HFP value. The central assembly is peaked using Eq. 3-6 and an outer assembly is reduced using Eq. 3-7 to preserve total power.

An additional requirement is imposed on the $F_{\Delta H}$ design limit for the core design: the peak $F_{\Delta H}$ rod for any assembly must not occur on the peripheral row. This requirement stipulates that the hot subchannel does not occur on the outer row because the outer row would be influenced by direct crossflow from the annulus channel between assemblies. This channel is not accurately simulated in the CHF tests and, therefore, not a valid channel for CHF to occur. Even though VIPRE-01 is capable of simulating these local conditions, there is no testing to benchmark or develop a valid CHF correlation for this geometry. Therefore, to ensure a crossflow neighboring channel remains within a tested configuration, the core design constraint is required.

3.10.4 Radial Flux Tilt

Radial flux tilt is a condition in which the power is not symmetric between azimuthally symmetric fuel assemblies and can have an impact on thermal margin because the plant is allowed, by operational limits (albeit for a limited time), to continue operation. For this brief period, an assembly can have a higher $F_{\Delta H}$, which is accounted for in the safety analysis. The design enthalpy rise peaking factor safety limit inherently accounts for the radial tilt, expressed as:

$$F_{\Delta H}^{OL} = F_{\Delta H}(1 + T_q) \qquad \text{Eq. 3-9}$$

where $F_{\Delta H}^{OL}$ = Operating limit enthalpy rise design peaking factor

$F_{\Delta H}$ = Design limit for core design calculations

T_q = azimuthal tilt.

The core operating limit $F_{\Delta H}$ design limit is met while accounting for radial tilt in nuclear analysis of any fission product (i.e., xenon) transients that disturb symmetric power peaking. The subchannel analysis, therefore, requires no additional methodology to account for radial tilt.

3.10.5 All Rods Out Power-Dependent Insertion Limit Enthalpy Rise Hot Channel Factor

The enthalpy rise hot channel factor is defined for all rods out (ARO) conditions. However, the safety analysis evaluates allowable operating conditions. The power-dependent insertion limit (PDIL) allows the core to be at 100 percent rated power with control rods inserted to the PDIL. With the enthalpy rise hot channel factor defined as an ARO maximum value, an additional peaking factor must be accounted for on the hot rod for PDIL-to-ARO augmentation peaking differences.

A nuclear analysis calculation determines the value for PDIL-ARO augmentation for all power levels. The subchannel analysis uses a bounding single value to be applied for use at every power level; a simplification such that only one value is applied as the factor for all transients, including those that initiate at partial powers. This value is cycle-specific based on loading patterns and control rod worths. However, a bounding value is used and must be confirmed by cycle-specific nuclear analysis calculations. As an example, the NuScale subchannel analysis will use a value of 4 percent as the PDIL-ARO $F_{\Delta H}$ augmentation factor for rodded operating conditions.

3.10.6 Determining the Bounding Radial Power Distribution

The radial power distribution for the subchannel basemodel is a bounding distribution expected to be used for future core designs that maintain a similar shuffle or loading pattern. This modeling method is justified from parametric sensitivity analysis in Section 6.4.2 which confirms that the radial power distribution far removed from the hot subchannel has a negligible impact on the MCHFR results. Therefore, the use of a radial power distribution with the hot rod at the design peaking limit is sufficient for any distribution in a cycle-specific core.

The bounding radial power distribution used in the basemodel and most transients is not representative of the actual core conditions, and as a result, the determination of MCHFR for meeting the acceptance criterion is only applicable for the hot rod and subchannel. Thus, the purpose of the bounding radial power distribution is to capture the hot subchannel flow conditions, which are dependent upon the surrounding crossflow neighbor channels. A “flat” power distribution is one in which nearly all the rods provide similar power, and therefore, flow conditions and this power distribution limit the amount of turbulent mixing and diversion crossflow in the hot subchannel. This is conservative for thermal margin calculations.

The approach for the subchannel methodology is to set the hot rod at the core operating limit value at HFP as discussed above in Section 3.10.3, as well as accounting for the factors discussed in Sections 3.10.4 and 3.10.5. The power distribution for an assembly

may be characterized by its “peak-to-average” ratio, which is the maximum $F_{\Delta H}$ rod in an assembly divided by the average $F_{\Delta H}$ for the assembly. A value closer to unity denotes a flat power distribution. Because a cycle-specific core design does not specifically have a distribution that has $F_{\Delta H}$ at the core operating limit value, a spectrum of peak-to-average $F_{\Delta H}$ values for each assembly throughout the cycle exposure in the equilibrium cycle design is utilized to inform a bounding distribution.

This method generates several thousand values. Assembly average relative power fraction values that were less than a minimum threshold (1.1 as an example) are filtered out because of the low assembly power. Taking into consideration the flattest peak-to-average ratio for the assemblies of interest and the distribution of assembly maximum $F_{\Delta H}$ values in relation to the core operating limit, a peak-to-average ratio for the limiting assembly of {{ }}$^{2(a),(c),\ ECI}$ was selected.

This value is then used to set a “slope” for the artificial power distribution of the core. As an example, the hot rod is set to {{ }}$^{2(a),(c),ECI}$ (example core operating limit of 1.5 with root sum of squares (RSS) uncertainty applied) and the remaining rods within the one-eighth central assembly are reduced by the slope and distance is from the hot rod. This approach keeps the hotter rods around the hot rod, which reduces the amount of potential turbulent mixing and diversion crossflow from the hot subchannel. The other assemblies are gradually reduced in power to preserve the power generated. This means the lumped rods that are used to represent partial or full assemblies must take into account the total number of rods when used in preserving the total power. An example radial power distribution for the subchannel basemodel is presented in Figure 3-7.

In this model the peak rod contributes heat to both the guide tube subchannel as well as the unit subchannel. The hot channel will sometimes shift between both channel types, depending on the transient. Such shifts are due to the specific thermal-hydraulic conditions, such as the heat rates, mass flux, and single-phase or two-phase conditions.

{{

}}2(a),(c),ECI

Figure 3-7. Example artificial radial power distribution for the basemodel

3.10.7 Deterministic Radial Power Distribution

The bounding radial power distribution used in subchannel analyses is further adjusted from the one developed in Section 3.10.6. The distribution in Figure 3-7 is adjusted by employing the penalties for $F_{\Delta H}$ measurement uncertainty (Section 3.12.2) and $F_{\Delta H}$ engineering uncertainty (Section 3.12.4) on the hot rod. These penalties include the measurement uncertainty on the radial peaking as well as the engineering uncertainty for enthalpy rise. The radial power distribution prior to applying uncertainty penalties retains the conservative peak-to-average for the hot assembly, while the rod in which MCHFR is determined accounts for the applicable uncertainties. In order to accommodate the slight increase on the hot rod, a small reduction in the peripheral assembly is performed to maintain normalization.

Uncertainties for the $F_{\Delta H}$ measurement and $F_{\Delta H}$ engineering tolerance factors are applied to the hot rod using RSS methods. Each of the uncertainties are composed of independent parameters from one another, which allows the use of RSS application to the hot rod uncertainties. The total uncertainty for the hot rod is {{ }}2(a),(c),ECI percent, with the calculation provided as an example.

{{

}}2(a),(c),ECI

3.10.8 Axial Power Distribution

The axial power distribution is the distribution of power along the height of the active fuel. This power peaking is expressed as a core-average (F_Z^{Core}), rod-specific (F_Z^{Rod}), or assembly-specific shape (F_Z^{Assy}). Thus, the axial power distribution is highly variable, dependent upon the core design, exposure, and power history. The axial power peaking is not a strictly imposed limitation on the core design, but it is inherently limited by the total peaking factor (F_Q) core operating limit.

The subchannel methodology incorporates a CHF-limiting axial power shape for use in all steady-state analyses as well as most transients. The FSAR Chapter 15.4 events in which control rods are withdrawn during the transient are not included because the axial flux shape used for this analyses is determined as part of the analysis of the event. The CHF-limiting shape is developed from a nuclear analysis calculation of bounding and representative power shapes for various configurations:

- core cycle exposure
- control rod configuration (ARO, PDIL, alignment uncertainty)
- xenon distribution
- core thermal-hydraulic conditions

These power shapes consider possible scenarios that can occur for normal and anticipated operation within an AO window. On the order of 4,000 shapes are evaluated. The calculation ensures that the axial power shapes developed for each power level are within the AO window. Figure 3-8 presents an example AO window that is considered the analytical limit for the core. This window will envelope an AO window placed in the COLR that would account for instrument delays and uncertainties. The axial power shapes developed from the nuclear analysis may or may not violate the AO analytical limit; however, operating limitations for axial offset will ensure that the analytical AO limit is protected. This means that any AOs beyond the bounds of the axial offset window need not be considered in the nuclear analysis power shapes analysis and subsequently are not applicable to the subchannel analysis.

The NuScale design does not incorporate a reactor trip based on measured AO, either in a CHF trip or direct AO trip. This means that the AO operating limits with any associated time requirements before action, must be enveloped by the analytical limit AO window used for the safety analysis. The neutron monitoring system algorithm that calculates AO is nonsafety-related for the NuScale design. Without a reactor trip on AO deemed a necessity, it was determined that operating limits can be monitored periodically with non-safety equipment, such as the in-core detectors.

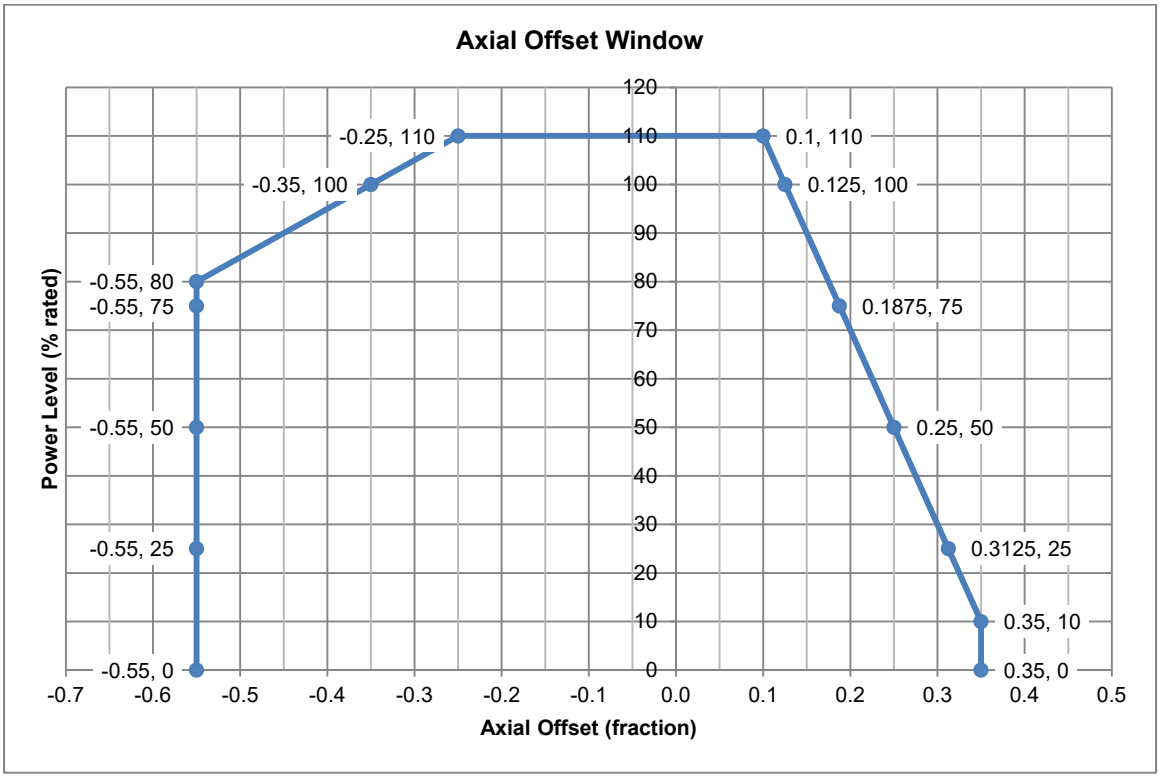

Figure 3-8. Example axial offset window

From the many potential permutations of the core-average axial power shape from the nuclear analysis, the CHF-limiting shape is obtained. Example power shapes generated by this process are presented in Section 6.1 (Figure 6-1). Subchannel analysis is sensitive to the axial power shape, with a top-peaked axial power shape being more limiting with respect to CHF than a bottom or mid-peaked shape for the same magnitude of peaking. For each power level (in appropriate increments), power shapes are provided with an emphasis on ensuring the shapes reach the widths of the AO window. Axial offset alone is not an indicator for the axial power shape, as the magnitude of F_Z and the axial elevation contribute to the MCHFR. Therefore, the axial power shape is selected as the one that results in the lowest MCHFR using the basemodel. A subchannel analysis calculation determines the limiting axial power distribution for use in steady-state and most transient analyses from which a bounding axial power shape for each provided power level is ascertained.

The CHF limiting axial power shape (based on core-average axial power) is sufficient to be used for most transient analyses. For the transients that are not characterized by control rod motion (non-SRP 15.4 events), the core-average axial power shape does not deviate significantly from the shapes already considered within the power shapes analysis, and therefore the subchannel limiting axial power shape is appropriate. The combination of the core-average axial power shape of initiating power level with the conservative radial power distribution and the system flow boundary conditions provides a conservative MCHFR calculation.

3.10.9 Standard Review Plan Section 15.4 Analyses

For the events involving control rod motion (SRP Section 15.4), an event-specific nuclear analysis is performed to determine control rod worth, radial power distribution ($F_{\Delta H}$ augmentation factor), and axial power distribution. The initial conditions for control rod motion transients start from the edges of the AO window as the edge of the window is a permissible condition prior to an event actuation. If a permissible normal operation power swing results in the core-average axial power shape at the edges of the window, then once rods leave the core for an uncontrolled bank withdrawal (UCBW) or single rod withdrawal, the core-average axial power shape has the potential to go beyond the AO limits. The potential to exceed the AO limits is for a brief amount of time; however, this would be unanalyzed space from the axial power shapes analysis. This is the reason for the necessity of nuclear analyses to provide axial power shapes in addition to radial peaking augmentation (if applicable) and control rod worth information for specific transients. Detail is provided Sections 4.7 to 4.10 as to what axial power shape is assumed for control rod reactivity design-basis events.

3.11 Numerical Solution

As discussed further in Section 5.1.2, VIPRE-01 has three solution schemes that are available for use: direct solution, iterative solution, or the RECIRC solution. The direct and iterative schemes require the flow to always be positive (upward), while the more robust RECIRC solution can accommodate localized reverse flow. The RECIRC solution has the ability to analyze more complex flow fields. For NuScale subchannel applications, all licensing calculations are performed using the RECIRC solution. The verification and validation for the mathematical modeling and application have been performed in References 8.2.2 and 8.2.3.

3.11.1 Convergence Criteria and Damping Factor Guidance

Recommendations on convergence criteria are provided in the VIPRE-01 User's Manual (Reference 8.2.3). These are recommendations from the code developers and are useful in most calculation conditions; however, severe inlet flow asymmetry (e.g., due to flow blockages) can prove difficult for the code to meet. Damping factors are used on the tentative solution for the axial and lateral flow field in the RECIRC calculation scheme and can impact the convergence of the solution. Simply "tuning" the value of the damping factors to enhance convergence is not desired.

This modeling method using damping factors is justified from parametric sensitivity analysis in Section 6.4.8 in which the applicability of the default convergence criteria and damping factors to be used for NuScale applications is demonstrated. The default values are applicable to use for most applications encountered for the NuScale core. For calculations in which the solution will not converge using these recommended values, the analyst is allowed to lower the damping factor value for the failed criterion (axial or transverse flow) using ACCELF or DAMPNG. Generally when decreasing the value of the damping factors, the user will need to increase the number of forced external iterations to ensure a false convergence is not reached.

3.12 Subchannel Uncertainties and Biases

There are several types of uncertainties that must be accounted for in subchannel safety analysis calculations, including those from analysis method, physical manufacturing design inputs to the model, and operating conditions. Each of these is discussed in more detail to explain how each is accounted for within the subchannel analysis methodology.

The application of uncertainties in the NuScale subchannel methodology is deterministic, which means that the uncertainty associated with a parameter is applied in the conservative direction without regard for the combination nature of uncertainties. This uncertainty treatment involves applying an uncertainty value in the conservative bias direction. For subchannel analysis, the direction and location of the biases implemented is indicated in Table 3-2.

3.12.1 Uncertainty in Analysis Method

The uncertainties in the analysis method consist of computer code uncertainty and CHF correlation uncertainty. The computer code uncertainty pertains to the effects from using distinct discretization in axial and radial nodalization and the approximations in the governing constitutive equations. Comparisons of code predictions to actual data for the condition ranges of application will usually eliminate the need for a penalty. Most of this test validation work has been performed in VIPRE-01 in Reference 8.2.5. Additional validation work is performed in benchmarking VIPRE-01 to COBRA-FLX, an approved subchannel analysis code owned by AREVA with an approved SER as described in Section 5.8. The results of the benchmarks demonstrate that VIPRE-01 results are in good agreement with the AREVA COBRA-FLX code for conditions anticipated for NuScale applications. The axial and radial nodalization used in Section 3.7 are the bases for the benchmark and it is determined that no penalty is needed for a computer code calculation bias.

The CHF correlation uncertainty is measureable and is included as part of the NuScale-specific CHF correlation within the 95/95 MCHFR safety limit (Section 3.3). CHF correlations are developed from the local conditions derived from a simulated subchannel model of the CHF test, using the subchannel software. This means that the uncertainty in the VIPRE-01 computer code is included in the CHF correlation itself. This has been the conventional industry practice and is also the approach for NuScale.

The CHF correlation development inherently accounts for VIPRE-01 code uncertainties and the 95/95 CHF design limit accounts for uncertainty in the CHF correlation. For this reason, no additional penalties for uncertainty in analysis method are added to the subchannel calculations.

3.12.2 Uncertainty in Operating Conditions

The operating boundary conditions that are input into the subchannel analysis must account for measurement uncertainty. Values for these uncertainties are based on the instrumentation used for monitoring, and therefore are plant specific. The measurement uncertainties consist of those related to:

- core power
- system flow
- core inlet temperature
- core exit pressure

The correct accounting for measurement uncertainties is an interface between the systems and subchannel calculations, and care is taken to ensure the uncertainty is applied once to either the systems or subchannel calculations.

The core inlet flow boundary condition accounts for the appropriate bypass flow that is not available for heat transfer. The bypass flow values used for the safety analysis are determined as analytical maximums rather than best-estimate values. The type of bypass flows applicable for NuScale core subchannel analyses are described in Section 3.8.4. The operating conditions uncertainties are listed in Table 3-2.

The measurement uncertainties for $F_{\Delta H}$ and $F_{\Delta H}^{U}$ are included as a multiplier on the hot channel $F_{\Delta H}$, that results in a direct increase in enthalpy rise and heat flux. The $F_{\Delta H}$ measurement uncertainty is based on the safety-related excore detectors used for protecting the core operating limit. The design limit $F_{\Delta H}$, as discussed in Section 3.10.3, does not include uncertainties. Because this is a measured value, the measurement uncertainty for this value must be applied. An example uncertainty associated with this instrumentation is a value of {{ }}$^{2(a),(c),ECI}$ percent.

3.12.3 Uncertainty in Physical Data Inputs

Physical data that is used in the VIPRE-01 subchannel analysis has an uncertainty and must be accounted for in a thermal margins analysis because small deviations from nominal are allowed. The following items applicable to VIPRE-01 and subchannel calculation methods are:

- enthalpy rise engineering uncertainty ($F^{E}_{\Delta H}$)
- heat flux engineering uncertainty (F^{E}_{Q})
- LHGR engineering uncertainty (F^{E}_{LHGR})
- radial power distribution uncertainty
- fuel rod bowing and assembly bowing uncertainties
- core inlet flow distribution uncertainty
- core exit pressure distribution uncertainty

Each uncertainty is further described in detail for how it is accounted for in the VIPRE-01 model and calculation or post-processing thermal margin determination in the following subsections.

3.12.4 Enthalpy Rise Engineering Uncertainty

The enthalpy rise engineering uncertainty ($F^{E}_{\Delta H}$) is a penalty factor that is applied on the hot channel to account for fabrication uncertainties related to allowable manufacturing tolerances. This factor is also referred to as the enthalpy rise hot channel factor. The enthalpy rise hot channel factor accounts for variations in pellet diameter, pellet density, enrichment, fuel rod diameter, fuel rod pitch, inlet flow distribution, flow redistribution, and flow mixing.

In the NuScale subchannel methodology, this factor is calculated in two parts. The rod power component of the hot channel factor, which accounts for fuel stack length and uranium loading uncertainties ($F^{E}_{\Delta H1}$), was calculated to be {{ }}$^{2(a),(c),ECI}$ percent, based on the methodology defined in Reference 8.2.9. The $F^{E}_{\Delta H2}$ hot channel factor is dependent upon the VIPRE-01 modeling and two-phase flow correlations when used in combination with the variation in subchannel flow area due to fuel rod pitch and outer diameter variations. To determine the flow area reduction factor, the change in MCHFR for several different operating conditions was investigated.

The biased sensitivity consisted of reducing the rod pitch by the tolerance, and increasing the fuel rod and guide tube outer diameters by their respective tolerances. This reduces the flow area by the largest amount and the impact on MCHFR is calculated. To determine the actual value of $F^{E}_{\Delta H2}$, the same benchmark sensitivities are re-run with nominal geometry and only the hot rod $F_{\Delta H}$ peaking factor increased by a

factor to result in the same MCHFR as the biased case. The results of the $F^{E}_{\Delta H2}$ flow area reduction factor was calculated to be {{ }}$^{2(a),(c),ECI}$ percent. Because these two factors are derived using different methods, combining them using the RSS method is appropriate.

For the $F_{\Delta H}$ hot channel factor uncertainty, the penalty factor is directly applied to the hot rod, which directly impacts the channel enthalpy rise and MCHFR. The $F_{\Delta H}$ radial power distribution for the licensing basemodel incorporates this factor. For the transients that use the fully-detailed model and pin-by-pin $F_{\Delta H}$ distribution, the hot channel factor for enthalpy rise is applied to the hot rod, independent of the location.

3.12.5 Heat Flux Engineering Uncertainty

The heat flux engineering uncertainty (F^{E}_{Q}) factor is a penalty factor that accounts for the manufacturing uncertainties that affect the local heat flux. This factor is often referred to as the heat flux hot channel factor. The heat flux hot channel factor is affected by variations in fuel enrichment, pellet density, pellet diameter, and fuel rod surface area. This is an interface with the fuels discipline, in which a value of {{ }}$^{2(a),(c),ECI}$ percent for F^{E}_{Q} is utilized as an example based on a RSS method for the fuel enrichment, pellet density, fuel rod outer diameter, and fuel pellet cross-sectional area. The methodology utilized to calculate this value is defined in Reference 8.2.9.

For application of the F^{E}_{Q} uncertainty, the heat flux from the conduction model is penalized. There is no method to account for this in VIPRE-01 that directly impacts only heat flux. Therefore, it is applied as a direct penalty to the VIPRE-01 calculated MCHFR. The equation for incorporating this penalty is shown in Section 3.3 as an increase on the CHF 95/95 limit, resulting in a reduced margin to the MCHFR calculated with VIPRE-01.

3.12.6 Linear Heat Generation Rate Engineering Uncertainty

The LHGR hot channel engineering uncertainty factor (F^{E}_{LHGR}) is similar to F^{E}_{Q}, with the only difference being that the fuel rod outer diameter is excluded because the fuel rod outer diameter does not significantly impact the LHGR of the pellet. A value of {{ }}$^{2(a),(c),ECI}$ percent for F^{E}_{LHGR} is used, based on the methodology defined in Reference 8.2.9. The F^{E}_{LHGR} hot channel factor is applicable for peak linear heat generation rate (PLHGR) FCM calculations. This uncertainty factor is used in Eq. 4-2 as a penalty on the PLHGR (Section 4.5.1).

3.12.7 Radial Power Distribution Uncertainty

The radial power distribution uncertainty is related to the software used to simulate the detailed core power distribution. This modeling method is justified from parametric sensitivity analysis in Section 6.4.2 in which different power distributions of the NuScale core demonstrate that rod powers a few rod rows beyond the hot rod or channel have a negligible impact on the MCHFR. With the hot rod in the subchannel model placed at the

design limit $F_{\Delta H}$ (see Section 3.10.6), and any nuclear analysis code uncertainty accounted for in the nuclear analysis calculation, no radial power distribution penalty needs to be applied.

For the asymmetric events that utilize augmentation factors, the relative change in $F_{\Delta H}$ is applied to the hot rod and no bias or uncertainty on results is required. For calculations that use a pin-by-pin or fully-detailed power distribution for $F_{\Delta H}$, it is conservative without additional factors in that the peak rod conditions are conservative. The sensitivity study of conditions far away from the hot rod having negligible effect on MCHFR remains true; thus, a radial distribution uncertainty does not need to be applied.

3.12.8 Fuel Rod and Assembly Bow Uncertainty

Fuel rod bow is a negative impact to CHF due to the flow area reduction in the hot channel flow. Fuel rod bowing may occur throughout the fuel cycle and is dependent upon fuel assembly geometry and upon both assembly and cycle exposure.

The necessity of a rod bow penalty is determined for MCHFR and LHGR applications. For MCHFR, a penalty is derived based on the magnitude of gap closure and the reduction in CHF to reach failure in bowed rods. Rod bowing effects on LHGR are dependent upon the nuclear analysis effects in the bowed locations due to a change in the fuel-to-moderator ratio.

The penalties for rod bow and assembly bow are applied externally to VIPRE-01 calculations by increasing the CHF analysis limit that is used for margin comparison, as defined in Section 3.3. The penalty is applied and determined based on the highest exposure of any assembly that is in the core, regardless of where the hot channel MCHFR occurs.

A rod bow total penalty of 3 percent is used in this report. The methodology utilized to calculate this value is defined in Reference 8.2.9. Thus, the CHF analysis limit used for thermal margin evaluations biases the 95/95 MCHFR design limit by the penalty for potential rod bowing.

Assembly bow is caused by different forces and results in in-core distortions of the fuel. The large flux gradients along the outer assemblies where the fresh fuel is loaded increase the potential for assembly bow to occur. Evaluation of assembly bow for NuScale is performed by the fuels discipline. As defined in Reference 8.2.9, CHF penalties are only applied for rod bow and not assembly bowing. Therefore no penalties for assembly bowing are considered in CHF calculations.

3.12.9 Core Inlet Flow Distribution Uncertainty

The core inlet flow distribution is discussed in Section 3.8.5. For the subchannel analysis methodology, a 5 percent inlet flow distribution uncertainty is applied to the hot or limiting assembly. The open lattice of the NuScale core allows flow redistribution to occur for inlet flow imbalances which mitigates the MCHFR impact.

3.12.10 Core Exit Pressure Distribution Uncertainty

A core exit pressure distribution uncertainty is not appropriate for NuScale subchannel analyses because the open upper plenum design allows pressure equalization to occur. Additionally, the boundary condition for core exit pressure is located in the lower riser branch component, where pressure equilibrium is expected. Therefore, no uncertainty for core exit pressure distribution is appropriate.

3.13 Bias and Uncertainty Application within Analysis Methodology

A summary of the uncertainties and biases applied in the subchannel methodology, including the definition of the conservative bias directions, is provided in Table 3-2. For a parameter designated to “Increase,” the actual values calculated by the system analysis are increased by the bias factor and vice-versa for parameters designated to “Decrease”.

Table 3-2. Example methodology parameter biases for subchannel MCHFR analyses

Parameter	Conservative Bias Direction	Example Bias	Location Applied	Reference Section
reactor power measurement uncertainty	increase	{{	subchannel or transients input	Section 3.12.2
core inlet flow rate uncertainty	decrease	}}$^{2(a),(c),ECI}$	subchannel or transients input	n/a
core exit pressure	increase	case dependent	subchannel or transients input	Section 3.12.2
core inlet temperature	increase	+5 °F	subchannel or transients input	Section 3.12.2
core inlet flow distribution uncertainty	decrease	5%	VIPRE-01 model hot assembly	Section 3.12.9
$F_{\Delta H}^{U}$ uncertainty	increase	{{	hot rod peak (RSS)	Section 3.12.2
$F_{\Delta H}$ rodded peaking	increase		limiting assembly peak	Section 3.10.5
$F_{\Delta H}^{E}$ engineering uncertainty	increase	}}$^{2(a),(c),ECI}$	hot rod peak (RSS)	Section 3.12.4
$F_{\Delta H}$ augmentation for asymmetric events	increase	varies, %	hot rod peaking	Section 3.10.1
F_{Q}^{E} engineering uncertainty	increase	{{ }}$^{2(a),(c),ECI}$	CHF analysis limit	Section 3.12.5
fuel rod bowing	increase	3%	CHF analysis limit	Section 3.12.8
fuel assembly bowing	n/a	none	n/a	Section 3.12.8
radial power distribution uncertainty	n/a	none	n/a	Section 3.12.7
core exit pressure distribution	n/a	none	n/a	Section 3.12.10

*This bias is indicated as {{ }}$^{2(a),(c),ECI}$ because the minimum design system flow rate accounts for uncertainties throughout the RCS loop. System transient simulations include the implementation of the flow loss uncertainties.

The boundary conditions input uncertainties in Table 3-2 are applied on the values calculated from transient analysis and subsequently input into VIPRE-01. The hot rod peaking is inclusive of all $F_{\Delta H}$ peaking factors, including the augmentation factor if needed. The basemodel radial power distribution includes all peaking values, except the augmentation factor. The inlet flow distribution penalty is applied to the entire assembly containing the hot rod. The basemodel already includes the Figure 3-7 distribution from Section 3.8.5; however, the fully-detailed model case will need to be applied appropriately as discussed in Section 3.8.5. The penalties that are applied on the CHF design limit use Eq. 3-4.

3.14 Mixed Core Analysis

Subchannel analysis with VIPRE-01 modeling is appropriate to evaluate MCHFR for multiple fuel types. VIPRE-01 can simulate the flow and enthalpy distribution with varying fuel types by accurately modeling the axial drag and form losses, as well as diversion crossflow from different fuel types next to one another in the core. It is expected that only hydraulically similar fuel assemblies will be placed in the core to avoid significant crossflow among assemblies. A difference in turbulent mixing coefficients among multiple fuel types in the core has a direct impact on MCHFR and flow redistribution.

For a full core of the same fuel design, the axial nodalization will be the one described in Section 3.7.2. However, a mixed core of multiple fuel types may require finer axial nodalization to capture the resolution of the flow redistribution due to geometric and hydraulic effects.

A mixed core analysis is performed by evaluating combinations of neighboring assemblies. VIPRE-01 is used to model multiple fuel types by applying each respective radial and axial geometry applicable for each fuel type. Hydraulic characteristics are correctly captured using VIPRE-01. The outcome of the mixed core analysis is a MCHFR penalty that is applicable for the transition core.

Transition core penalties are applied for all subchannel analyses in which multiple fuel types are present within the core. The transition core penalty is defined in terms of CHF points. The transition core penalty is applied as an increase on the CHF analysis limit discussed in Section 3.4. The subchannel analysis for the reload cycle consists of a single fuel type (fresh or new design), with the VIPRE-01 calculated MCHFR compared to the CHF analysis limit increased by the transition core penalty for margin to CHF considerations.

3.15 Methodology-Specific Acceptance Criteria

The subchannel analysis methodology has been developed to conservatively model the NuScale core and calculate thermal margins for SAFDLs, and, if necessary, determine the number of fuel failures as input for radiation dose assessments. This ensures the NuScale core specifically meets the requirements of General Design Criterion 10. The following methodology acceptance criteria must be satisfied to ensure a valid MCHFR is calculated by VIPRE-01.

- The local mass flux, equilibrium steam quality, and pressure at the location and time of minimum CHFR is within the CHFR correlation applicability range.
- The MCHFR must occur in a channel geometry for which there is a valid CHF correlation (a unit cell containing 4 fuel rods, or guide tube or instrument tube cell each of which contain three fuel rods).

- The MCHFR must not occur on a peripheral subchannel of an assembly when using the fully-detailed one-eighth core model.
- The hot channel must occur adjacent to the hot rod.
- The hot rod from the VIPRE-01 MCHFR calculation must be the rod with the highest $F_{\Delta H}$ peaking factor.
- The VIPRE-01 calculation must satisfy all selected convergence criteria for the results to be considered valid. If convergence cannot be met with the selected default values or methods described in Section 3.10.1, justification must be provided to ensure that the relaxed acceptance criterion does not result in invalid results. If the calculation still does not converge, an assessment of the calculated results needs to be provided to prove acceptability.
- The MCHFR calculations must be performed using the VIPRE-01 RECIRC numerical solution.

4.0 Transient-Specific Applications Methodology

The methodology described throughout Section 3.0 is applied as a standard technique for modeling all steady-state calculations and transients. In most cases the FSAR Chapter 15 transients are analyzed using the base model discussed holding the bounding radial and axial power distributions constant during the event. This is because the radial and axial power distributions are conservatively developed and many of the Chapter 15 accidents do not perturb the axial and radial power distributions. For example, the radial power distribution used bounds the predicted peak power distribution throughout the entire operating cycle, considers the insertion of CRAs, and includes uncertainties. This was previously discussed in Section 3.10.3. For accidents that start at lower than full power, the peak rod power is increased in accordance with Eq. 3-8.

In addition, as discussed earlier, the radial power distribution surrounding the hot rod channel is conservatively flat to minimize energy exchange out of the hot channel. The axial power distribution as discussed in Section 3.10.8, is determined by selecting the most limiting axial flux shape based on analysis of thousands of power shapes generated by operation over the full range of allowed operating conditions. This analysis includes different control rod positions, cycle exposures, xenon distributions, and core thermal hydraulic conditions. A bounding axial flux shape is selected at 5%, 25%, 50%, 75%, and 100% power. In analyzing the transient events these bounding shapes are assumed to exist throughout the event. For many events such as increases or decreases in heat removal, there is no significant change in axial or radial power distribution. However, for events that involve CRA motion, an event-specific neutronics analysis is performed to determine the peak radial power distribution and then the bounding radial power distribution is augmented such that the peak rod power matches the peak from the event-specific analysis. The axial power shape from the event-specific neutronics analysis is used if it is more conservative than the bounding axial power shape.

The transient analysis code NRELAP5 calculates pressure, flow, inlet temperature, and power level as a function of time during the transient. For each event, several limiting cases are identified for further analysis and then the VIPRE-01 subchannel basemodel is used to determine the subchannel flow, enthalpy, quality, void fraction, and CHFR for all of the limiting cases. As discussed in the next section, the CHFR is calculated based on a steady state CHF correlation.

In summary, the typical subchannel analysis entails changes to the basemodel for the following:

- Boundary conditions from transient analysis such as NRELAP5, including uncertainties and biases as discussed in Section 3.12.2 and shown in Table 3-2.
- Limiting axial power shape that corresponds to the initiating power level.
- Radial power distribution augmentation (if necessary) for events that initiate at partial powers using Eq. 3-6 to determine operating limit peaking. The initial peaking value

is determined as a ratio relative to the HFP core operating limit value. This augmentation factor is applied to all rods in the central assembly using Eq. 3-4 (which preserves the peak-to-average ratio for hot assembly) and reduced from the outer assembly using Eq. 3-5. This augmentation factor is only in reference to the increased allowable peaking for the core operating limit value, which is different than the augmentation factor for SRP Section 15.4 events.

It should be noted that for the example cases in this topical report, the full power $F_{\Delta H}$ is 1.50, and after including uncertainties it is {{ }}$^{2(a),(c),ECI}$. The limiting 95/95 CHFR is 1.17 but with the penalties that are applied is 1.262.

Table 3-3 summarizes the axial and radial power distribution assumptions used in the Chapter 15 analyses. Each of the event categories are discussed in more detail in subsequent section.

Table 3-3. Radial and Axial Power Distribution Assumed in Chapter 15 Event Subchannel Analysis

Event	FSAR	Radial Shape	Axial Shape
Decrease in FW Temperature	15.1.1	Bounding	Bounding
Increase in FW Flow	15.1.2	Bounding	Bounding
Increase in Steam Flow	15.1.3	Bounding	Bounding
Open SG Relief	15.1.4	NA	NA
Steamline Break (pre-trip)	15.1.5	Bounding	Bounding
Steamline Break (post-trip)	15.1.5	No Return to Power	No Return to Power
Loss of Containment Vacuum	15.1.6	Bounding	Bounding
Loss of Electrical Load	15.2.1	Bounding	Bounding
Turbine Trip	15.2.2	Bounding	Bounding
Loss of Condenser Vacuum	15.2.3	Bounding	Bounding
Closure of MSIV	15.2.4	Bounding	Bounding
Steam Pressure Regulator Failure	15.2.5	Bounding	Bounding
Loss of AC Power	15.2.6	Bounding	Bounding
Loss of Normal Feedwater	15.2.7	Bounding	Bounding
Decrease in Flow	15.3	NA	NA
CRA or Bank Drop	15.4.3	Bounding + Augmented	Shape at pre-event power
CRA Misalignment	15.4.3	Bounding + Augmented	Shape at pre-event power
Single CRA Withdrawal	15.4.3	Bounding + Augmented	Shape at post-event power
Fuel Assembly Misload	15.4.7	Bounding + Augmented	Shape at full power
Uncontrolled Bank Withdrawal – at power	15.4.2	Bounding at pre-event power	Shape at pre-event power
Uncontrolled Bank Withdrawal – at zero power	15.4.1	Bounding for zero power	Bounding for zero power
Rod Ejection	15.4.8	Separate Methodology	Separate Methodology
Increase in RCS Inventory	15.5	Bounding	Bounding
Decrease in RCS Inventory	15.6	No CHF Assessment	

Additionally, presented in this section are transient-specific methodologies, such as fuel rod conduction and changes required to the general methodology for unique event applications.

4.1 Transient Critical Heat Flux Applications

The NuScale CHF correlations are developed from steady-state data. For subchannel safety analysis calculations, a correlation is used in FSAR Chapter 15 design-basis event analyses to determine the MCHFR as a function of time. From a phenomenological standpoint, steady-state CHF data is conservative relative to transient CHF data because there is a lag time in creating the vapor blanket on the fuel rod surface. This was supported by the NuScale CHF testing described in Reference 8.2.7, which showed that transient CHF was higher than steady-state CHF. Steady-state CHF correlations are appropriate to use in subchannel application space for transient MCHFR calculations.

The above conclusion has been confirmed by industry experience. The VIPRE-01 applications validation manual (Reference 8.2.5, Section 6.7) describes work that was performed to exercise the CHF calculation in transients using steady-state CHF correlations. The SER (Reference 8.2.1) also focused on this application. The results of the review indicate that transient CHF for power ramps, flow, decay, and mild depressurization are higher than steady-state CHF. The use of steady-state CHF correlations in most transients will conservatively predict the CHF.

For the CHF calculations using VIPRE-01 for depressurization events, the rate of depressurization must be below 20 psi/second. This is based on Reference 8.2.1 (Section 2.3) in which a study was performed for a 20 psi/second depressurization. The results showed that transient CHF was bounded by using a steady-state CHF correlation. Therefore, as a methodology restriction the CHF calculation cannot be performed for depressurizations faster than 20 psi/second for NuScale applications.

4.2 Time Step Size

Specification of VIPRE-01 transient forcing functions for transients obtained from the system analysis code (transient discipline interface) must have an adequate time step resolution. Specifically, fast transients require that simulations need to be performed in sufficiently small time steps to capture the CHF behavior adequately.

4.3 Courant Number

NuScale uses the existing VIPRE-01 correlations for subcooled boiling, which necessitates ensuring that the Courant number SER requirement ($N_c > 1$) is satisfied (Section 2.3). The Courant number (N_c) is defined as the axial mass velocity times the time derivative, where u is the axial flow velocity, Δt is the transient time step, and Δx is the axial node size.

$$N_c = u\frac{\Delta t}{\Delta x} \qquad \text{Eq. 4-1}$$

Selection of the transient time step is achieved on a case-by-case basis based on the axial nodalization and the coolant velocity to ensure that the SER requirement is satisfied.

VIPRE-01 uses an implicit solution technique, which precludes any time step limitations relative to numerical stability. The subcooled models used in VIPRE-01 that are of the profile-fit type, however, may affect the state of convergence through their dependence on the selection of transient time step. Satisfying the condition $N_c > 1$ decreases the likelihood of the transient solution failing to converge in boiling transients. If convergence problems occur, the calculation terminates and sufficient information is output by VIPRE-01 to allow the user to determine the state of convergence of each simulation.

4.4 Fuel Rod Conduction Model Methodology

The modeling of the fuel rod is important because the conduction of the heat through the fuel rod directly impacts thermal margin to CHF for transients. The heat flux is a function of the conductivity of the fuel pellet, the pellet-to-clad gap conductance, and the clad thermal conductivity. The clad conductivity does not change significantly during transients, however, the fuel conductivity and gap conductance both change with exposure and during transients and must be accounted for. The gap conductance changes due to the presence of fission gases in the rod and also due to changes in the size of the gap due to rapid changes in power. If the gap conductance decreases the heat flux decreases (MCHFR increases) and the fuel centerline temperature increases. If the gap conductance increases, the heat flux increases (MCHFR decreases) and the fuel centerline temperature decreases. The same relationship applies to the fuel pellet conductivity. These impacts are taken into account in the fuel conduction methodology. For transient CHFR calculations, typically a conservatively high fuel conductivity and gap conductance is assumed to maximize heat flux (and reduce MCHFR). For transient fuel temperature calculations, the opposite typically occurs, namely a low gap conductance and low fuel thermal conductivity is assumed. These effects are not particularly significant for slow transients, but can be important for faster transients where the heat flux lags the power increase in the fuel. Because of the opposite directions of conservatism for MCHFR and fuel temperature analyses and variability of the bias directions, all transients are analyzed with both bounding high and low heat transfer inputs, with the most limiting used for licensing analysis

The fuel rod heat transfer for safety analysis calculations is performed using VIPRE-01, which uses a one-dimensional conduction model for the fuel rod, starting from the centerline of the fuel pellet outward to the cladding surface. The VIPRE-01 conduction model was approved for licensing calculations in the original generic VIPRE SER based on comparisons to fuel performance codes. To ensure that the VIPRE-01 fuel conduction calculations are conservative this methodology requires that the entire range of possible

time-in-cycle parameters are evaluated using the COPERNIC fuel performance code, including exposure, uranium enrichment, gadolinium enrichment, gap conductance, and fuel density. The VIPRE-01 model is calibrated to ensure that it produces conservative temperatures for each fuel design.

In VIPRE-01, the key component of interest is the fuel rod heat flux, which is used for determining the flow and enthalpy distribution, and also in calculating the MCHFR to ensure thermal margin to the cladding integrity. The fuel rod heat flux is dependent upon the stored energy in the fuel rod. The simplified options in VIPRE-01 to control the predicted temperature are: (1) power peaking within the radius of the pellet, (2) fuel theoretical density, and (3) gap conductance.

Calibration of VIPRE-01 fuel temperature predictions to the fuel performance analyses is performed for the fuel average, fuel surface, and cladding surface temperatures for each cycle. Fuel-design specific calibration results in temperature predictions that are conservative for MCHFR. The conservative bias for MCHFR is a high initial temperature of the fuel as well as a high gap conductance. This allows the amount of heat in the fuel to be conservatively high and transferred to the coolant the fastest.

As the subchannel analysis determines MCHFR on the hot rod, the basis for the temperature benchmark is made on the hot rod at each time in life. At the beginning of cycle (BOC), the hot rod will represent the core operating limit $F_{\Delta H}$ peaking with a representative axial peaking shape. At the end of cycle (EOC) exposure, the hot rod peaking will be conservative based on the least exposure, meaning the $F_{\Delta H}$ peaking value will remain high. Realistically, the hot rod would change locations gradually throughout the cycle; however, using the operating limit peaking throughout the cycle is conservative. The EOC condition for material properties is conservative for exposure-dependent effects.

In summary the fuel conduction methodology is:

1. Compare VIPRE-01 calculated fuel temperatures to COPERNIC over the full range of cycle operating conditions and calibrate VIPRE-01 if necessary.

2. For each transient use both high and low heat transfer inputs, with the most limiting input and results reported for licensing analysis.

4.5 Fuel Centerline Melt

A SAFDL, if exceeded, results in fuel failure due to fuel pellet overheating, also referred to as FCM. This SAFDL must be precluded for all AOOs and evaluated for all other FSAR Chapter 15 design-basis events. The FCM limit is evaluated by either a steady-state LHGR protection limit or a peak fuel melt temperature limit, depending on the transient. The steady-state LGHR limit applies to most transients for NuScale, as they are slower progressing events that do not require Doppler reactivity to end the transients. Fast transients, those which result in a power increase in the form of a pulse

in which the heat flux lags and are Doppler inhibited, are treated and analyzed differently.

The FCM calculations performed for each transient are also evaluated for MCHFR because some transients initiate at a lower power level and may not reach a high peak power, but that power change may be severe enough to be limiting for FCM.

By definition, if the PLHGR or peak hot spot fuel centerline temperatures are below the FCM limit, then no fuel failure will occur.

4.5.1 Steady-State Fuel Centerline Melt Analysis

The fuel performance code and applied methodology for determining the fuel melt curves is an interface in which a steady-state FCM limit is provided. It is a functional limit used to ensure fuel melting does not occur for all types of fuel present in the core and provided in the form of a 'kW/ft' linear heat rate value that is based on rod histories for the applicable core design.

The melt limit for design-basis events that are mitigated by a reactor trip are generically treated as steady-state limits because the neutron power of the fuel rod internally and the heat flux escaping are in near-equilibrium. Because the neutron power and heat flux are coupled for reactor trip events, the FCM limit may be protected by a PLHGR calculation. The LHGR calculation accounts for the total peaking in the core, and using the transients discipline interface (such as NRELAP5), the calculation accounts for peak power throughout the transient. The equation to determine the PLHGR is:

Eq. 4-2

$$\mathrm{PLHGR}\left(\frac{\mathrm{kW}}{\mathrm{ft}}\right) = \frac{\mathrm{Q_{peak}}}{\mathrm{N_{Assy}} \cdot \mathrm{N_{rods}} \cdot \mathrm{L_{activefuel}}} * \mathrm{F_{\Delta H}^{OL}} * \mathrm{F_{PDIL-ARO}} * \mathrm{F_{\Delta H}^{U}} * \mathrm{F_{aug}} * \mathrm{F_Z} * \mathrm{F_{LHGR}^{E}} * \mathrm{F_{rod\_bow}} * \left(\frac{1000\mathrm{kW}}{\mathrm{MW}}\right)$$

where

Q_{peak}	=	Peak power for transient, in MW.
N_{Assy}	=	Number of assemblies in the core
N_{rods}	=	Number of fuel rods within each assembly
$L_{activefuel}$	=	Heated length of the core, in feet.
$F_{\Delta H}^{OL}$	=	Operating limit enthalpy rise peaking factor at HFP. If the peak power is below full power, the enthalpy rise peaking factor is increased using the operating limit peaking equation in Section 3.10.3 for the peak power.

$F_{PDIL-ARO}$	=	Rodded enthalpy rise peaking augmentation factor to account for the peaking increase from PDIL-to-ARO control rod location (Section 3.10.5)
$F_{\Delta H}^{U}$	=	Measurement uncertainty for the radial peaking factor based on detector measurement uncertainty, which is used to meet the limitations in the COLR. (Section 3.12.2)
F_{aug}	=	Radial peaking augmentation factor for asymmetric transients
F_Z	=	Axial peaking factor for the transient peak power (Q_{peak}). This value is the highest axial peaking value that corresponds to the limiting axial power shape (power-dependent) from the axial power shapes analysis. For powers beyond 110 percent power, use of the 110 percent F_Z value is conservative.
F_{LHGR}^{E}	=	Hot channel factor for LHGR, as discussed in Section 3.12.6.
F_{rod_bow}	=	LHGR rod bow penalty augmentation. This penalty is applied if any assembly average exposure reaches a value at which the combination of uncertainties is greater than deterministic application of F_Q measurement and F_{LHGR}^{E}. The penalty augmentation is applied as (1 + $\gamma_{rod-bow}$), where $\gamma_{rod-bow}$ is the rod bow penalty.

4.5.2 Fast Transient Peak Fuel Centerline Temperature Analysis

The behavior of fast transients is significantly different than those of slow transients. Fast transient events are characterized by a rapid reactivity spike that is mitigated by Doppler feedback. The neutron power is increased dramatically in an extremely short period of time, on the order of milliseconds. A steady-state limit is not appropriate because the heat flux from the fuel rod significantly lags the increase in reactivity.

The acceptance criterion for the FCM for fast transients is based on a fuel centerline temperature rather than a linear heat generation limit. The safety limit for the FCM temperature is dependent on exposure and gadolinia enrichment.

The peak fuel centerline temperature is evaluated with VIPRE-01. Both the transient power and the peaking factors used for the MCHFR calculation are used for the hot rod, as the radial peaking and axial power shape at the time of transient peak power for the hot rod capture the total peaking of the fuel rod. The initial stored energy of all fuel rods in the core is biased to a bounding large value using conservative values of the specific heat and thermal conductivity material properties for UO_2.

Additional conservatisms used in the fuel centerline calculation are the gap conductance value and heat transfer coefficient, which are biased to bounding small values in order to reduce the rate at which heat leaves the fuel rod. The gap conductance value is biased to smaller bounding values for each exposure consistent value. The peak fuel centerline temperature is then evaluated with VIPRE-01 in a separate calculation from MCHFR and captured for all simulated time steps for the hot rod.

4.5.3 Fuel Centerline Melt Limit Margin

The amount of margin for FCM calculations using the PLHGR method for steady state is:

$$\text{LGHR margin (\%)} = \frac{\text{LHGR}_{\text{limit}} - \text{PLGHR}}{\text{LHGR}_{\text{limit}}} \times 100 \qquad \text{Eq. 4-3}$$

The margin for fuel centerline temperatures for fast transients is:

$$\text{CM margin (°F)} = \text{TEMP}_{\text{limit}} - \text{TEMP}_{\text{max}} \qquad \text{Eq. 4-4}$$

4.6 Main Steam Line Break (SRP Section 15.1.5)

The main steam line break (MSLB) transient for the NuScale design behaves differently than for traditional PWRs. An MSLB event is generally split into two phases: pre-trip and post-trip. The analysis is performed for each phase and the physics are unique for each phase.

As an example, a conventional PWR design has two secondary coolant trains each with a steam generator, although many conventional designs have four steam generators. As a result, the two steam generators are located 180 degrees from one another. When an MSLB occurs on one side, that steam generator undergoes a blowdown which increases the heat transfer from the primary fluid located inside the tubes. The unaffected steam generator remains intact and heat transfer remains constant. As the MSLB side heat transfer increases, the core inlet temperature is no longer uniformly symmetric and results in core power redistribution on the cooler inlet side. The discussion of how each phase of the MSLB is handled for traditional PWRs is discussed below.

Pre-trip: This is analyzed similarly to the other core cooldown transients (SRP Section 15.1) except that a PWR MSLB causes temperature asymmetry in the downcomer and core inlet. As a result, the core power is redistributed to the cooler inlet temperature side and a radial peaking augmentation factor is needed on the hot assembly similar to other reactivity anomaly transients (SRP Section 15.4).

Post-trip: This is a challenging transient scenario for conventional PWRs. Once the reactor trips, the worth of the control rod insertion must assume that the worst rod is stuck out. Therefore, once the reactor coolant entering the core is cooler, the core can become re-critical. The control rods alone might not provide enough negative reactivity, thus a safety-related boron injection system can be used to mitigate the return to power. Even though the power is much lower than normal operation, the concentration of the power in the location of the stuck control rod can challenge MCHFR limits. To evaluate MCHFR for this event, standard local condition CHF correlations are not used; CHF correlations that were specifically developed for rod bundles at low pressures are used.

The challenges faced by traditional PWRs are removed by inherent design features for the NuScale reactor. A brief discussion of MSLB event sequence is provided below:

Pre-trip: The NuScale steam generator design as discussed in Section 3.8.6 prevents an MSLB on one side from resulting in core inlet temperature asymmetry. Therefore, this phase can be analyzed as a typical CHF analysis.

Post-trip: The control rod design and worth provides enough negative reactivity to keep the reactor subcritical with the worst rod stuck out and without any boron injection. Reactor coolant temperatures following a MSLB event remain high enough that a potential return to power is of no concern in the immediate term. A generic long-term cooling analysis will address the potential return to power with temperatures nearing the reactor building pool temperature. The power at this time will be only be from decay heat. The CHF SAFDL for the long-term cooling analysis will be met using NRELAP5 correlations and methods.

In summary, the conventional PWR design MSLB methodology required special treatment and analysis methods. The NSSS design features for the NuScale reactor make the MSLB event similar to other SRP 15.1 cooldown events, and therefore allows use of the same subchannel analysis method.

4.7 Asymmetric Core Transients (SRP Section 15.4)

For most design-basis events, the core radial power distribution is not perturbed and the radial power distribution defined in Section 3.10 is appropriate because it bounds the core design. However, for SRP Section 15.4 events analyzed with subchannel methodology, the radial power distribution undergoes redistribution due to control rod movement. With the radial peaking redistribution, the subchannel radial power distribution must be modified to account for the increase.

For each event discussed in this section, a peaking augmentation factor is implemented. This factor is the maximum ratio of the post-event $F_{\Delta H}$ divided by the initial condition $F_{\Delta H}$. In each event, the radial peaking augmentation factor is calculated and applied to the basemodel peaking factor for the central limiting assembly as an increase for the entire assembly using Eq. 3-6, while reducing an outer assembly using Eq. 3-7. The use of the operating limit $F_{\Delta H}$ peaking factor for the initial power level in combination with the $F_{\Delta H}$ augmentation factor is conservative. Thus, if the event is initiated from a reduced power level, an augmentation increase in $F_{\Delta H}$ for the higher allowable operating limit peaking factor from Section 3.10.5 is applied using Eq. 3-6 and Eq. 3-7.

The axial power shape for the control rod or bank drop event is the initial power level limiting power shape. This axial power shape is more top-peaked than the core-average axial shape would be after the rod or bank has dropped. If the transient results in the core power returning to higher than the initial power level, conservatism can be removed by using the axial power shape that corresponds to the transient peak power.

4.7.1 Control Rod Misoperation: Control Rod or Bank Drop (SRP Section 15.4.3)

The control rod or bank drop occurs when a single rod or an entire bank from the control group or shutdown group drops into the core. This event is characterized by a sudden drop in reactor core power. In those instances when the rod worth is not significant enough to shut the core down (k_{eff} < 1), the constant demand of the secondary side causes a decrease in core inlet temperature, which results in a power increase at EOC because of a highly negative moderator temperature coefficient.

4.7.2 Control Rod Misoperation: Control Rod Misalignment (SRP Section 15.4.3)

The control rod misalignment is an event in which a single control rod or multiple control rod assemblies are out of alignment with the remaining rods in the control rod assembly bank. The alignment can be higher or lower than the expected rod position. A misalignment can occur because of the uncertainty in the rod position from its indicated or expected position. A limiting misalignment occurs when the core is operating at steady state, full power, with the rods inserted to the PDILs except one rod is left withdrawn. This is a postulated condition as the rod position indicators will alarm when the rods are out of alignment beyond the position uncertainty. Another postulated limiting misalignment is three of the control rods are at the ARO position and one rod is misaligned at a low power PDIL position.

The misalignments analyzed include those for control rod position uncertainty, a postulated single rod misaligned into a low power PDIL position, and the misaligned rod to the ARO position with others remaining at the full power PDIL. The postulated misalignment of the rods inserted to the PDIL but with one rod fully inserted is not a credible condition for the NuScale core. Reactor hold points will prohibit the movement of rods for that severe of a peaking distortion and is not analyzed for NuScale.

4.7.3 Control Rod Misoperation: Single Rod Withdrawal (SRP Section 15.4.3)

The single rod withdrawal transient occurs when a control rod is set at the PDIL and is postulated to withdraw. The single rod withdrawal adds positive reactivity and the core power increases. The core power distribution becomes asymmetric, power peaking can challenge the MCHFR SAFDL, and the reactor will trip due to high power.

The axial power distribution used in the MCHFR analysis for single rod withdrawal is the post-event core average limiting top-peaked axial power shape. The axial power shapes provided for positive AO cases are more limiting than the negative AO cases. The combination of the axial power shape and radial power distribution described above is different than the method used in Sections 4.7.1 and 4.7.2. It was determined that the combination of the conservative safety analysis limit $F_{\Delta H}$ peaking factor used with an $F_{\Delta H}$ augmentation factor to account for asymmetry with the post-event top-peaked core-average axial power distribution results in a conservative treatment. The method of using an augmentation factor to account for the peaking increase, in addition to the

conservative operating limit $F_{\Delta H}$ peaking factor, results in an $F_{\Delta H}$ more severe than would actually occur after the single rod withdrawal.

If additional margin is needed, the operating limit $F_{\Delta H}$ peaking factor can be reduced to correspond to the $F_{\Delta H}$ factor for the power level at the time of MCHFR. This can be used to replace the $F_{\Delta H}$ that corresponds to the initial condition power level. For instance, a 25 percent rated power single rod withdrawal transient may reach 85 percent rated power at the time of MCHFR. Instead of using the $F_{\Delta H}$ peaking factor for the initial 25 percent power case, the operating limit value can be changed to that of 85 percent rated power.

4.7.4 Fuel Assembly Misload (SRP Section 15.4.7)

The inadvertent loading of a fuel assembly in the incorrect location, among other possible deviations from the designed assembly, can cause power distribution anomalies from the expected core design power distribution. This infrequent event can challenge the MCHFR as well as SAFDL due to changes from designed peaking. Because this event is static, a transient calculation is not performed. Anticipated undetectable deviations in the power distribution will not affect the global RCS parameters. Therefore, thermal margins are not significantly impacted.

The spectrum of potential misload scenarios for the core and corresponding augmentation factor is determined by nuclear analysis. The misload augmentation factor is calculated as ratio of the maximum $F_{\Delta H}$ at full power after the misload to the maximum $F_{\Delta H}$ at full power.

$$F_{aug}^{Misload} = \frac{F_{\Delta H}^{Misload}}{F_{\Delta H}^{Core\_Design}} \qquad \text{Eq. 4-5}$$

where

$F_{aug}^{Misload}$ = misload augmentation factor

$F_{\Delta H}^{Misload}$ = maximum $F_{\Delta H}$ rod value for any time in cycle for after misload

$F_{\Delta H}^{Core\_Design}$ = maximum $F_{\Delta H}$ rod value for the core design

The subchannel analysis evaluates the maximum allowed augmentation factor that results in MCHFR at the CHF analysis limit. This means the MCHFR should include all penalties exterior to the VIPRE-01 calculation as shown in Eq. 3-4. The VIPRE-01 calculations use the steady-state full power boundary conditions adjusted by the uncertainties listed in Table 3-2. The axial power shape is the CHF limiting hot full power shape determined from the axial power shapes analysis.

The key result of the misload subchannel analysis is the maximum allowed radial peaking augmentation factor. Each cycle-specific nuclear analysis confirms that the maximum augmentation factor calculated is not violated.

4.8 Uncontrolled Bank Withdrawal at Power (SRP Section 15.4.2)

The UCBW transient is characterized as an increase in power from the positive reactivity addition by the control rod withdrawal. The core power increase and the mismatch with the steam demand results in an increase in core temperature and MCHFR is challenged.

The transient analysis considers a spectrum of reactivity insertion rates for the positive reactivity addition by the control rods. The power range neutron excore detectors provide high power and high flux rate core protection. For cases in which the reactivity insertion is sufficiently slow, the high pressurizer pressure and level setpoints are credited in the analysis.

A spectrum of insertion rates are evaluated with maximum and minimum reactivity feedbacks because the reactor trips and timing of the trips that mitigate the event are different. Different power levels are also evaluated to ensure the adequacy of the trip logic availability to prevent MCHFR.

For NuScale subchannel analysis, the $F_{\Delta H}$ power distribution used for the control bank withdrawal is symmetric, meaning that the power distribution developed in the basemodel is applicable. For the UCBW events that are initiated at a partial power, an augmentation factor for the increased allowable $F_{\Delta H}$ radial peaking is applied. This is performed as discussed in Section 3.10.3 using Eq. 3-6 and Eq. 3-7. The default axial power shape used is the initial core average shape, however a post-event core average limiting axial power shape may be used.

4.9 Uncontrolled Bank Withdrawal at Subcritical or Low Power (SRP Section 15.4.1)

The uncontrolled bank withdrawal at subcritical (UCBWS) or low power event is similar to UCBW at power, except the event can result in a rapid insertion of positive reactivity. This event is characterized as a fast transient as it is limited in power excursion due to Doppler feedback. This feedback limits the power of the event enough that even with delays in the module protection system, the transient is terminated by a reactor trip.

The radial power distribution is symmetric for the bank withdrawal event, meaning that an augmentation factor for power asymmetry is not necessary. However, because the operating limit $F_{\Delta H}$ peaking factor for HZP is larger than the HFP value, the power distribution must be adjusted. Additionally, at zero power, the PDIL-ARO augmentation factor is larger than at full power. Because the peak-to-average ratio used in setting the $F_{\Delta H}$ power distribution remains valid for the low power cases, a simple multiplier is used on the $F_{\Delta H}$ radial distribution for the UCBWS transient. The multiplier is performed using Eq, 3-6 and Eq. 3-7, with the augmentation value determined by accounting for the applicable peaking increase.

The axial power distribution used for the UCBWS is the CHF limiting shape for HZP from the axial power shapes analysis because this axial power shape for the initial condition of zero rated thermal power is limiting. The axial power shapes analysis uses an analytical limit on AO, and is used as the bounds to which the axial power shape may swing for zero power. A post-event core average limiting axial power shape may be used as well.

4.10 Spectrum of Rod Ejection Accidents (SRP Section 15.4.8)

Subchannel analysis of the control rod ejection accident design-basis event is described in Reference 8.2.11.

5.0 VIPRE-01 Qualification

As described in References 8.2.2 through 8.2.6, broad qualification of VIPRE-01 has been performed by the VIPRE-01 developers primarily for PWRs. This qualification work included comparisons with other subchannel codes for several PWR plants, as well as comparisons to a wide range of experimental data from single-phase and two-phase flow tests, void and quality relation data, fuel rod temperature measurements, heat transfer tests, and CHF tests. As a result of this extensive work, the code developers concluded that VIPRE-01 is applicable to thermal-hydraulic analysis of reactor cores in normal steady-state operation and off-normal transients. Additionally, the NRC has performed audit calculations with the COBRA-IV code to provide an additional comparison with VIPRE-01. These calculations concluded that VIPRE-01 is acceptable for use generically in PWR licensing analyses subject to a specific submittal. Since then, VIPRE-01 has been qualified by a number of utilities and vendors for PWR licensing applications (Reference 8.2.13 - 8.2.16).

In the following sections, a detailed review of the fundamental assumptions of VIPRE-01 modeling and correlations utilized with respect to NuScale applications are reviewed. Specifically, deviations from traditional PWR applications are assessed to ensure proper application of VIPRE-01 to the NuScale system. A thorough basis for the usage of the fuel rod conduction model is presented. A review of the void-drift phenomena and its effect on NuScale licensing applications is provided. Finally, additional VIPRE-01 benchmark calculations with the COBRA-FLX code and comparison with three experiments are presented and discussed.

5.1 VIPRE-01 Mathematical Modeling

The NuScale implementation of VIPRE-01 does not alter the fundamental computational method and solution scheme of the code. All the mathematical models selected and discussed herein were previously supplied in VIPRE-01 and were not changed by NuScale. The modeling choices described in this report were developed in a manner consistent with standard industry practice for VIPRE-01 use.

5.1.1 Conservation of Mass and Energy

As stated in Reference 8.2.2, “the basic computational method of VIPRE-01 comes from COBRA-IIIC. Both codes use the subchannel analysis concept in which a problem is divided into a number of quasi-one-dimensional channels that communicate laterally by diversion crossflow and turbulent mixing. Conservation equations of mass, axial and lateral momentum, and energy are solved for the fluid enthalpy, axial flow rate, lateral flow per unit length, and momentum pressure drop. The flow field is assumed to be incompressible and homogeneous, although models are added to reflect subcooled boiling and concurrent liquid/vapor slip. Fluid properties are functions of the local enthalpy and a uniform but time-varying system pressure with an option to add the effects of local pressure drop. Like COBRA-IIIC, VIPRE-01 uses an implicit boundary value solution that repeatedly sweeps the computation mesh, rather than a marching

solution that solves the flow field one step at a time solely on the basis of upstream information. The boundary value solution propagates flow disturbances throughout the computation mesh with no time step or axial node size restriction for numerical stability."

The following sections review the flow field model solution in VIPRE-01 (Section 2 of Reference 8.2.2) to determine if any aspects of the modeling methodology in VIPRE-01 would not be applicable to the NuScale reactor design or operating conditions.

5.1.1.1 Mixture Balance Equations

The integral balance laws (Eq. 2.1-6 through 2.1-8 of Reference 8.2.2) for mass, energy, and momentum apply to a single-component, single-phase, or two-phase mixture. The following simplifying assumptions are made in consideration of the intended applications of VIPRE-01:

- The flow is at sufficiently low speed that kinetic and potential energy are small compared to internal thermal energy (U2/2 << i so that e = i).
- Work done by body forces and shear stresses in the energy equation are small compared to surface heat transfer and convective energy transport.
- Heat conduction through the fluid surface is assumed small compared to convective energy transport and heat transfer from solid surfaces.
- The phases are in thermodynamic equilibrium, i.e., $T_l = T_v = T_{sat}$ when both phases are present. Empirical models for non-equilibrium subcooled boiling are applied later, but the basic equations still assume thermal equilibrium.
- Gravity is the only significant body force in the momentum equation $\left(\vec{F} \cong \vec{g}\right)$
- Viscous shear stresses between fluid elements are assumed small compared to the drag force on solid surfaces.
- The fluid is incompressible, but thermally expandable.

Each of seven assumptions remains valid for the NuScale design. While the design is significantly different from conventional PWRs in many respects (as summarized in Section 7.5), it remains a PWR and satisfies these fundamental assumptions characteristic of all PWRs. With respect to the thermally expandable flow assumption, this means that the density and transport properties vary only with the local temperature (enthalpy). The local pressure does not affect the properties unless the local pressure option is used. Fluid properties are computed with the local enthalpy and a uniform system pressure. This approach is valid as long as the pressure drop is small compared to the system pressure. This pressure drop versus system pressure is valid for NuScale conditions.

All of the simplifying assumptions made on the mass, energy, and momentum equations remain valid for the NuScale design and conditions, and the final equations used in VIPRE-01 can be used for analysis at NuScale.

5.1.1.2 Subchannel Formulation of the Basic Equations

The VIPRE-01 modeling manual (Reference 8.2.2) discusses the development of the equations for the subchannel control volume. The NuScale fuel design is similar in radial geometry and configuration to standard PWR fuel designs. VIPRE-01 subchannel modeling for NuScale is performed in a similar manner as for other PWRs. As a result, the basic subchannel equations remain valid for the NuScale design.

5.1.2 Numerical Solution Methodology

As described in Reference 8.2.2, VIPRE-01 has two main solution options that can be selected by the user. The normal upward flow solution (subroutine UPFLOW) resembles the one used in COBRA-IIIC, and includes both direct and iterative options. The recirculation scheme (subroutine RECIRC) was adapted from COBRA-WC and allows for reverse and recirculating flows. Each scheme iteratively solves the same set of finite difference equations and uses the same models and correlations for heat transfer, wall friction, fluid state, and two-phase flow as specified in the input.

The difference between UPFLOW and RECIRC is in the manner by which the flow and pressure fields are obtained. With the UPFLOW option, a combination of the axial and lateral momentum equations are solved for the pressure gradient in each channel at an axial level. The new channel pressure gradients are used to update the local pressures. The new lateral pressure difference is then applied to the lateral momentum to yield the crossflows. The new axial flows are computed with the continuity equation, using the flows at the last axial level and the new crossflows. With the RECIRC option, tentative axial flow and crossflows are obtained at each level with the respective momentum equations, using information from the last iteration. The tentative flows and pressures are then adjusted to satisfy continuity by a Newton-Raphson procedure.

Both UPFLOW and RECIRC yield essentially the same results. RECIRC must be used whenever axial flows are expected to become locally small or could reverse direction at any time during the simulation, or if the crossflows become large when compared to the axial flow. UPFLOW is limited to positive axial flows with crossflows less than the axial flow. The iterative and the direct solution methods in UPFLOW cannot calculate flow reversals and usually have great difficulties with low-velocity, buoyancy-dominated flow conditions, while the RECIRC solution was designed for problems of this type.

Because the NuScale design uses natural circulation, there are more conditions in which the system could encounter low-velocity axial flow. The following table compares UPFLOW and RECIRC solution methods with NuScale operating conditions. The table shows that the RECIRC method is best suited to NuScale application.

Table 5-1. Comparison of UPFLOW and RECIRC solution methods in VIPRE-01

Condition	UPFLOW	RECIRC	NuScale Conditions	Best Option
axial flow direction	positive only	positive, downward, recirculating	positive, potentially recirculating (not likely even under accident conditions)	RECIRC
axial flow velocity	forced flow	can handle low axial flow	natural circulation (lower flow rates than forced flow)	RECIRC
crossflow	crossflow << axial flow	can handle low axial flow	axial flow will still dominate crossflow, but less than standard PWRs	RECIRC
two-phase slip	no	yes	yes	RECIRC
non-equilibrium subcooled boiling	no	yes	possible at low flow, hot fuel conditions	RECIRC

5.2 Water Properties Ranges of Applicability

VIPRE-01 has available as a default the internal EPRI water properties, which are functions that fit water properties data over a wide range of applicability. The expressions for temperature and specific volume are valid from 0.1 to 6,000 psia. The expressions for specific enthalpy are valid from 0.1 psia to the critical point of 3208.2 psia, and for enthalpies from 3.0 to 1,750 Btu/lb_m. VIPRE-01 ensures the water properties functions are not used outside their range.

NuScale has a full-power nominal pressure value of 1850 psia. As defined in Table 3-1, an example CHF correlation has a pressure range of 300 to 2300 psia. Therefore, the expected range of use of VIPRE-01 is well within the valid range of the water properties internal functions. As a result, VIPRE-01 accurately predicts water properties over the entire NuScale reactor operating range.

5.3 Axial Friction Factor

In single-phase flow, the most important constitutive relations are pressure losses due to wall friction and form drag at sudden area contraction or expansions, such as spacer grids, orifice plates, or other physical obstructions in the one-dimensional flow field. The single-phase friction factor (f) used in VIPRE-01 is obtained from the formula

$$f = a * Re^b + c \qquad \text{Eq. 5-1}$$

Where Re = Reynolds number (based on channel hydraulic diameter). The constants a, b, and c have been determined from experimental data of single-phase flow in smooth tubes. Axial friction factors are fuel design-dependent and defined as a fuels interface.

5.4 Two-Phase Flow Correlations

There are 44 possible combinations of two-phase flow correlations that may be selected as VIPRE-01 input. These correlations are grouped into three major categories of (i) subcooled void fraction, (ii) bulk quality and void fraction, and (iii) two-phase friction multiplier. Not all combinations are appropriate for all problems; for a given application suitable combinations must be identified and subjected to further numerical evaluations to justify the choice.

A selection process was used to choose the set of correlations appropriate for the NuScale application. The process used to achieve this objective was:

1. Examine the NuScale reactor operating point and the various plausible reactor conditions to determine the two-phase flow regimes that are predominant during normal and off-normal conditions.
2. Determine which correlations are most applicable to the flow conditions dominant under NuScale normal and off-normal conditions.
3. Review the modeling assumptions of each correlation identified, as well as the available application knowledge base to develop several appropriate groups of correlations. This includes a detailed review of References 8.2.5 and 8.2.24 through 8.2.29.
4. Evaluate the performance and behavior of VIPRE-01 when used with each of the correlation combinations under a wide variety of possible NuScale normal and off-normal conditions.
5. Based on the analytical results, recommend one of or more correlation combinations for use in NuScale analysis.

Using this process, four combinations of VIPRE-01 two-phase flow combinations were selected for further evaluation as defined in Table 5-2.

Table 5-2. Two-phase flow correlations grouped by modeling assumptions

Combination Name	Subcooled Void Correlation	Bulk Void Relation	Two-Phase Flow Friction Multiplier
EPRI-EPRI-EPRI	EPRI	EPRI	EPRI
LEVY-HOMO-HOMO	Levy	Homogeneous	Homogeneous
LEVY-ZUBR-HOMO	Levy	Zuber	Homogeneous
LEVY-ARMA-ARMA	Levy	Armand	Armand

The four combinations of the VIPRE-01 two-phase flow models shown above were evaluated at several operating conditions that span NuScale normal and off-normal conditions, including full power, extreme elevated power (MCHFR=1), low power, low pressure, and high pressure. Displayed in Table 5-3 are results for the full-power conditions in which MCFHR is effectively identical. At more extreme conditions, larger differences in MCHFR and local conditions are observed, as expected, with the general trends consistent across all sets of operating conditions.

Table 5-3. Comparison of two-phase flow correlations at NuScale full-power conditions

Name	MCHFR	Diff. (CHF Points)	Axial Level (in)	Mass Flux at MCHFR	Equil. Quality at MCHFR
EPRI-EPRI-EPRI	{{				
LEVY-HOMO-HOMO					
LEVY-ZUBR-HOMO					
LEVY-ARMA-ARMA					}}2(a),(c),ECI

The EPRI-EPRI-EPRI combination (above) is used for licensing analysis, with the requirement that the same combination be used for the following purposes:

- CHF correlation analysis
- Mixing parameters
- Pressure loss coefficient development

A comparison of the heat transfer correlation data base range to NuScale operating conditions is presented in Table 5-6. As stated above, the data base range is just one indication of applicability. Code-to-code benchmarking, including with experimental comparison evaluations (Section 5.9) provides an additional strong basis to holistically demonstrate applicability to the safety analysis of the NuScale design. For additional perspective, the computer codes for core thermal-hydraulics simulation currently used in the industry use correlations that are approximately representative of the parameter ranges of interest for the codes. This is acceptable due in part to the comprehensive process in which the qualification of a code to the application occurs. Other than the CHF correlations, most models, such as VIPRE-01 two-phase flow correlations, are used outside the ranges characterizing their databases.

Table 5-4. Comparison of two-phase correlation database range to NuScale

EPRI Correlation	Pressure (psia)	Mass Flux (Mlbm/hr-ft^2)	Inlet Subcooling (F)	Heat Flux (Mbtu/hr-ft^2)	Equilibrium Quality (%)
subcooled void	200 - 1,000	0.0288 - 1.10	0.5 - 25.9	< 0.1	-
bulk void	600 - 2,000	-	-	-	< 45
two-phase flow friction	600 - 1,300	0.37 - 3.25	-	-	< 80
Example NuScale (Normal/Off-Normal)	1,700-2,200	0.1–0.5	94-200	< 0.029	< 20

5.5 Heat Transfer Correlations

As with flow correlations, selection of heat transfer correlations to describe the boiling curve is of key importance. Reference 8.2.3 provides a description of the heat transfer correlations available for modeling various regions of the boiling curve, consisting of single-phase forced convection, subcooled boiling, saturated nucleate boiling, transition boiling, and film boiling. There are numerous possible combinations of correlations that may be chosen for VIPRE-01. The combination of correlations presented in Table 5-5 was selected for NuScale applications.

Table 5-5. Heat transfer correlations selected for NuScale use

Boiling Curve Segment	Correlation	Abbreviation
single-phase forced convection	EPRI	EPRI
subcooled nucleate boiling	Thom+EPRI	THSP
saturated nucleate boiling	Thom+EPRI	THSP
transition boiling	Condie-Bengtson	COND
film boiling	Groeneveld 5.7	G5.7

A comparison of heat transfer correlation data base range to NuScale operating conditions is presented in Table 5-6. As noted in Reference 8.2.3, "*many of the correlations are routinely applied to conditions far beyond their data bases.*" In other words, the data base range is just one indication of applicability. As with the two-phase flow correlations, code-to-code benchmarking, including with experimental comparison evaluations (Section 5.9) presented in this report, provide an additional basis to holistically demonstrate applicability to the safety analysis of the NuScale design.

Table 5-6. Comparison of heat transfer correlation database ranges to NuScale

Correlation	Pressure (psia)	Mass Flux (Mlbm/hr-ft^2)	Heat Flux (Mbtu/hr-ft^2)	Equilibrium Quality (%)
THSP	750 - 2,000	0.77 - 2.80	<0.5	n/a
COND	-	“High Flow”	-	-
G5.7	490 - 500	0.590 - 3.0	-	10 – 90
Example NuScale (Normal/Off-Normal)	1,700 - 2,200	0.1-0.5	< 0.029	< 20

The EPRI single phase forced convection correlation (Dittus-Boelter) is traditionally utilized over a broad range of conditions.

5.6 Summary of Two-Phase and Heat Transfer Correlations Used

A summary of the correlations qualified for NuScale use as described in Sections 5.4 and 5.5 is provided in Table 5-7. For NuScale subchannel applications, all licensing calculations are performed with these correlation options. These correlations are identical with those used in the derivation of the NSP2 CHF correlation (Reference 8.2.7), which ties the prediction of CHF, along with thermal margins, to the underlying CHF test data. This further strengthens the applicability of these correlations for application to the NuScale design.

Table 5-7. Two-phase flow and heat transfer correlation selection for VIPRE-01

Correlation Option	Description
EPRI	EPRI subcooled void correlation
EPRI	EPRI void/flowing-quality correlation
EPRI	EPRI two-phase friction multiplier
EPRI	EPRI single phase forced convection heat transfer
THSP	Thom nucleate boiling correlation (plus single-phase correlation)
THSP	Thom nucleate boiling correlation (plus single-phase correlation)
COND	Condie-Bengtson transition boiling correlation
G5.7	Groeneveld 5.7 film boiling correlation

5.7 Fuel Rod Conduction Model

The VIPRE-01 conduction model solution has been verified in Reference 8.2.5. In this reference, the VIPRE-01 conduction equation results were benchmarked to test data as well as analytical problems, demonstrating that the fuel rod temperature predictions radially and axially were acceptable. To provide additional assurance that the temperature predictions for the VIPRE-01 fuel rod conduction model are suitable for NuScale applications, VIPRE-01 temperature predictions are calibrated against fuel

design-specific results from the fuel performance code COPERNIC (Reference 8.2.40) as described in Section 4.4. COPERNIC is a code specifically developed for fuel temperature calculations. COPERNIC was demonstrated to be applicable to the NuScale design in Reference 8.2.9.

5.7.1 Fuel Pellet Power Distribution

Power generation within the fuel pellet is generally lower at the centerline and outer surface of the fuel pellet. The pellet power peaking distribution is selected in such a way that it results in conservatively predicted temperature measurements when compared to fuel performance predicted values. To obtain the proper temperature resolution within the pellet, a sufficient number of radial nodes within the pellet peaking are used to ensure the fuel centerline, average, and outer surface temperatures are conservatively higher than the COPERNIC code.

5.7.2 Gap Conductance

Cladding temperatures are dependent upon the properties of the pellet-clad gap, which changes with exposure. Typically, the pellet-clad gap decreases with exposure. For transient analyses that are specific to time-in-life, the gap conductance is input to bias the cladding outer wall surface temperature high for CHF calculations. Higher gap conductance values increase the rate at which the heat is transferred to the coolant. A constant gap conductance is applied for all transient time steps and is input as a constant value axially. These approximations are conservative because the value is set to bound the hot spot clad surface temperature from fuel performance simulations. A higher gap conductance at all axial levels increases the subchannel enthalpy and reduces the MCHFR. Similarly, conservative assumptions, which may be opposite of inputs that result in conservative MCHFR, are utilized to ensure fuel centerline melt temperatures calculated are conservative.

In the NuScale natural circulation design, the flow and power are coupled, i.e. lower power results in lower flow and higher power results in higher flow. For this reason, there is no design-basis event that results in a flow reduction with power remaining high (such as loss of coolant flow for conventional PWR design). Therefore, all transient analyses that are not time-in-life reactor kinetics-specific (SRP Section 15.4) utilize EOC gap conductance values for conservatism. Chapter 15.4 events analyzed at BOC conditions use a conservatively high BOC gap conductance value that matches the fuel performance benchmark.

5.8 VIPRE-01 Code-to-Code Benchmark Analyses

AREVA NP, Inc. has recently developed the subchannel analysis code COBRA-FLX that is based on COBRA-IIIC/MIT-2 (Reference 8.2.17). This code has been reviewed and approved by the NRC for use in performing subchannel simulations in PWRs (Reference 8.2.18). Utilizing COBRA-FLX with the approved AREVA methodology for core thermal-hydraulic analysis, including selection of two-phase flow models and correlations, a

series of comparisons have been performed. This in effect shows a benchmark of VIPRE-01 to COBRA-FLX for comparable conditions.

These code-to-code comparisons are not the same as the full scale code-to-code benchmark analyses that have been performed by other VIPRE-01 users. This is because no operating plant data is yet available for the NuScale reactor. Instead, these code comparisons are intended to serve as an additional method for qualifying the selected combination of two-phase flow and heat transfer models and correlations in VIPRE-01 for the NuScale analyses.

5.8.1 Inter-Bundle Diversion Cross Flow Experiment

Reference 8.2.19 documents the Inter-Bundle Diversion Cross Flow (IBDCF) series of experiments utilized by AREVA for an experimental benchmark for COBRA-FLX. A benchmark of both the test data and comparison to the COBRA-FLX results with VIPRE-01 was performed. Specifically, VIPRE-01 was utilized to analyze the measured test data and determine the VIPRE-01 lateral resistance loss coefficient appropriate for NuScale subchannel analysis.

The purpose of this series of experiments was to evaluate VIPRE-01 predictions for crossflow to measured test data and determine the VIPRE-01 lateral resistance loss-coefficient appropriate for the NuScale subchannel analysis. Adiabatic crossflow experiments were performed by Alliance Research Center on two, identical, half-length full-scale fuel assemblies that were half-pitch in one direction. Each fuel assembly consisted of an 8x15 fuel rod array. Placed side by side, these form an 8-by-30 fuel rod array, which represented a full bundle in one direction while also modeling the bundle-to-bundle interface in the center.

The system test pressures ranged from 25 to 50 psia, with fluid temperatures ranging from 80 to 105 degrees F. The bundle velocity ratio at the inlet (V_1/V_2) was also varied for each test case and ranged from a nearly uniform flow distribution (0.95) to cases representing a complete flow blockage at one bundle inlet (0.0). Data for a total of 15 different test cases were provided for analysis in VIPRE-01. Analysis with simple models is used to validate VIPRE-01 for more complex reactor core calculations. The IBCDF benchmark calculations allow comparisons of code behavior at a fundamental level utilizing measurements from simpler geometries. This comparison gives confidence the local fluid conditions are represented adequately for NuScale applications.

In the VIPRE-01 benchmark, the IBDCF data is used in the same manner as by AREVA for the COBRA-FLX validation. Specifically, the velocity ratio information (V_1/V_2) is used as available, without separating into individual components. The velocity ratios are utilized to provide flow distribution information for the two assemblies axially considering the effects of asymmetric inlet flow conditions. Code predictions of these tests are compared to the measured data to evaluate VIPRE-01's capability to resolve the local flow field.

An evaluation of the adequacy and appropriateness of the IBDCF data was performed as summarized in Table 5-8. In this case, the test bundle half-height geometry for conventional PWR fuel matches the actual geometry of the NuScale design.

Table 5-8. Applicability of IBDCF experiment characteristic features to NuScale

IBDCF Test Feature	Applicability to NuScale
Two half bundle test apparatus	This configuration is appropriate for obtaining flow field information for the NuScale design.
Three spacer grids positioned within the mixing region	The configuration matches the NuScale fuel design which consists of two end grids and three mid-span grids. Therefore, IBDCF data represent the NuScale design with even better fidelity than conventional PWR fuel designs.
Two half-length assemblies	The IBDCF test assemblies were half the typical PWR assembly height used to justify subchannel codes for conventional PWR designs. NuScale fuel assemblies are approximately the same height as the IBDCF test assemblies. Therefore, IBDCF data represent the NuScale design with even better fidelity than conventional PWR fuel designs.
Assemblies are 15x15 lattice, two side by side (half-pitch in one direction) to form a total of 8x30 array.	The IBDCF data has been used to validate subchannel codes for analysis of PWRs with 17x17 lattice designs. Therefore, the data is equally applicable to the NuScale design.
System temperature range: 85°F -105°F	The tests were conducted under isothermal and single-phase conditions. The results have successfully been used to validate subchannel codes for the analysis of PWRs. Therefore, the data is equally applicable to the NuScale design.
Incremental pressure measurements taken along the axial length of the two bundles, the flow distribution was calculated based on the measured axial pressure profile	Mid-channel flow measurements are possible only using Doppler flowmeters. Deducing flow velocities using pressure measurements under single-phase flow conditions is accurate.
The test simulations differed from each other according to the inlet velocity ratio between the two simulated fuel bundles.	For the two half-pitch assemblies (8x15) positioned next to each other, the inlet flow rates were varied to generate crossflow. The ability of subchannel codes with generalized modeling and computational capabilities to predict crossflow was verified by using this test configuration. This validation to other similar geometries is the basis for qualification through test data. Therefore, this test configuration is also applicable and appropriate for the qualification of VIPRE-01 analysis of the NuScale design.

The VIPRE-01 two-channel input of the test geometry modeled each half-bundle as a single channel characterized by the appropriate geometry conditions. This allowed the comparison of axially averaged velocity ratios (V_1/V_2) to case-specific velocity ratios determined using the measured pressure profile. A VIPRE-01 four-channel model was also developed that modeled the each half-pitch bundle as two channels instead of one for sensitivity study purposes.

Test results obtained for both the two-channel and four-channel models with the VIPRE-01 RECIRC solution scheme show good agreement with the measured test data. The results compared were the velocity ratio between channels as a function of axial location (elevation). The VIPRE-01 results were within ±2.5 percent for all test values. Figure 5-1 and Figure 5-2 provide example two-channel and four-channel model results for the normalized velocities. Test 131 was for a near uniform inlet velocity ratio (0.95) while Test 135 was for a condition in which the flow velocity ratio was 0.0. Not all 15 test results are shown, but the trend of all analyses corresponds to the selected cases presented.

{{

}}2(a),(c)

Figure 5-1. Example Inter-Bundle Diversion Cross Flow test (131)

{{

}}2(a),(c)

Figure 5-2. Example Inter-Bundle Diversion Cross Flow test (135)

For the lateral resistance input, direct comparison of VIPRE-01 and COBRA-FLX results were made for average axial and crossflow velocities of a four-channel case (Case 147) with inlet flow for only one bundle (flow velocity ratio of 0.0). For all channels, VIPRE-01 and COBRA-FLX show excellent agreement, validating the capability of VIPRE-01 to reproduce IBDCF cases in which flow blockages exist. Figure 5-3 provides a representative example comparison of the two code results.

{{

}}2(a),(c)

Figure 5-3. Example Inter-Bundle Diversion Cross Flow test (147)

Given good results in comparison with experiment velocity profiles for nearly uniform and completely blocked flow channels, a lateral resistance loss-coefficient VIPRE-01 value of 0.5 (recommend code default) can be used for NuScale subchannel analyses.

5.8.2 Reactor Core Simulations

After flow velocity profile benchmarking with the IBDCF test, the next evaluation analyzed the larger NuScale basemodel at full-power operating conditions. First, the VIPRE-01 fluid and thermodynamic behavior with various combinations of void and two-phase friction multiplier correlations was evaluated. In this case, no existing measurements or tests are available for assessing performance. Therefore, the comparison was made to a second subchannel thermal-hydraulic code. The VIPRE-01 results were compared to COBRA-FLX results of equivalent models with the consistent flow and heat transfer correlations and the EPRI-1 CHF correlation. Because all correlation CHF calculations require a converged fluid solution from the thermal-hydraulics code, CHF calculations can be performed through post-processing. In this analysis, the CHFR results were manually calculated for COBRA-FLX because the EPRI-1 correlation is not available directly in that code.

VIPRE-01 CHFR results are minimally impacted by the combinations of correlations selected. Steady-state and transient CHFR results for both the NuScale 24-channel basemodel and 51-channel (lump51) models show excellent agreement between the two codes. The steady-state difference never exceeded 0.9 percent and the MCHFR location more than 0.2 percent relative to the calculated COBRA-FLX values. The transient case

results showed slightly larger differences at 2.2 percent overall and 1.1 percent at the MCHFR. Results for both the steady-state and transient calculations are acceptable. In addition, the location of MCHFR is consistent across all cases. Examples of axial CHFR comparisons for the 24-channel basemodel and 51-channel models (lump51) of the NuScale reactor core are presented in Figure 5-4 and Figure 5-5 respectively.

{{

}}2(a),(c),ECI

Figure 5-4. Example 24-channel steady-state model hot channel CHFR comparison

{{

}}2(a),(c),ECI

Figure 5-5. Example 51 channel transient channel model hot channel CHFR comparison

Small variances in conditions were observed in the hot channel and peripheral subchannels, specifically void fraction, pressure drop, and mass flux. This is not unexpected and, as the results shown above indicate, the effect on CHFR is small. Pressure drop across all cases was identical, regardless of the combination of correlations used or modeling geometry. Void fraction and mass flux for all cases show similar behavior until the fluid begins to void at mid-plane in the bundle. Above approximately 50 inches, VIPRE-01 predicts a slightly higher void fraction for the remainder of the bundle. Differences in void fraction are quite small, with trend and behavior in good agreement for the entire length of the channel. Crossflow from the hot channel to each of its adjacent channels was also monitored. Using various combinations of void and two-phase friction correlations does not significantly impact the agreement of the code results.

Overall, results for the VIPRE-01 cases agree in both behavior and magnitude with the COBRA-FLX predictions. This behavior is consistent in the hot channel as well as its adjacent channels (limiting locations), which are the most important locations for ensuring adequately conservative licensing analyses. Qualitatively, this code-to-code behavior comparison is further justification that VIPRE-01 can adequately predict local conditions for NuScale fuel designs and operating conditions.

5.8.3 Conclusion

The results of the code-to-code benchmarking show that VIPRE-01 and COBRA-FLX have comparable behavior. This additional code-to-code benchmark of VIPRE-01 at NuScale operating conditions advances qualification beyond what has been done previously in PWR applications. For NuScale applications, this is a demonstration of the applicability of VIPRE-01 with the selected model options, single-phase and two-phase fluid flow, and heat transfer models for steady-state and transient thermal-hydraulic calculations for the core conditions.

5.9 VIPRE-01 Experimental Benchmark Analyses

NuScale also performed benchmarking of three additional subchannel experiments not included in the VIPRE-01 test suite approved in Reference 8.2.3. This benchmarking was done to provide additional evidence that individual phenomena applicable to the NuScale analysis can be adequately predicted by VIPRE-01. The NuScale phenomena of interest are single-phase and two-phase flow, turbulent mixing, and flow redistribution. In addition, it was desired to ascertain whether these experiments would provide additional modeling recommendations. Table 5-9 provides a summary of these three experiments, including a description of the phenomena of interest.

Table 5-9. Summary of phenomena-specific tests benchmarked to VIPRE-01

Test	Test Data	Category	Phenomena	Ref.
CNEN-Studsvik 4x4 bundle isothermal flow	axial mass flux at the exit	single-phase unheated flow	turbulent mixing	8.2.31
Combustion Engineering 15x15-rod bundle inlet jetting			flow redistribution	8.2.32
Studsvik 3x3-rod bundle two-phase flow	axial mass flux & quality at the exit	two-phase heated flow	turbulent mixing	8.2.38

In the benchmarking process, the following key characteristics of VIPRE-01 comparisons to the data were specified:

- As a modeling check, the initial conditions, e.g., pressure, flow, power distribution, inlet subcooling, should be consistent with experimental conditions.
- Axial channel average void fraction or related parameter, e.g., enthalpy, is consistent with measurements.
- Evaluation of data comparisons for various unequal phase velocity options. This is used to make modeling recommendations based on the best comparison of radial distribution of subchannel void fractions at given axial locations.

The wide range of conditions of the experimental tests generally included NuScale geometry and thermal-hydraulic conditions as shown in Table 5-10.

Table 5-10. Range of experimental parameters compared to NuScale subchannel analysis

Experiment	Power Density (kW/ft)	Mass Flux (Mlbm/hr-ft^2)	Pressure (psia)	Inlet Subcooling (F)	Inlet Enthalpy (Btu/lbm)	Flow Area (in^2)	Wetted Perimeter (in)	Heated Perimeter (in)
CNEN – Studsvik 4x4	-	0.50-4.0	-	-	-	0.10-0.30	1.9	1.9
CE 15x15	-	1.5	15	-	-	0.23 -0.39	2.0	2.0
Studsvik 3x3	7.7-47	0.67-1.5	992-1,047	18-74	459-523	0.10-0.23	1.5	1.5
Experimental Range	7.7-47	0.50-4.0	15-1,047	18-74	459-523	0.10-0.39	1.5-2.0	1.5-2.0
Example NuScale (Normal/Off-Normal)	< 3.3	0.1 - 0.5	1,700 - 2,200	94 - 200	404 - 524	0.136	1.175	1.175

5.9.1 CNEN-Studsvik 4x4 Bundle Isothermal Flow

5.9.1.1 Purpose

Experiments were performed to evaluate the velocity field in a square lattice geometry typical of fuel at the Studsvik Laboratory (Reference 8.2.31). Flow distribution experiments were carried out with a 16-rod test section at single-phase subcooled conditions.

5.9.1.2 Test Loop

The test section consisted of a square channel with 16 heater rods arranged in a 4x4 array. The cross-section was designed in such a way that the corners were rounded. This results in lower flow area for corner channels than normal PWR-type corner channels. The test dimensions are provided in Table 5-11 and the test layout is shown in Figure 5-6. Experiments were carried out at inlet mass fluxes of 0.5, 1, 2, 3, and 4 Mlbm/ft^2-hr. For each condition, mass flux at the exit of the entire test section was obtained. The experiment results were presented as average mass distribution at center, side and corner locations as a function of bundle average mass flux (the normalized difference between local value and the bundle average value). Although the test section has heated rod capability, the experiments were performed with unheated conditions at ambient temperature.

Table 5-11. Studsvik 4x4 test dimensions

Description	S.I. Units	English Units
number of rods	16	16
rod diameter	15.06 mm	0.593 inches
rod length	1400 mm	55.1 inches
rod heated length	1000 mm	39.4 inches
grid location	700 mm	27.5 inches (center of test section)
grid loss coefficient	0.3	0.3
pitch	19.3 mm	0.76 inches

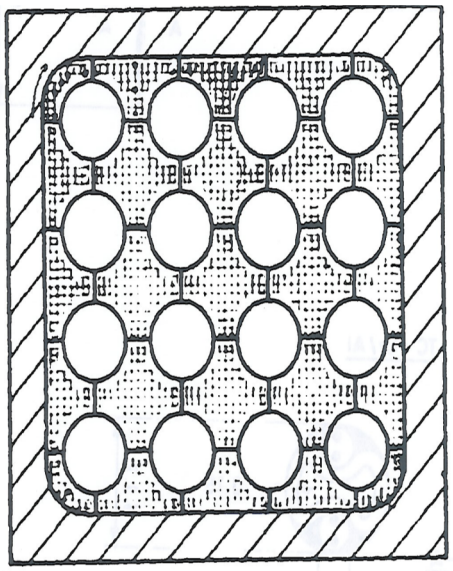

Figure 5-6. Studsvik 4x4 test layout

5.9.1.3 Key Parameters

The experiment consisted of five tests at different flow conditions specified. Measurements of flow and temperature were made at the exit of the test section using a special probe working as a pitot tube and thermocouple, capable of traversing in two radial directions. Mass velocity distribution was obtained at the exit of the test section at various radial locations for the center, side, and corner cell locations to obtain the flow velocity field.

5.9.1.4 VIPRE-01 Model

A VIPRE-01 model consisting of 25 channels with 16 rods was created to model the experiment. Mass flux at the exit of each subchannel was measured during the experiments. The data was presented as a function of average regional mass flux. VIPRE-01 calculates the mass flux at the exit of each channel modeled. Therefore, the mass flux at the center, sides, and at the corner location was calculated. The mass flux distribution is then calculated as a ratio of the difference in local mass flux and bundle average mass flux to the bundle average mass flux. Figure 5-7 shows the mass flux distribution comparison between VIPRE-01 and experimental data for the three measurement locations (center, side, and corner) for the five different test conditions.

5.9.1.5 Results

Pressure information was not available from Reference 8.2.31, so a sensitivity study was performed at different pressures. Initial calculations were performed at pressures of 20 psia, 50 psia, and 100 psia. It was observed that mass flux ratio remains essentially the same for all three pressure conditions. Hence, a pressure of 100 psia was chosen for simulation with VIPRE-01. The tests were run at ambient temperature and an inlet enthalpy of 40 Btu/lbm was used to yield a temperature of 72 degrees F.

The VIPRE-01 results compare well with the data; all predicted mass flux values fall within 5 percent of the measured data. VIPRE-01 also predicts the effect of increasing bundle average mass flux on individual channel mass flux distribution very well. Corner channel mass flux distribution is close to the data. The flow distribution calculated by VIPRE-01 for single-phase conditions shows behavior consistent with the measured experimental data. This comparison shows that VIPRE-01 is capable of making accurate predictions of mass flux. The predictions are better for corner channels than for side or center channels.

{{

}}2(a),(c)

Figure 5-7. CNEN – Studsvik 4x4 flow distribution experiment comparison with VIPRE-01

5.9.2 Combustion Engineering 15x15 Rod Bundle Inlet Jetting

5.9.2.1 Purpose

A set of experiments were performed by Combustion Engineering to examine the influence of inlet geometry on the flow in the entrance region of a PWR fuel assembly (Reference 8.2.32).

5.9.2.2 Test Loop

A 15x15 fuel assembly was utilized for the testing as depicted in Figure 5-8.

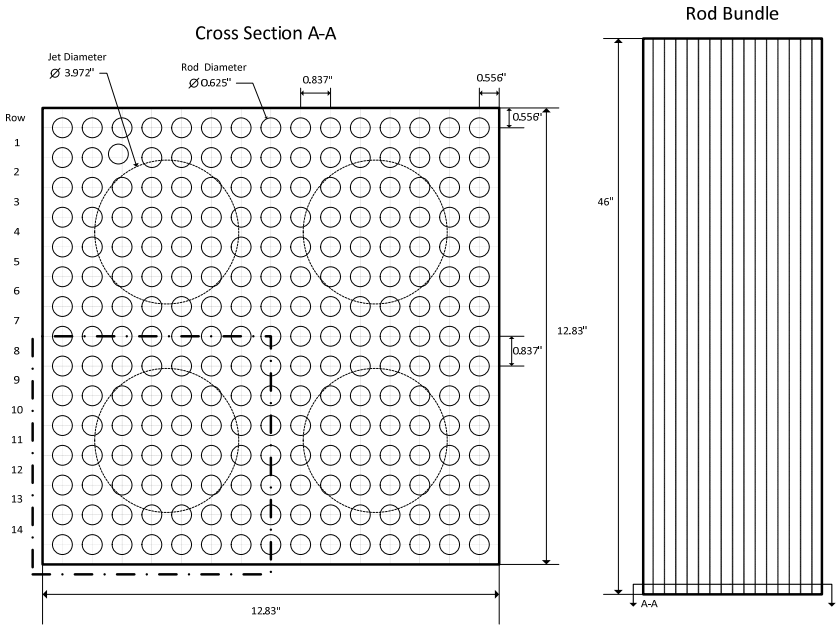

Figure 5-8. CE 15x15 rod bundle geometry

5.9.2.3 Key Parameters

Velocity profiles were obtained at various axial elevations for an inlet volumetric assembly flow rate of 2,000 gpm. The flow entered the rod bundle through four jets at the inlet of the fuel assembly as shown in Figure 5-9. This configuration represents one of the common core inlet conditions for current PWR plant designs. The measured data contains velocity profiles for rows 7 and 11, which represent locations that are tangent to the jet boundary, and across the jet, respectively. These locations are shown in Figure 5-11.

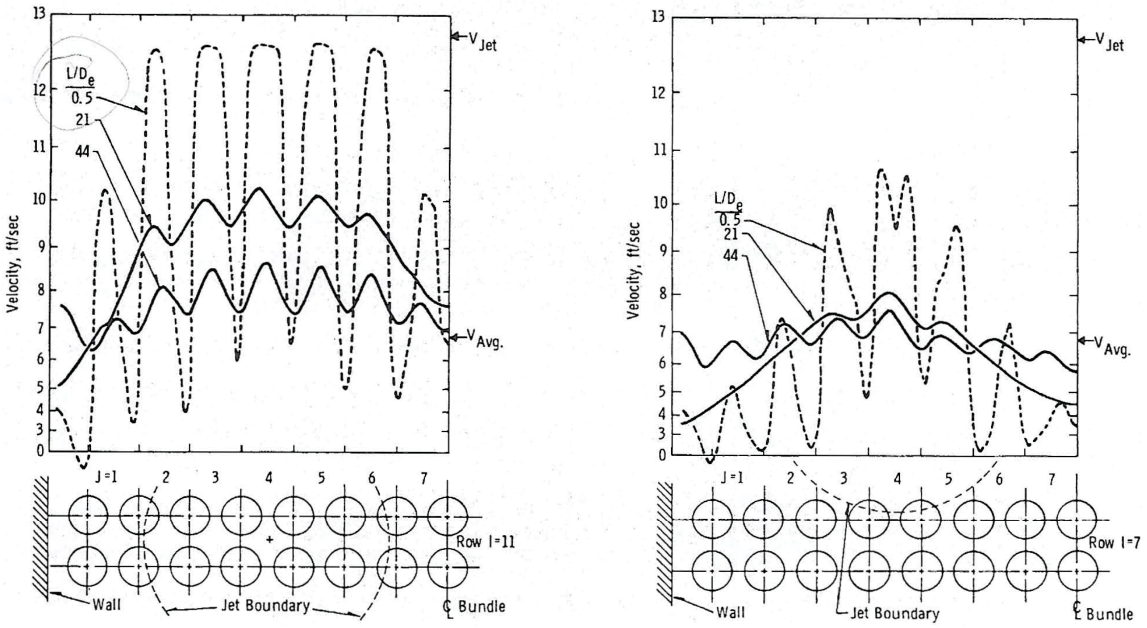

Figure 5-9. Across jet (Row 11, left) and tangent to jet (Row 7, right) velocity profiles

5.9.2.4 VIPRE-01 Model

The cross-section of the test section shows symmetry in the two radial directions and the inlet flow conditions to the test were uniform. Therefore, one-fourth of the bundle was modeled by NuScale which translates into a 64 channel VIPRE-01 model. The total axial length was divided into one-inch axial nodes. Reference 8.2.32 did not specify inlet water conditions other than stating that the experiment was a cold water test and the total flow rate was 2,000 gpm. The VIPRE-01 analysis assumed 15 psia for the assembly exit pressure, a 60 degrees F inlet temperature, and no heat flux for the boundary conditions. The inlet jet created by the large hole in the lower plate was modeled using an entrance velocity profile chosen to approximate the shape of the opening.

5.9.2.5 Results

VIPRE-01 results are interpolated from the output data based on the distance from the wall in the test configuration. Overall, the velocity profile matches the experimental data. It is expected that some differences would be observed as the experiment data is measured by a traversing probe, which covers a number of locations within the subchannel, while VIPRE-01 calculates the average value at the center of the subchannel. For both Row 7 and Row 11, measured data compare more accurately near the inlet jets (L/De = 0.5) than at the other locations as depicted in Figure 5-10 and Figure 5-11.

The results further from the jets show larger differences as depicted in Figure 5-12 and Figure 5-13 (for an L/De = 44). As expected, the pronounced jetting effects observed at entry (at L/De = 0.5) appear to become significantly reduced by the time the flow reaches L/De = 44. The velocity profile between jets (row 7) stabilizes more quickly than that across the jet, which is also an expected result. Experimental data obtained by means of a traversing probe affords generating continuous, therefore more realistic, velocity profiles. The accurate correspondence of local minima in the measured velocity profile to the gaps between rods (Figure 5-9) indicates the effectiveness of using a travelling probe. VIPRE-01 models subchannels with radial homogeneity and, as a result, predictions do not include wall effects that give rise to the more pronounced unevenness observed in the data. The trends predicted by VIPRE-01 agree with measurements. It is also observed from the comparisons that if the measured data are reduced to subchannel specific averaged mass flow velocities, they compare well with the VIPRE-01 predictions. The test section is modeled with the highest available modeling accuracy in VIPRE-01 where all subchannels are individually modeled. VIPRE-01 modeling of CHF tests is also performed according to the same methodology where each subchannel in the test section is modeled. Local thermal-hydraulic conditions used to derive the CHF correlation are in fact the subchannel averaged values at the most limiting location. The reactor thermal safety, i.e. the proximity to SAFDL, is in turn determined using average subchannel conditions, a method widely used in the nuclear industry to circumvent the modeling limitations in currently available thermal-hydraulic codes. Overall, the average experiment measured profile data typically matches the VIPRE-01 predictions within 10 percent or less.

{{

}}2(a),(c)

Figure 5-10. CE 15x15 velocity profile experiment comparison for Row 7, L/De = 0.5

{{

}}2(a),(c)

Figure 5-11. CE 15x15 velocity profile experiment comparison for Row 11, L/De = 0.5

{{

}}2(a),(c)

Figure 5-12. CE 15x15 velocity profile experiment comparison for Row 7, L/De = 44

{{

}}2(a),(c)

Figure 5-13. CE 15x15 velocity profile experiment comparison for Row 11, L/De = 44

In conclusion, the VIPRE-01 calculated velocity profile trends are similar to the measured velocity profile. The calculated velocity profile matches better with the measured velocity profile at the bottom of the test section than the top. Additionally, the jet effects are predicted accurately through the axial length of the test section. This comparison shows VIPRE-01 accurately predicts trends for mass flux in single-phase, unheated flow conditions with flow inlet distribution effects present.

5.9.3 Studsvik 3x3 Rod Bundle Two-Phase Flow

5.9.3.1 Purpose

Reference 8.2.38 describes a set of 12 different heated rod bundle test runs designed to study mass flux and quality profiles at the fuel bundle exit. The previous two tests specifically analyzed the hydraulic model and correlation performance of VIPRE-01 for PWR fuel assembly conditions without heat addition. This test, performed by Studsvik, provides data for analyzing the code performance of similar hydraulic conditions with heat addition.

5.9.3.2 Test Loop

The test was performed using nine heated rods in a 3x3 array with a uniform, axially heated length of 59 inches. The test also included two slightly different diameter rods, 0.4823 inches (Rods 1-6) and 0.4724 inches (Rods 7-9). The smaller rods were in an unheated row. The non-uniform radial power gradient specification sets Rods 1-3 at 70

percent of the total power, Rods 4-6 at 30 percent of the total power, and zero power in Rods 7-9. Figure 5-14 shows the 3x3 rod bundle test diagram.

Data was collected across four split channels divided at the rod centers. Figure 5-14 depicts both the rod array with the specified power distribution and the location of each of the four split channel measurement positions.

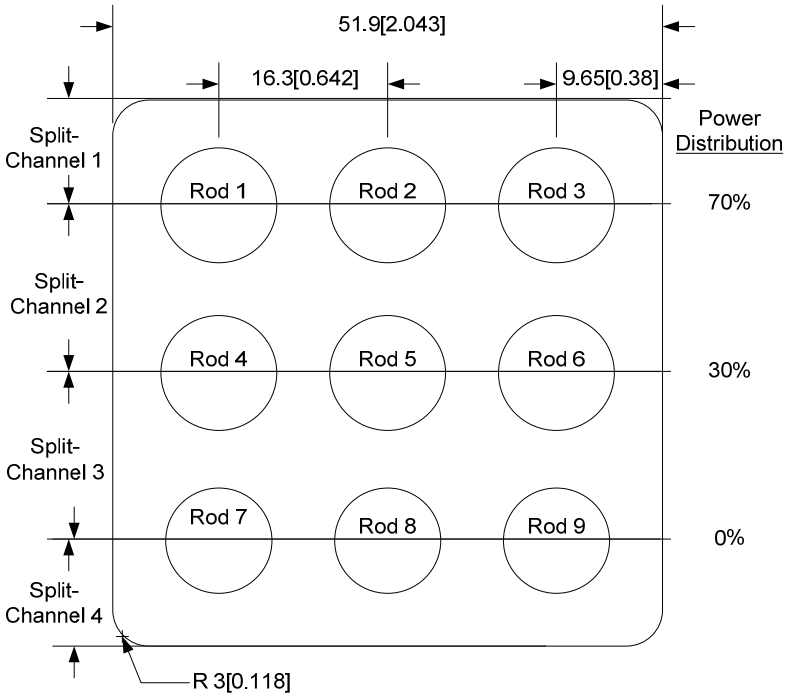

Figure 5-14. Studsvik 3x3 rod bundle two-phase flow test diagram, values in mm [in]

5.9.3.3 Key Parameters

In this test, data was obtained to study the mass flux and quality profiles at the exit of the heated and unheated rod segments. Average mass flux and steam quality were measured at the bundle exit for each of the four split channels. A total of twelve separate tests were performed with this configuration at various pressures, inlet temperature, inlet flow, and heat flux conditions as follows:

Pressure = 992 – 1047 psia

Inlet temperature = 474.7 – 528.7 °F

Inlet flow = 0.67 – 1.53 Mlbm/hr-ft^2

Heat flux = 0.234 – 0.311 MBtu/hr-ft^2

5.9.3.4 VIPRE-01 Model

A VIPRE-01 subchannel model for the test configuration was developed to calculate mass flux and quality for comparison to measured results. This model has 16 channels around the 9 rods of the test and used one-inch axial nodes. In order to compare the predicted results to the measured data, the VIPRE-01 data from the four channels in the model corresponding to each split channel were averaged.

5.9.3.5 Results

In all simulations, VIPRE-01 results for the measured mass flux and exit quality distributions compare well with the experimental results. The calculated values are within 10 percent of the measured experimental data reported. Note that the error bars in the figures represent the standard error of the mean for the measured data. Split channel 1 shows the highest quality, which is expected because it contains the highest power rods. The quality in the other split channels is gradually lower due to the presence of lower power rods. Mass flux predictions showed higher variation, but all but four split channels were within measurement error. In addition, the expected trend of lower mass flux resulting in higher quality conditions was observed in the test sequence.

Figure 5-15 and Figure 5-16 show VIPRE-01 predictions compared to measured experimental data for exit quality and mass flux for the lowest inlet flow test (0.668 Mlbm/hr-ft^2). Similar plots are presented in Figure 5-17 and Figure 5-18 for the highest flow test (1.531 Mlbm/hr-ft^2). This experiment analysis confirms that VIPRE-01 adequately predicts mass flux and quality distributions in two-phase heated flow with turbulent mixing and void-drift.

{{

}}2(a),(c)

Figure 5-15. Studsvik 3x3 lowest flow test (1085) exit quality experiment comparison

{{

}}2(a),(c)

Figure 5-16. Studsvik 3x3 lowest flow test (1085) mass flux experiment comparison

{{

}}2(a),(c)

Figure 5-17. Studsvik 3x3 highest flow test (1038) exit quality experiment comparison

{{

}}2(a),(c)

Figure 5-18. Studsvik 3x3 highest flow test (1038) mass flux experiment comparison

5.9.4 Conclusion of Experimental Benchmark Analyses

Based on the results presented for the three additional experimental benchmarks, the VIPRE-01 code performed adequately. Benchmarking to these experiments was done to provide additional evidence that VIPRE-01 performance for individual phenomenon applicable to the NuScale analysis is well-predicted. The single-phase and two-phase flow results are consistent between VIPRE-01 and the experimental data, particularly with respect to flow distribution, void, and quality data. Analysis of these additional three sets of experimental data further validate performance of the VIPRE-01 turbulent mixing, flow distribution, two-phase mixing, and void-drift capabilities. This is particularly relevant in illustrating the range of usefulness of the code's homogeneous equilibrium model for two-phase flow, including the NuScale selection of two-phase flow models.

The conditions evaluated in these experiments add to the benchmarks that represent the operating environment anticipated for the NuScale core.

Table 5-10 shows that the aggregate range of these additional experiments represents a reasonable portion of anticipated NuScale operating conditions. Therefore, these three experimental benchmarks further demonstrate the applicability of VIPRE-01 to NuScale subchannel models and analyses.

5.10 Void-Drift and the Drift-Flux Model

In two-phase flow conditions, there is a strong tendency for the voids to migrate to more open and higher velocity regions. This phenomenon is referred to as void-drift. Because this phenomenon is driven by the void distribution among subchannels, it is typically not considered in conventional PWR subchannel analysis as documented in Reference 8.2.5. The stated basis for this is "*since the homogenous codes, such as VIPRE-01 and COBRA, produce reasonable bundle-average results, despite not being able to correctly resolve the details of the two-phase flow field, this modeling deficiency has little impact on the usefulness of the code and is tacitly ignored.*" For NuScale applications, this phenomena was further investigated to ensure VIPRE-01 is appropriate for NuScale applications.

The VIPRE-01 flow solution is based on the homogeneous flow model and includes constitutive models to account for subcooled boiling and two-phase slip, as discussed in the preceding sections. The code handles a wide range of flow conditions with this formulation in both steady-state and transient analysis. Limitations exist, however, due to the modeling assumptions and correlations used. The drift-flux model overcomes some of the shortcomings of the homogeneous model. In particular, it eliminates the convergence problems that can arise in transient boiling calculations due to phase slip being accounted for empirically.

VIPRE-01 has options for empirical subcooled void relations to model subcooled boiling. Bulk void correlations can be selected by user input to model the effects of liquid/vapor relative velocity (slip). Under certain conditions (e.g., with small time steps), use of the

void correlations in a transient analysis can lead to instabilities in the numerical solution and unrealistic results. These problems can occur with or without subcooled boiling, but subcooled boiling tends to magnify the problem. The instabilities occur in the flow solution and are a result of the interdependencies of the parameters involved. The empirical void relations used are a function of mass flow rate. Because the time derivative in the continuity equation involves density which depends directly on the void fraction, there is an implicit dependency of the flow rate on itself. This can create, in effect, a self-generating flow and therefore cause unstable conditions. The drift-flux model uses a transport equation to calculate the void fraction and provides the appropriate time-rate-of-change value to stabilize the calculation.

The drift-flux model treats the flow as a homogeneous mixture for momentum, but special consideration is given to the relative motion between phases. The motion of the whole mixture is determined by the mixture momentum equation and the relative motion is taken into account by a kinematic constitutive equation. The velocity fields are defined in terms of the mixture velocity and the drift velocity of the vapor phase. The field equations consist of the three mixture equations for continuity, energy, and momentum, along with an additional equation for vapor mass conservation.

A modified version of VIPRE-01 was created by NuScale, including appropriate software verification and validation, to investigate the effect of void-drift in the lateral direction implemented in the continuity, energy, and axial momentum equations. The void-drift model implemented was based on that presented in Reference 8.2.20 through Reference 8.2.24. The Chexal-Lellouche drift-flux formulation was utilized in conjunction with the void-drift model.

Verification and validation of both the void-drift model and the use of the drift-flux model was performed through experimental benchmarks of Reference 8.2.25 through Reference 8.2.38. The NuScale geometry and thermal-hydraulic conditions are well within the range of conditions of these experimental tests. Taken in aggregate and for the purposes of validation of drift-flux and void-drift modeling, the experimental benchmarks are considered applicable to NuScale conditions.

With the modified code, a set of sensitivity cases applicable to NuScale conditions was performed with and without the void-drift model activated to confirm consistency with void fraction and MCHFR trends. For these cases, the predicted void fractions differed by less than 0.9 percent (relative difference) and CHFR differed by less than 0.02 CHFR points for all sensitivity cases. These results indicate the void-drift phenomenon has a negligible impact on NuScale applications. Therefore, the standard VIPRE-01 model without the effect of lateral void-drift is acceptable for NuScale analyses.

6.0 Example Calculation Results

Calculation analyses and results are presented in this section to demonstrate the application of the methodology described in this report. These results are for illustrative purposes only. NuScale design values are provided in the FSAR. Results are provided in this section for steady-state and transient simulations.

6.1 General Inputs

In addition to the example inputs provided throughout the report, namely Table 3-2 and Table 5-7, tabulated inputs utilized for the analyses are provided in Table 6-1 and Table 6-2.

Table 6-1. Tabulated inputs for example calculations

Description	Units	Value
core power at 100% power	MW	160
system flow at 100% power	kg/s	537.3
inlet temperature at 100% power	°F	486.6
nominal system pressure	psia	1850
core average axial power shape	relative	top-peak
core average axial power peaking	factor	1.3
fuel rod pitch	In.	0.496
active core height	In.	78.740
rod outer diameter	In.	0.374
rod inner diameter	In.	0.326
guide tube outer diameter	In.	0.482
pellet outer diameter	In.	0.3195
fuel rod length	In.	85.00
total bypass flow (of system flow)	%	8.5
turbulent mixing factor	factor	{{ }}2(a),(b),(c),ECI
lateral resistance factor	factor	0.5
turbulent momentum factor	factor	{{ }}2(a),(c),ECI

Table 6-2. Example loss coefficients [K=A*Re^B+C]

Grid	A	B	C
bottom nozzle + grid	{{		
middle grids			
top nozzle + grid			
axial friction			}}2(a),(c),ECI
Note: K= Loss Coefficient, Re= Reynolds Number			

Section 3.10.8 defines the methodology used to determine the limiting axial power distribution for the steady-state and transient analysis. Specifically, nuclear analysis is utilized to generate possible power shapes that can occur inside or on the edge of the axial offset window. Figure 6-1 provides a trace plot of the shapes input into the subchannel analysis in order to determine the bounding shape with respect to MCHFR for each power level. The result of this analysis determines the power shape at each power level that results in the minimum MCHFR. These shapes are then used in subchannel analysis.

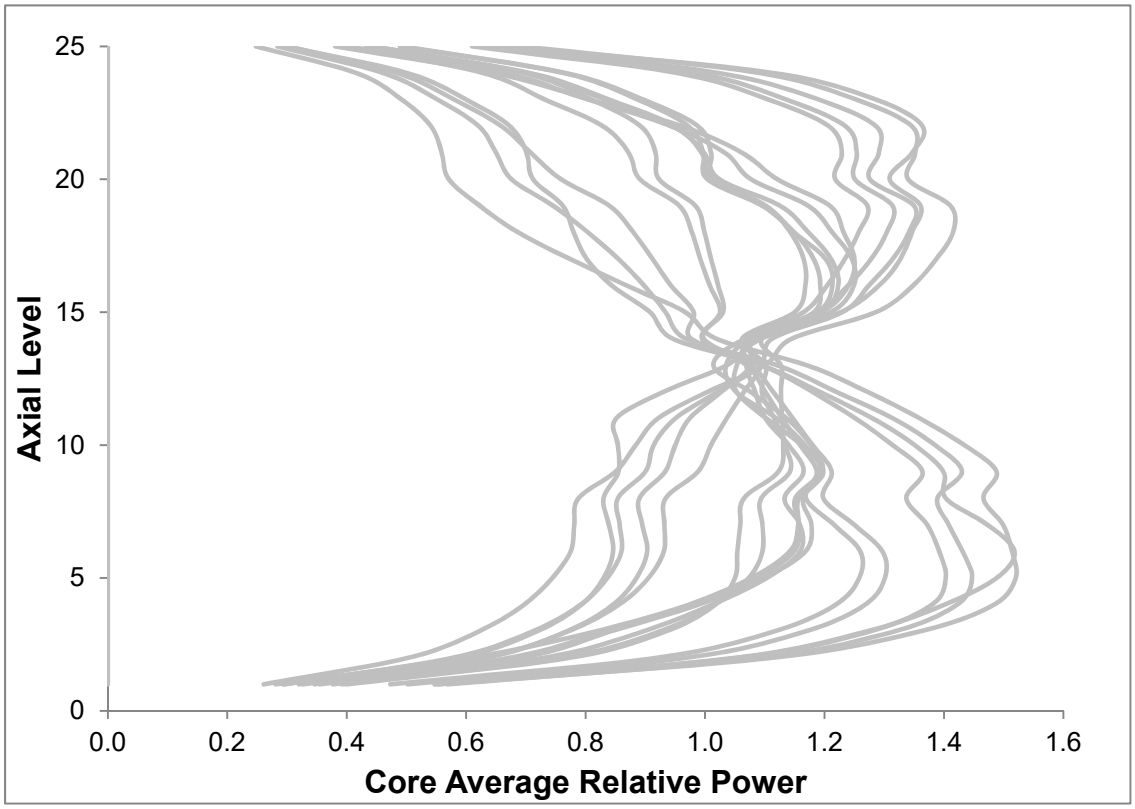

Figure 6-1. Example limiting axial power shapes from axial offset window

6.2 Steady-State Case

Steady-state calculations at HFP utilizing the 24-channel basemodel along with the methodology presented in this report and example inputs are provided. Additionally, results for a lumped 51-channel intermediate model (lump51) and a fully-detailed model are provided. The MCHFR for the basemodel at HFP conditions is 2.360.

Table 6-3. Summary of example steady-state results

Case Name	MCHFR (≥ 1.262)	Hot Channel Equilibrium Quality
basemodel	2.360	0.007
lump51	2.361	0.007
detailed	2.359	0.007

Comparison plots for the three steady-state models (basemodel, lump51, detailed) are presented to define the similarities and the acceptance of the behavior of the models. Figure 6-2 through Figure 6-4 provide void fraction, mass flux, and CHF ratio at each axial elevation in the hot channel of each model. These comparison plots demonstrate close agreement between models and expected effects, such as the spacer grids reducing mass flux.

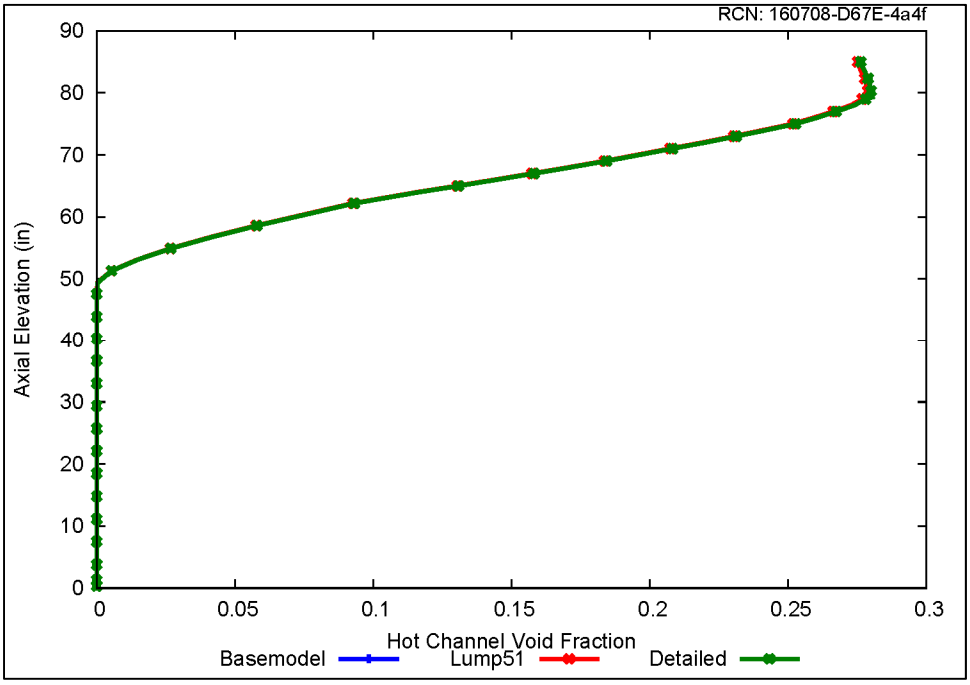

Figure 6-2. Example hot channel void fraction vs. elevation

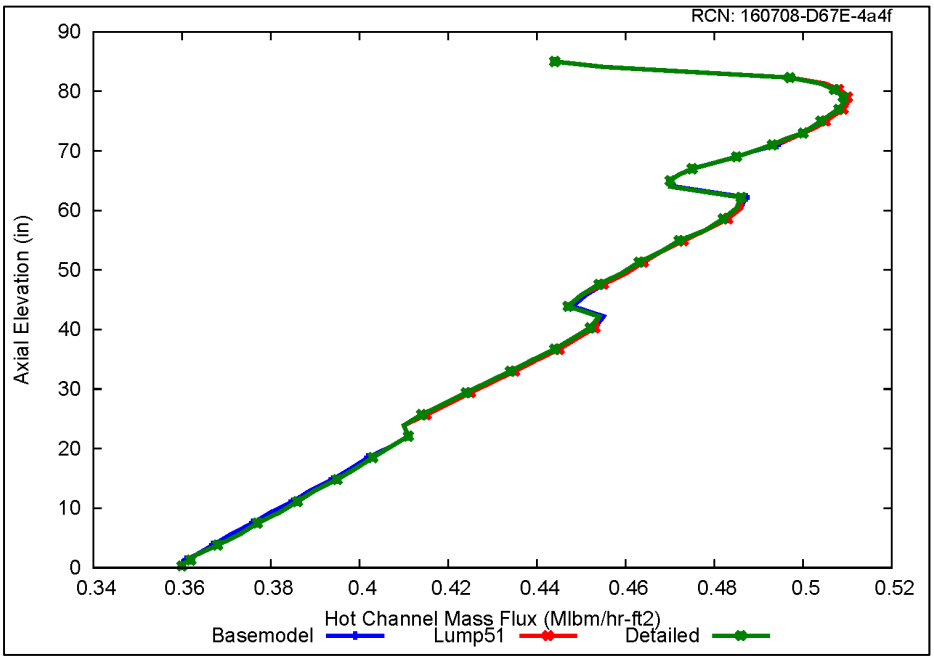

Figure 6-3. Example hot channel mass flux vs. elevation

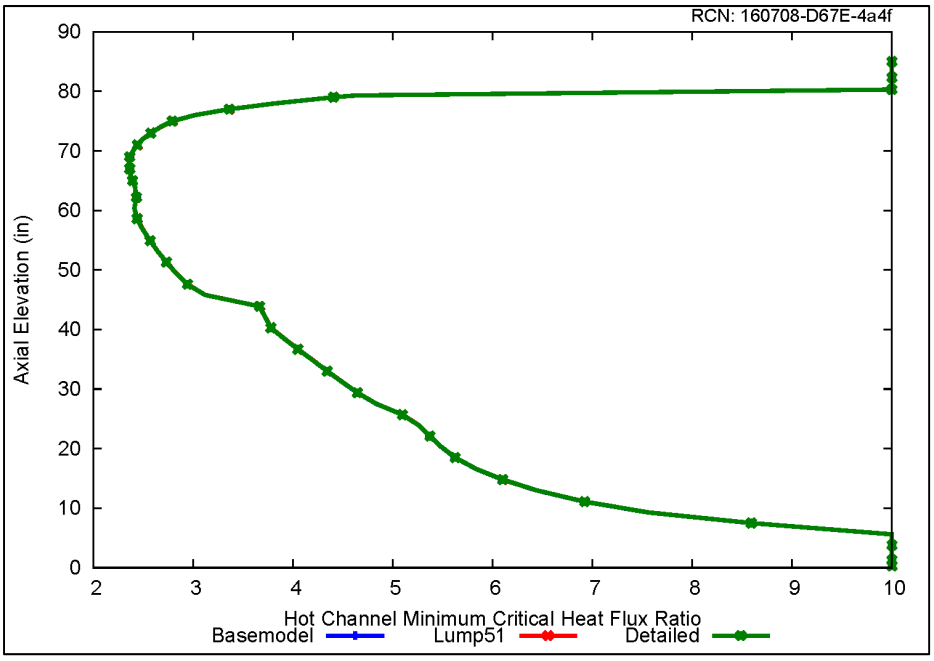

Figure 6-4. Example hot channel critical heat flux ratio vs. elevation

Figure 6-5 provides an isothermal pressure drop across the core to demonstrate that the grid losses are applied correctly. A near-zero power (0.01 MWt) was utilized to obtain a case with no significant temperature difference between the core inlet and exit.

{{

}}2(a),(c),ECI

Figure 6-5. Example basemodel isothermal core pressure drop vs. elevation

6.3 Transient Cases

Three transients that represent the key types of design-basis transients expected for the NuScale design are selected for example purposes. Table 6-4 provides a description of the transients along with the corresponding section from the standard review plan.

Table 6-4. Example transient subchannel calculations

SRP Section	Description
15.1	Decrease in Temperature with Power Increase
15.2	Increase in Core Inlet Temperature
15.4	Power Escalation from Rod Movement

These three transients were selected to span the main types of design-basis transients for the NuScale design. Each event is characterized by a different forcing function: a power increase, an increase in inlet temperature, or flow rate changes as a result of changes in power. Normalized forcing functions and resulting MCHFR plots are presented in Figure 6-6 through Figure 6-11 for the three transients. For all cases, the VIPRE-01 simulations (in addition to MCHFR) correspond to expectations. Additionally, all convergence and methodology criteria, including the Courant limit criterion, are satisfied.

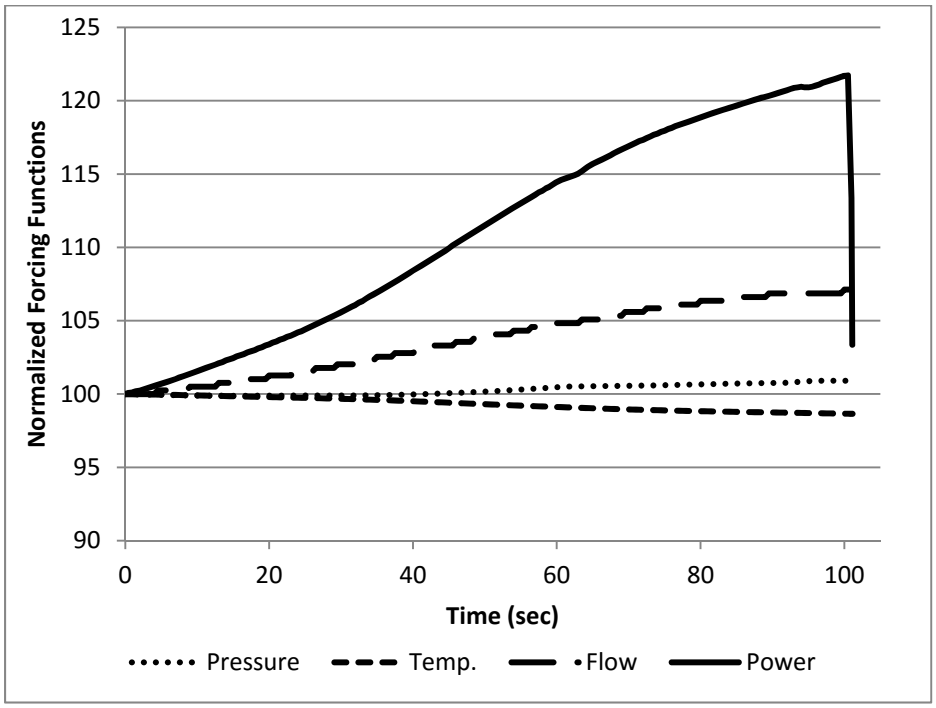

Figure 6-6. Example Chapter 15.1 normalized transient boundary conditions

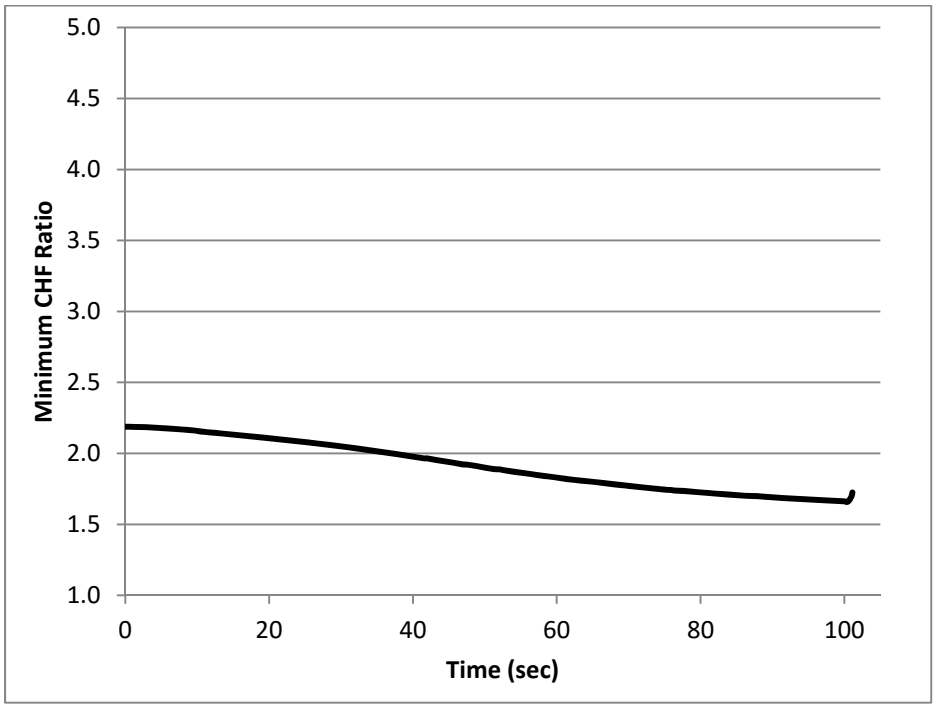

Figure 6-7. Example Chapter 15.1 minimum critical heat flux ratio

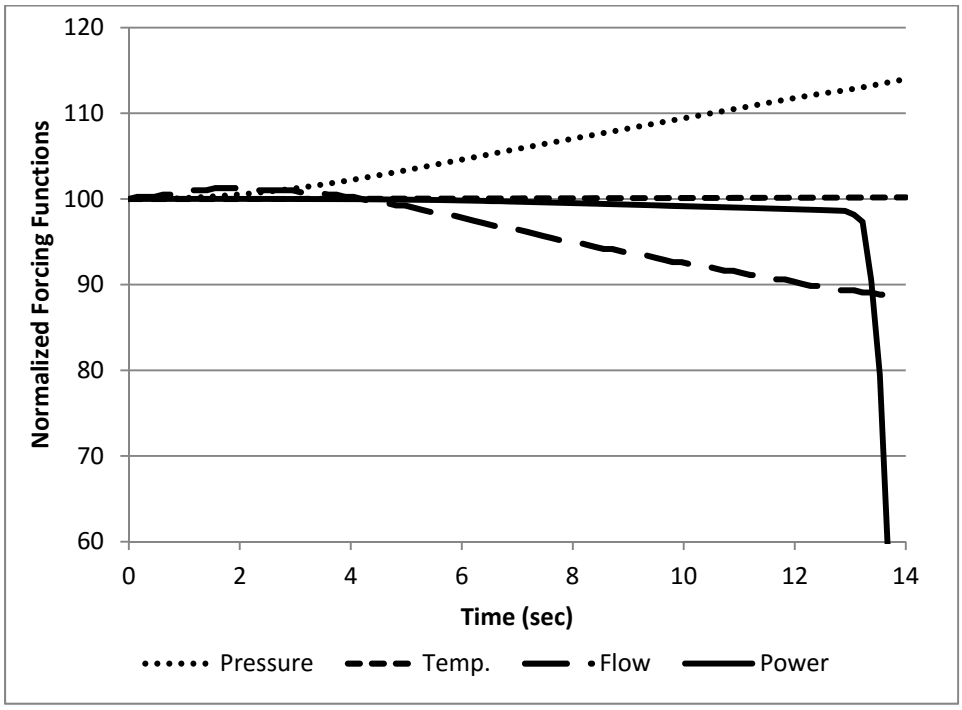

Figure 6-8. Example Chapter 15.2 normalized transient boundary conditions

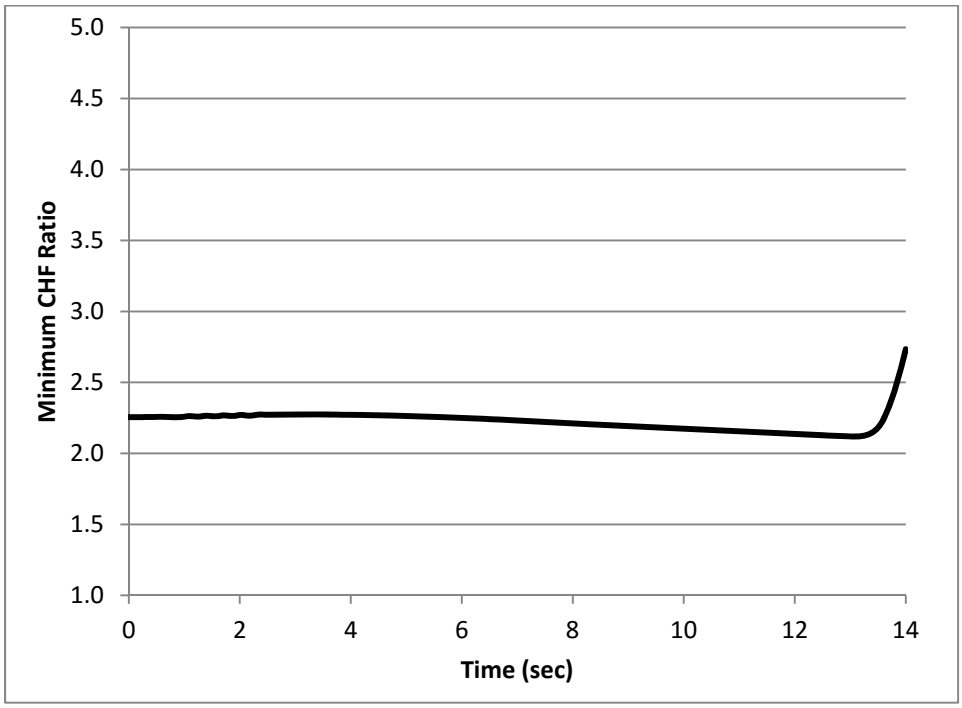

Figure 6-9. Example Chapter 15.2 minimum critical heat flux ratio

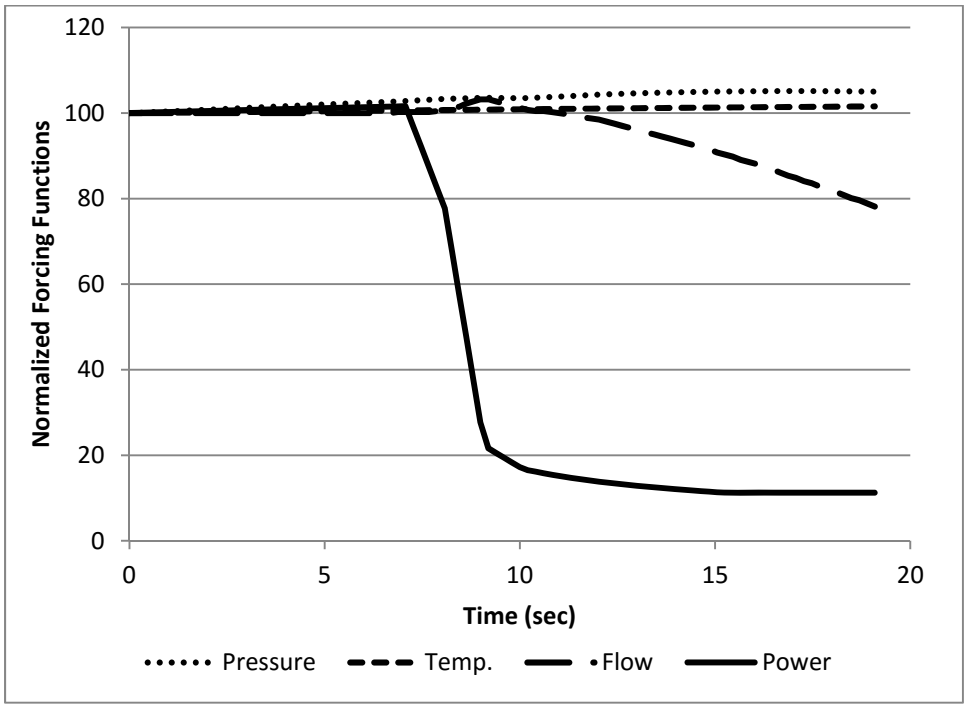

Figure 6-10. Example Chapter 15.4 normalized transient boundary conditions

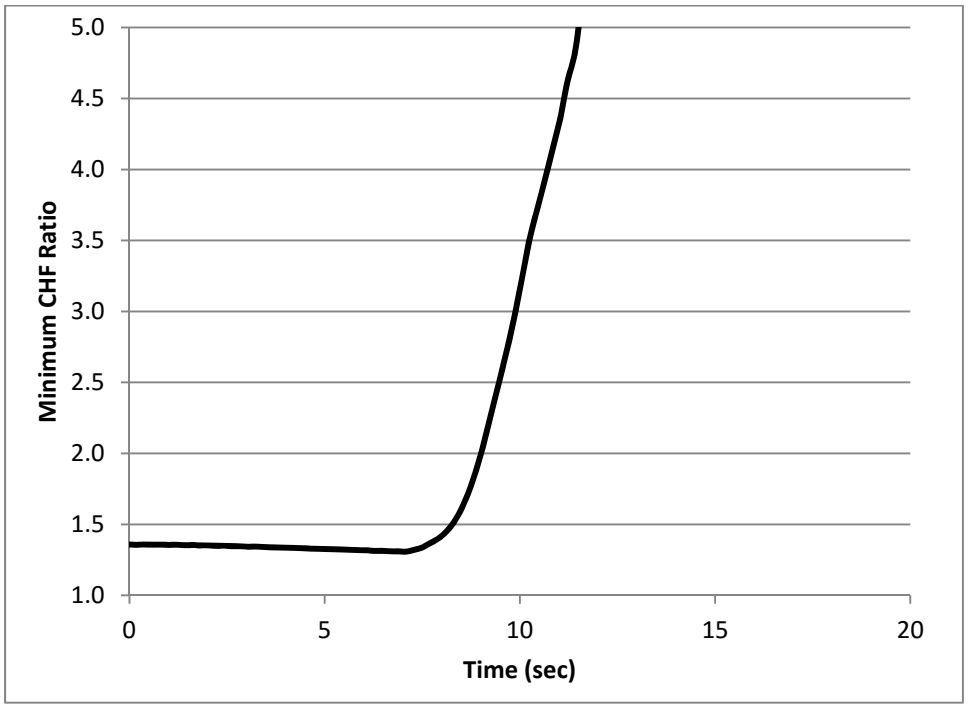

Figure 6-11. Example Chapter 15.4 minimum critical heat flux ratio

In addition to the three transients presented, Table 6-5 presents ranges of NuScale conditions representative of all design-basis events analyzed utilizing the methodology defined in this report.

Table 6-5. Summary of example off-normal range of conditions in subchannel analysis

Description	Units	Min	Max
System Pressure	psia	1,700	2,200
Inlet Mass Flux	Mlbm/h-ft^2	0.1	0.5
Linear Heat Generation Rate	kW/ft	0.2	3.3
Equilibrium Quality at MCHFR	%	-40	20
MCHFR	ratio	1.3	n/a

A scatter plot of example NuScale conditions is provided in Figure 6-12. The map itself is taken from Reference 8.2.2. The red data points demonstrate that the NuScale design is similar to conventional PWRs, for which VIPRE-01 was designed, with respect to equilibrium qualities and flow regime.

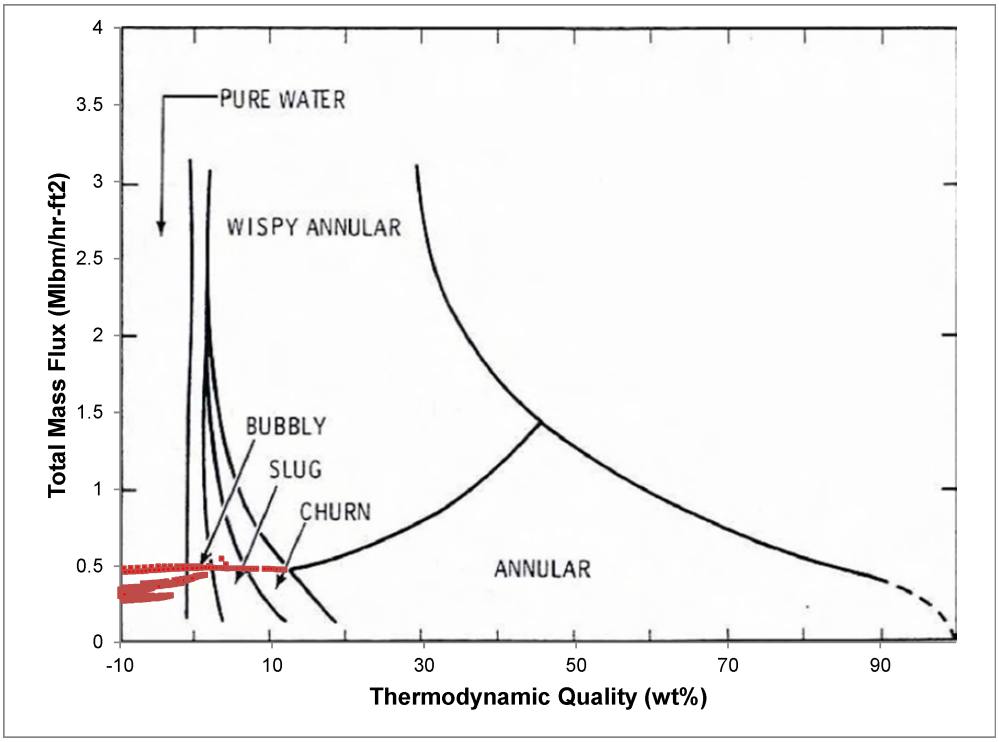

Figure 6-12. Bennett Flow Regime Map with Example Off-Normal Conditions at MCFHR

6.4 Parametric Sensitivity Analysis

The deterministic methodology described throughout Section 3.0 relies on simplified modeling techniques that ensure conservative results with respect to MCHFR. In addition to the generalized sensitivity analysis presented in the previous section, a set of parametric sensitivities are presented to further justify the modeling techniques used. In the tabulated presentation of key outputs, light grey highlighting is used to signify the reference case, from which other cases are compared to in the form of percent difference or CHF points.

6.4.1 Radial Geometry Nodalization

The two lumped models and the fully detailed model are compared for six different operating conditions defined in Table 6-6. The three models compared are the 24-channel basemodel (‘Basemodel’), 51-channel model (‘Lump51’), and the fully detailed model consisting of 1388 channels (‘Detailed’). The nodalization is confirmed to accurately maintain the hot channel flow field (void fraction, mass flux, and crossflow profiles versus elevation) and result in a conservative MCHFR. Benchmarking was performed for high pressure, low pressure, low power and flow, high power and flow, and high radial peaking augmentation.

As a result of the parametric sensitivities performed, the radial nodalization is confirmed to accurately maintain the hot channel flow field and result in a conservative MCHFR. The largest deviations in MCHFR were 0.1 CHF point or less, which is an insignificant difference. Sensitivities included high and low flow, high and low pressure, and high radial peaking augmentation. In all cases, the hot channel was adjacent to the hot rod, and the elevation, hot channel, and hot rod were consistent between all radial nodalizations.

Table 6-6. Radial geometry nodalization minimum critical heat flux ratio comparison

Description	Basemodel	Lump51	Detailed	Lump51 Diff. (CHF Points)	Detailed Diff. (CHF Points)
full power	2.360	2.361	2.359	-0.1	0.1
high power & flow	1.203	1.204	1.202	-0.1	0.1
low power & flow	10	10	10	0.0	0.0
low pressure	1.335	1.336	1.335	-0.1	0.0
high pressure	1.325	1.325	1.324	0.0	0.1
high radial peak	1.715	1.716	1.715	-0.1	0.0

6.4.2 Radial Power Distribution

In order to study the operating power environment outside the limiting assembly, best-estimate power distributions were utilized for all assemblies except the hot assembly, which utilized the same artificial power distribution. The best-estimate power distributions were from the BOC, middle of cycle, and EOC.

The radial power distribution more than a few rows removed from the hot subchannel has a negligible impact on the MCHFR results. In other words, analysis of different power distributions of the NuScale core demonstrate that rod powers a few rod rows beyond the hot rod or channel have a negligible impact on the MCHFR.

Table 6-7. Radial power distribution results

Power Distribution Outside Center	MCHFR	Diff. (CHF Points)	Axial Level (in)	Mass Flux at MCHFR	Equilibrium Quality at MCHFR	Heat Flux at MCHFR
Artificial	2.291	n/a	68.0	0.480	0.010	0.184
BOC	2.292	0.1	68.0	0.477	0.010	0.184
MOC	2.292	0.1	68.0	0.477	0.010	0.184
EOC	2.291	0.0	68.0	0.478	0.011	0.184

6.4.3 Axial Geometry Nodalization

Analysis of different axial node heights demonstrates that {{ }}2(a),(c),ECI nodes (as an example) are sufficient to accurately predict the flow field. The sensitivity is limited to the CHF region, which is defined in Section 3.7.2 as the space between the fourth spacer grid and the end of the active fuel length in which CHF is observed to occur. A sensitivity study was performed with four additional cases in which the node height in this region was adjusted to {{ }}2(a),(c),ECI.

As a result of the parametric sensitivities performed, the axial nodalization is confirmed to accurately maintain the hot channel flow field and result in a conservative MCHFR. The largest deviations in MCHFR for cases with smaller nodalization than nominal were 1.0 CHF point or less, an insignificant difference. As the nodalization size increases, the difference in MCHFR is more pronounced (but in a conservative direction). Sensitivities included top-peaked and middle-peaked power shapes. In all cases, the hot channel was adjacent to the hot rod, and the elevation, hot channel, and hot rod were consistent between all axial nodalizations.

Table 6-8. Axial geometry nodalization minimum critical heat flux ratio comparison

Level Height (in)	MCHFR	Diff. (CHF Points)
{{		
		}}2(a),(c),ECI

6.4.4 Inlet Flow Distribution

Several inlet flow distributions were studied to understand the effect of inlet flow distribution on flow and CHF. For all phenomena examined, the differences in the hot channel after approximately a third of the active fuel length are nearly identical for different magnitudes of inlet flow maldistribution. Even at large maldistributions of 15 percent, the hot channel axial flow converges to the same mass flux at the same axial location as small maldistributions due to crossflow. This is shown in Figure 6-16. As a result of increased maldistribution, the core exit void fraction and equilibrium quality proportionally increase, leading to approximately linear decreases in MCFHR. A doubling of the nominal maldistribution from 5 percent to 10 percent results in a deviation in MCHFR of 1.0 CHF point or less, an insignificant difference. Additionally, for a given radial power distribution, there was a general insensitivity observed to the inlet distribution gradient, with the largest deviation between gradients at the same maldistribution magnitude of 1.0 CHF point.

Figure 6-14 shows the impact of maldistributions of 3, 5, 10, and 15 percent on CHFR. As can be seen from the figure, there is essentially no impact on MCHFR.

Additionally, a comparison of the basemodel to the fully-detailed model with one distribution gradient was performed for three sets of operating conditions of HFP, high power, and high radial peaking for four magnitudes of maldistribution. For all phenomena examined, the differences in the hot channel between the two radial nodalizations are nearly identical. The largest deviation in MCHFR observed is 0.2 CHF point, an insignificant difference.

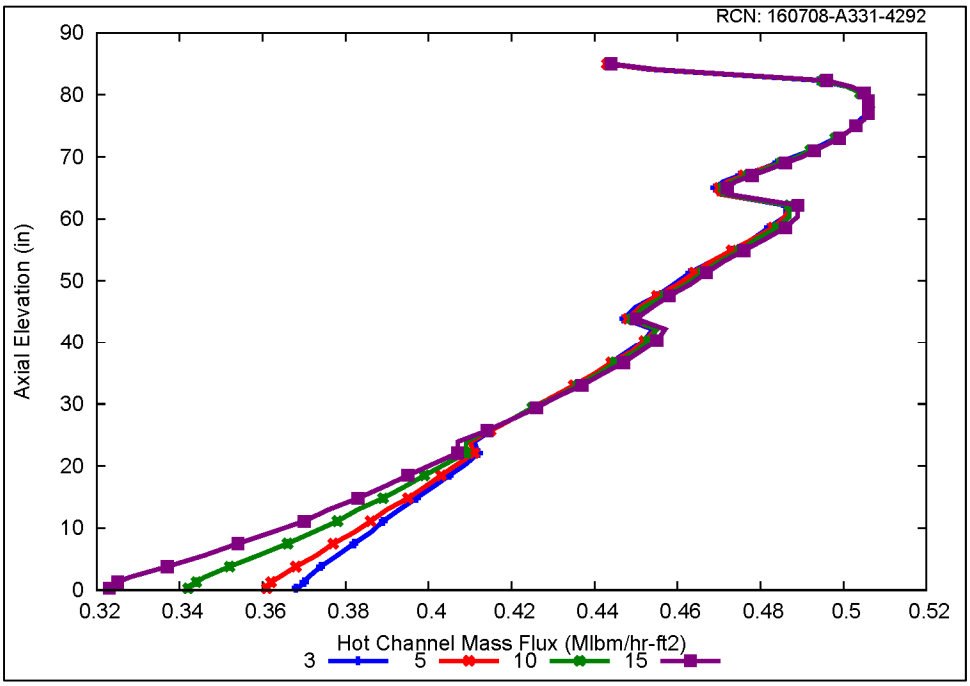

Figure 6-13. Inlet flow distribution baseline mass flux vs. axial elevation

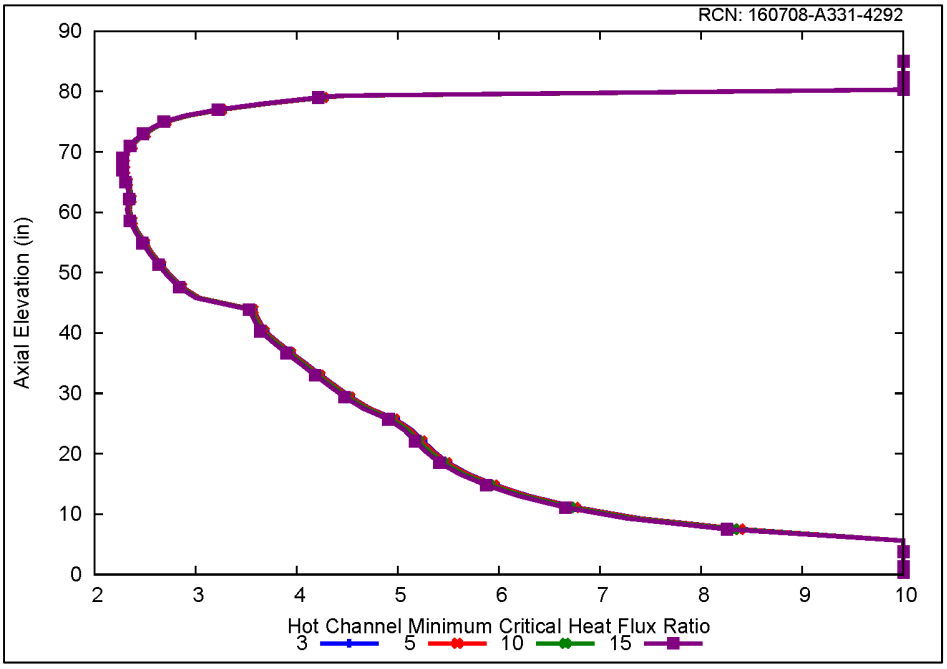

Figure 6-14. Inlet flow distribution baseline hot channel CHFR vs. axial elevation

Reducing the inlet flow to the limiting fuel assembly by 15 percent shows no discernible impact on the MCHFR. The lower rate of mass flow due to natural circulation in the NuScale reactor coupled with the smaller core radius compared to conventional PWRs promotes rapid flow redistribution once the flow enters the core.

6.4.5 Turbulent Mixing Parameter

A study of the impact of variation of the turbulent mixing coefficient (ABETA) on the MCHFR was performed by varying this value between the minimum possible value (0.0) to a relatively large value as compared to that observed in NuScale testing. Three different operating conditions spanning full power, high power, and high radial peaking were utilized to ensure the trends observed apply to all NuScale conditions.

As a result of decreased thermal mixing, the core exit void fraction and equilibrium quality proportionally increase, leading to an approximately linear decrease in MCFHR. A doubling of the nominal coefficient results in a deviation in MCHFR of {{ }}$^{2(a),(c),ECI}$ CHF points or less, a moderately significant impact. In all cases, the hot channel was adjacent to the hot rod, and the elevation, hot channel, and hot rod were consistent between all turbulent mixing coefficient values studied. The elevation at which MCHFR is predicted is identical for each nodalization option.

It is concluded that MCHFR is not very sensitive to ABETA as evidenced by a {{ }}2(a),(c),ECI percent increase in ABETA resulting in a {{ }}2(a),(c),ECI point change in CHF.

Table 6-9. Turbulent mixing factor minimum critical heat flux ratio comparison

Turbulent Mixing	Full Power		High Power		High Peaking	
	MCHFR	Difference (CHF Points)	MCHFR	Difference (CHF Points)	MCHFR	Difference (CHF Points)
{{						
						}}2(a),(c),ECI

6.4.6 Turbulent Momentum Parameter

A study of the impact of the turbulent momentum factor on predicted MCHFR was performed by varying this value between the minimum and maximum possible values {{ }}2(a),(c),ECI for two different operating conditions. The recommended value is {{ }}2(a),(c),ECI. Table 6-10 provides tabulated comparisons of the cases for MCFHR. For all phenomena examined, the axial profiles in the hot channel between different factors were nearly identical. The largest deviations in MCHFR were {{ }}2(a),(c),ECI CHF point or less, an insignificant difference. In all cases, the hot channel was adjacent to the hot rod, and the elevation, hot channel, and hot rod were consistent between all turbulent momentum parameter cases. The elevation at which MCHFR is predicted is the same for each operating condition.

Table 6-10. Turbulent momentum factor minimum critical heat flux ratio comparison

Turbulent Momentum	Full Power and Flow		High Power and Flow	
	MCHFR	Difference (CHF Points)	MCHFR	Difference (CHF Points)
0.0	{{			
0.2				
0.4				
0.6				
0.8				
1.0				}}2(a),(c),ECI

6.4.7 Grid Loss Coefficients

The impact of the grid spacer loss coefficient on the hot rod MCHFR is determined by varying this value between a range of values from 20 percent less to 20 percent greater than the design value. Varying the homogeneous grid loss coefficient does not result in a significant MCHFR response, as shown in Table 6-9, which is an expected result where the inlet flow rate is assumed not to change in response. Application of grid loss coefficients reduced from a smaller array rod bundle to a larger rod array is conservative since non-uniform effects such as those resulting from the presence of the wall tend to become smaller as their proximity to the hot channel decreases. The reduction of pressure loss data to obtain uniform grid loss coefficients assumes radial homogeneity, which is maintained in application. In all cases, the hot channel parameters are nearly identical. The largest deviations in MCHFR are {{ }}$^{2(a),(c),ECI}$ CHF point or less, an insignificant difference. In all cases the hot channel was adjacent to the hot rod, and the elevation, hot channel, and hot rod were consistent between all grid spacer losses. The elevation at which MCHFR is predicted is identical for each loss coefficient evaluated.

Table 6-11. Grid spacer losses minimum critical heat flux ratio comparison

Grid Loss Coefficient	MCHFR	Difference (CHF Points)
-20%	{{	
0		
+20%		}}$^{2(a),(c),ECI}$

6.4.8 Numerical Solution Parameters

Nominal axial flow, lateral flow, and pressure and energy numerical solution damping and convergence limits are confirmed to accurately maintain the hot channel flow field and result in a conservative MCHFR. Specifically, the VIPRE-01 inputs FERROR, ACCELF, WERRX, DAMPING, WERRY, and ITRYM were varied to both more and less restrictive values than the nominal values defined for NuScale use. For all phenomena examined with nominal or more restrictive numerical solution options, the differences in the hot channel observed are negligible. The largest deviations observed in MCHFR were 0.2 CHF point or less, an insignificant difference.

6.5 General Input Sensitivity Analysis

6.5.1 General Methodology

General sensitivity analysis methodologies are used throughout this section and are provided here for reference. The sensitivity analyses are used in the subchannel methodology to determine the appropriate biasing direction for an input in order to yield a conservative solution and relative importance of inputs.

Another important use of this analysis is to check for the possibility of a non-linear system with corresponding feedback effects. It is important to check for a non-linear system as parameter importance and bias directions are not consistent in such systems. Thus, in the case of a non-linear system, conditional bias directions would have to be established in order to ensure a robust deterministic methodology. A review of the input parameters ranked importance by linear, rank, and quadratic regression indicates clear consistency for each case individually, but also between different cases. This is a strong indication that subchannel analysis of the NuScale design, as performed with a deterministic methodology, results in the modeled system behaving largely as a linear system (i.e., consistent importance and bias directions). A statistically based nonparametric input sampling process is implemented through automated software tools. Input parameters are randomly varied across their pertinent range of values within the input deck and run as a single sample whose output file gives a value.

The partial rank correlation coefficient (PRCC) value is also calculated. A positive value means that the effect of the input on the output is the same (i.e., an increase of the value of the input leads to an increase of the value of the output). A negative PRCC value means the effect is the opposite (an increase in input leads to a decrease in output).

The primary indicator of importance is the incremental R^2 from the quadratic regression model. An input is not sufficiently important if it has an incremental R^2 less than 0.02. A high incremental R^2 (close to 1.0) indicates that an input is highly influential on the evaluated system output.

6.5.2 Application to Subchannel Analysis Inputs

Six steady-state cases that span a variety of normal or off-normal conditions are defined in Table 6-12. These cases are selected to be representative of subchannel analysis conditions in the NuScale design. At lower powers (starting at less than 50% rated power) the calculated MCHFR becomes large. Values of MCHFR significantly greater than 1.0, both for the same correlation and comparing between different correlations, become less and less physically meaningful. As a result, steady-state sensitivity analysis at low powers is not performed.

Table 6-12. Sensitivity case summary

Case Name	Description	Core Power (% Rated)	Pressure (psia)	Core Inlet Temperature (°F)
100	Hot Full Power	100	1,850	497
120	Higher Power/Flow	120	1,850	492
80	Lower Power/Flow	80	1,850	502
lo_pr	Low Pressure	100	1,700	Min (420)
hi_pr	High Pressure	100	2,200	Max (525)
min	Minor Importance	100	1,850	497

Table 6-13 presents the inputs sampled for the sensitivity analysis utilizing uniform distributions. Engineering judgment is utilized for minimum and maximum bounds of an input for those inputs in which tolerances are not currently available. For those inputs in which minimum and maximum bounds, or a tolerance, is documented this basis is provided. The sampling of transient input forcing functions is not performed.

Table 6-13. Summary of sampled input

Description	Units	Nominal	Uncertainty	Min	Max
Core Power at 100% Power	MW	160	2%	156.8	163.2
System Flow at 100% Power	kg/s	587	12.5%	513.6	660.4
Inlet Temperature at 100% Power	°F	496.1	5	491.1	501.1
System Pressure	psia	1850	35	1815	1885
Pitch Assembly	in	8.466	0.005	8.461	8.471
Pitch Rod	in	0.496	0.002	0.494	0.498
Rod Diameter	in	0.374	0.002	0.372	0.376
Guide Tube Diameter	in	0.482	0.002	0.480	0.484
Axial Power	-	1.3	0.2	1.1	1.5
F-delta-H Bias	-	1.0	-	1.00	1.12
Lateral Resistance Factor	-	0.5	0.4	0.1	0.9
Turbulent Momentum Factor	-	{{ }}$^{2(a),(c),ECI}$	-	{{	}}$^{2(a),(c),ECI}$
Turbulent Mixing Factor	-	{{ }}$^{2(a),(b),(c),ECI}$	-	{{	}}$^{2(a),(b),(c),ECI}$
Frictional Loss Coefficient	-	0.204	20%	0.163	0.245
HMP Spacer Grid Loss Coefficient	-	{{	20%	{{	
HTP Spacer Grid Loss Coefficient	-	}}$^{2(a),(c),ECI}$	20%		}}$^{2(a),(c),ECI}$

Utilizing the general sensitivity analysis criteria defined previously to analyze the results of the seven cases, a number of observations are made. As described, the quadratic regression, PRCC, and adjusted R^2 values are the main basis for these observations. In all cases, the adjusted R^2 indicated fair performance with quadratic values ranging approximately from 0.7 to 0.85. A review of all the sensitivity results indicates that this fair performance is likely a combination of (i) a cubic relationship between MCHFR and axial power shape and (ii) the number of total inputs perturbed. It is judged that it is unlikely that the roughly 0.7 adjusted R^2 is caused by non-linear effects and the resulting sensitivity analysis is judged to be fairly reliable.

The quadratic regression criteria consistently aligned across all cases and with the PRCC rankings. As a result, eight inputs for the steady-state cases are classified as the most important. As mentioned earlier, a positive PRCC value means that the effect of input on the output is the same. As an example, the axial shape PRCC value is always positive. As the axial shapes are sorted from top (1) to bottom (4), an increase in shape number (more bottom peaked) results in an increased MCHFR. Stated the other way, a decrease in shape number (more top peaked) results in a decreased MCHFR.

The one main exception is that of system pressure in which the bias direction is not consistent across all cases. This is due to the unique features of the NSP2 correlation as defined in Reference 8.2.7. As a result, case dependent bias directions on pressure should be utilized to ensure a conservative calculation of MCHFR. The turbulent moment parameter does exhibit one instance of an inconsistent bias direction; however, the calculated PRCC and incremental R^2 values are sufficiently small such that it may be discounted as statistical noise. Table 6-14 presents rankings the key parameters (as defined by the quadratic regression criteria) for steady-state full power results. The resulting relative importance and bias directions are in alignment with expectations. In all but the low pressure case, the rankings of importance, based on the magnitude of PRCC values, are identical. In this case, there are minor differences in the relative rank of the top four parameters and the addition of pressure into the top eight.

Table 6-14. Key steady-state full power PRCC Values

Description	Conservative Bias	PRCC Values				
		100	120	80	hi_pr	lo_pr
Axial Power	Larger	-0.773	-0.773	-0.760	-0.738	-0.664
F-delta-H Bias	Larger	-0.724	-0.729	-0.711	-0.701	-0.670
System Flow	Smaller	0.577	0.576	0.544	0.597	0.343
Axial Shape	Top-Peaked	0.452	0.453	0.472	0.470	0.513
Core Power	Larger	-0.251	-0.252	-0.234	-0.252	-0.217
Inlet Temperature	Larger	-0.217	-0.197	-0.213	-0.224	-0.136
Turbulent Mixing Factor	Smaller	0.104	0.102	0.094	0.109	0.085
Pitch Rod	Smaller	0.085	0.082	0.072	0.088	0.043

Not all inputs satisfied the quadratic regression criteria as being significantly important. However, it is desired to provide the biasing directions for all inputs. Therefore, a second case at hot full power was run with the inputs deemed most important by the other steady-state and transients cases set to constant values and only the minor importance or unimportant inputs allowed to be sampled. As a result, acceptable statistics for all inputs were obtained. Therefore, this analysis provides a basis for defining the appropriate input biases, which are defined in Table 6-15. All biasing directions are expected based on prior experience and NuScale subchannel analysis.

Table 6-15. Direction of bias to minimize MCHFR

Description	Conservative Bias	Significance
Axial Power	Larger	High
F-delta-H Bias	Larger	High
System Flow	Smaller	High
Axial Shape	Top-Peaked	High
Core Power	Larger	High
Inlet Temperature	Larger	High
Turbulent Mixing Factor	Smaller	High
Pitch Rod	Smaller	High
Rod Diameter	Smaller	Medium
System Pressure	Case Dependent	Medium
HTP Spacer Grid Loss Coefficient	Larger	Medium
Frictional Loss Coefficient	Larger	Medium
Turbulent Momentum Factor	Smaller	Medium
Pitch Assembly	Smaller	Medium
Guide Tube Diameter	Larger	Medium
HMP Spacer Grid Loss Coefficient	Larger	Low
Lateral Resistance Factor	Larger	Low

6.5.3 General Sensitivity Analysis Conclusions

The results from the example input sensitivity analysis performed for the subchannel analysis are used in the methodology to determine the appropriate biasing direction for an input in order to yield a conservative solution. In addition, this example analysis may be utilized as a supporting determination of the linear nature with respect to sensitivity analysis (i.e., consistent biasing directions) of the system modeled. A high-level summary and conclusions of the example sensitivity analysis with respect to subchannel analysis is provided below:

- Subchannel analysis utilizing the recommended deterministic methodology behaves largely as a linear system.
- Consistent top input importance rankings.
- Consistent bias directions throughout cases (except for pressure as described).
- Axial peaking is the single most important input, with a top peaking the most limiting.
- A relatively large uncertainty range of system flow (12.5%) results in a relatively large importance.
- An important input is smaller rod pitch, as it reduces the channel flow area.

- Smaller turbulent mixing factor is both significant and limiting.
- System pressure is not consistent across all cases due to unique features of the NSP2 correlation as defined in Reference 8.2.7. As a result, case dependent bias directions on pressure should be utilized to ensure a conservative calculation of MCHFR.

7.0 Summary and Conclusions

A general overview of the specific methodology utilized for steady-state and transient subchannel analysis has been presented. Design calculations will use this methodology for assessing thermal margin and to determine if fuel failure will occur due to inadequate heat removal capability through CHF and FCM. The methodology is developed to meet the relevant expectations of Section 4.4 and Chapter 15 of the SRP.

The thermal design analysis methodology for NuScale subchannel analysis has been presented with the basis for the subchannel model development and application. A fully-detailed pin-by-pin model in addition to lumped-channel models are used to resolve the desired enthalpy and flow field, with specific focus on the hot channel. This methodology is applied as a standard technique for modeling steady-state calculations and transients. Example calculations and corresponding sensitivity analysis were provided in order to demonstrate applicability of the methodology. Detailed descriptions of the model nodalization, boundary conditions, radial power distributions, and uncertainties and biases are provided.

An extension of the qualification of VIPRE-01, previously performed for PWRs, to NuScale applications is presented. This includes a detailed review of the fundamental assumptions of the models and correlations utilized as a basis for using the fuel rod conduction model, review of the void-drift phenomena and its effect on NuScale licensing applications, and additional VIPRE-01 benchmark calculations to the COBRA-FLX code, and three additional experiments. As a result, it has been demonstrated that VIPRE-01 is appropriate for NuScale licensing applications.

7.1 VIPRE-01 Safety Evaluation Report Requirements

As described in this report, the NuScale application of VIPRE-01 fulfills the requirements specified in the generic VIPRE-01 SER (Reference 8.2.1). A summary of the NuScale fulfillment of each requirement is provided below:

1. **Post-CHF:** The methodology described in this report does not include use of VIPRE-01 for post-CHF calculations.
2. **CHF Correlation:** NuScale CHF correlations are demonstrated to be valid for design-specific experimental data. The test bundles represent the fuel geometry and spacer grid design, and the test points adequately cover the parameter ranges, such as pressure, coolant mass velocity, and quality, that characterize the reactor operation. VIPRE-01 is used to reduce the experimental CHF data to obtain local thermal-hydraulic conditions. The CHF correlation is used with VIPRE-01 for the calculation of event-specific CHFR values and limits. In alignment with current practice, the CHF correlation is submitted in a separate topical report for NRC review (Reference 8.2.7).

3. **Modeling Assumptions:** This topical report is the separate documentation describing NuScale's intended use of VIPRE-01 and the justification for specific modeling assumptions, choice of particular two-phase models and correlations, heat transfer correlations, CHF correlation and limits, and input values of plant specific data. Table 7-1 provides information on what part of this topical report addresses the topics identified under this item.
4. **Courant Number:** The VIPRE-01 user must check that the transient time step, axial nodalization, and coolant velocity utilized ensure satisfaction of the Courant number requirement. Section 4.3 describes the methodology for addressing this requirement.
5. **Quality Assurance:** VIPRE-01 will be used for licensing calculations in accordance with NuScale quality assurance program description (Reference 8.2.41). In order to implement this methodology, the restrictions and conditions defined in the topical report must be met (see Section 7.2). Additionally, all subchannel calculations performed with VIPRE-01 must follow applicable software configuration and usage procedures that include requirements for error and warning documentation, error reporting, applicability of models and correlations for each application, and usage of code inputs and outputs.

The NuScale application of VIPRE-01 also fulfills the requirements specified in the generic VIPRE-01 MOD-02 SER (Reference 8.2.1). A summary of the NuScale fulfillment of each requirement is provided below:

1. **BWR Models:** Water tube channel modeling and leakage flow path connections are specific to BWR applications. Bypass flow (including guide tube flow) is modeled in a similar manner to conventional PWR applications and described in Section 3.8.4. An evaluation of drift-flux modeling is described in Section 5.10, in which a negligible effect on NuScale applications was observed.
2. **GEXL Correlation:** NuScale does not perform CPR calculations for BWR fuel with VIPRE-01.
3. **Code Limitations:** Section 2.2 of Reference 8.2.6 describes several two-phase flow conditions, local pressure phenomena, and a free-field not dominated by wall friction that are not applicable to NuScale applications. Section 6.3 and Figure 6-12 demonstrate that the NuScale design is similar to conventional PWRs, for which VIPRE-01 was designed, with respect to equilibrium qualities and flow regime.

   With regard to the applicable range of constitutive correlations, closure relationships used in CHF analyses are the same that were used in deriving the CHF correlation from the testing database as stated in Section 7.2.2. As NuScale utilizes the CHF testing database for the applicable range of the given closure relationships, not based on the ranges of the derived empirical closure models (subcooled boiling, bulk boiling, two-phase friction), this condition is satisfied.
4. **Input and Procedures:** The input and modeling options and corresponding justification presented in this report meet this requirement and are summarized in

Table 7-1. The quality assurance procedures required for usage with VIPRE-01 are described in SER Requirement #5.

Table 7-1. Summary of NuScale modeling assumptions

Topic for Justification	Value	Section in the Topical Report
CHF correlation and limit	NSP2, 1.17 (example)	3.3
turbulent mixing coefficient	{{ }}2(a),(b),(c),ECI (example)	3.9
turbulent momentum factor	{{ }}2(a),(c),ECI	3.9
crossflow resistance factor	0.5	5.8.1
axial friction losses	Blasius formulation	3.6, 5.3
choice of particular two-phase flow correlations	EPRI correlations	5.4
heat transfer correlations	EPRI, THSP, COND, G5.7	5.5
fuel rod modeling	calibration to fuel performance data	5.7
slip ratio	not used	n/a
grid loss coefficient (fuel-design specific)	fuel-dependent	6.1 (example)
axial friction loss coefficient (fuel-design specific)	fuel-dependent	6.1 (example)
run control parameters	default options or guidance specified	3.11

7.2 Criteria for Establishing Applicability of Methodology

The generalized methodologies presented in this topical report are based upon modeling assumptions. For completeness, the following set of criteria for establishing the applicability of these methodologies is provided. An applicant or licensee that uses the methodology of this topical report must satisfy these criteria in order to establish applicability. Any deviation from these criteria must be explicitly defined and justified.

7.2.1 General Criteria

The following criteria are required for a valid MCHFR calculation:

- The local mass flux, equilibrium quality, and pressure at the location and time of MCHFR is within the correlation applicability range.
- The MCHFR must occur in a channel geometry for which there is a valid CHF correlation (a unit or guide tube or instrument tube cell).
- The MCHFR must not occur on a peripheral subchannel of an assembly when using the fully-detailed one-eighth core model.

- The hot channel must occur adjacent to the hot rod.
- The hot rod from the VIPRE-01 MCHFR calculation must be the rod with the highest $F_{\Delta H}$ peaking factor.
- The VIPRE-01 calculation must satisfy all selected convergence criteria for the results to be considered valid. If convergence cannot be met with the selected default values or methods described in Section 3.10.1, justification must be provided to ensure that the relaxed acceptance criterion does not result in incorrect or premature results. If the calculation still does not converge, an assessment of the calculated results needs to be provided to prove acceptability.
- Axial nodalization within the region in which MCHFR is predicted to occur must be sufficiently small to resolve the flow field such that parametric sensitivity analysis results in a change of less than five CHF points for a halving of the nodalization size. Additionally, an aspect ratio (ratio of adjacent cell heights) of less than three must be maintained.
- Use of the RECIRC numerical solution.
- Use of heat transfer and two-phase flow correlation options defined in Table 5-7.
- Rate of depressurization must be below 20 psi/second.
- Fast transients require that simulations are performed in sufficiently small time steps to capture the CHFR behavior adequately.
- Water properties for temperature and specific volume are valid within the VIPRE-01 application range.
- Fuel pressure drop must be significantly less (by a factor of 10) than the minimum system pressure evaluated with the uniform pressure option or the local pressure drop option must be used.

7.2.2 Critical Heat Flux Correlation

The methodology presented in this report is independent of a specific CHF correlation. However, any application of the subchannel methodology is limited by the following restrictions:

- Application explicitly states that an approved CHF correlation is used.
- The CHF correlation is used within its applicable parameter ranges.
- Local conditions are simulated with VIPRE-01 to predict the test data.
- Use of the same two-phase flow model options used for local condition simulations.
- Applicable to the fuel design (including spacer grids) being analyzed.
- Fuel design-dependent (or bounding) turbulent mixing coefficient (ABETA) is defined and utilized in analysis.

7.2.3 Nuclear Analysis Discipline Interface

The Nuclear Analysis interfaces are:

- Core designs must exhibit one-eighth core or quarter-core symmetric pattern.
- Peak $F_{\Delta H}$ rod for any assembly must not occur on the peripheral row.
- Axial power shapes (general and SRP Section 15.4-specific)
- Core operating limit $F_{\Delta H}$ design limit is met accounting for radial tilt in nuclear analysis of any fission product (i.e., xenon) transients that disturb symmetric power peaking.
- Calculate value for PDIL-ARO augmentation for all power levels.

7.2.4 Transients Discipline Interface

The transient analysis requirements are:

- For events in which one or more parameters are outside the CHF correlation range applicability, such as low flow rate after reactor trip, the transients discipline calculation ensures all SAFDLs are satisfied.
- Either the transients discipline calculation, such as NRELAP5, or the subchannel analysis calculation must account for measurement uncertainties in core power, system flow, inlet temperature, and core exit pressure.
- The flow boundary condition must be system flow (as opposed to core flow) such that the subchannel methodology accounts for all components of bypass flow.

7.3 Cycle-Specific Confirmations

In general, the subchannel analysis presented is generic to a given core design (i.e., not cycle-specific) and does not need to be repeated each cycle. However, each unique core design must be checked to ensure the subchannel analysis is valid. As a result, the following cycle-specific confirmations with respect to subchannel analysis only (i.e., other confirmations may be required) must be performed for each cycle.

- Cycle-specific axial power shapes are bounded by that used in the generic bounding analysis.
- Hot rod in assembly shall not be on assembly periphery.
- Eight-core or quarter-core symmetric pattern.
- Hot full power $F_{\Delta H}$ at all exposures is less than COLR $F_{\Delta H}$.
- PDIL-ARO augmentation for all power levels maximum cycle-specific augmentation factor calculated is bounded by that used in the generic bounding analysis.

- Fission product (i.e., xenon) transients that disturb symmetric power peaking preserve radial tilt less than allowed by COLR.
- Fuel misload analysis confirms that the maximum cycle-specific augmentation factor calculated is bounded by that used in the generic bounding analysis.

7.4 Key Fuel Design Interface Requirements

The subchannel analysis methodology presented is generic to a given fuel design, and does not need to be reformulated for a different design. However, each unique fuel design requires significant inputs into the subchannel analysis. The following is a minimum list of required fuel design inputs that must be provided for each fuel design evaluated with this methodology:

- An approved CHF correlation valid for the fuel design.
- Basic geometry, flow loss coefficients, friction factors, etc.
- Guide tube bypass flow.
- Heat flux engineering uncertainty factor.
- Linear heat generation rate engineering uncertainty factor.
- Assembly and row bow uncertainty factors.
- Calibration of VIPRE-01 fuel rod conduction model to fuel performance code.
- Melting temperature equation to calculate fast transient FCM safety limit.

7.5 Unique Features of the NuScale Design

A summary of the unique features of the NuScale design that affect the analysis of core thermal hydraulics is identified and summarized.

- Natural circulation (including lower flow than conventional PWRs) results in a number of differences in the design and operation of a NuScale Power Module. As a result, CHF testing at lower flow rates is required and documented in Reference 8.2.7. Additionally, Section 5.0 provides justification for why VIPRE-01 and selected models are appropriate for lower flows.
- The stable startup system provides the initial flow for zero-power events. Therefore, all subchannel analysis includes this forced flow (approximately 10 percent rated flow) as applicable.
- A lower power density in the NuScale design results in unique heat transfer conditions. CHF testing at lower heat fluxes is required and documented in Reference 8.2.7. Additionally, Section 5.0 provides justification for why VIPRE-01 and selected models are appropriate for lower heat fluxes.

- A reactor core that is half the active fuel length, a fifth of the total assemblies, and a thicker reflector result in flatter radial and axial power distributions.
- The trend of MCHFR from the NuScale CHF test data indicates that CHF increases with decreasing pressure but can be case dependent. This is addressed by applying the appropriate directional bias for the specific NuScale application. A more in depth discussion is provided on this trend in Reference 8.2.7.
- The integral steam generator has the primary flow on the shell side and the secondary flow through the tubes. This increases thermal mixing and eliminates the possibility of an asymmetric inlet core temperature distribution.
- Unlike conventional PWRs, there is no reactor trip based on measured AO in the safety-related module protection system as described in Section 3.10.8. Rather an LCO on AO window prevents the reactor from being operated outside of analyzed conditions. The benefit of this is a simpler design to analyze, build, operate, and maintain.

A comparison of the NuScale design to a conventional PWR is provided in Table 7-2. The NuScale design is different in many respects as summarized above. However, the VIPRE-01 code is utilized in a similar manner and remains valid for NuScale applications as described and justified in this report.

Table 7-2. Comparison of NuScale reactor core design to conventional PWR

Parameter	Units	NuScale	Typical 4-Loop PWR (Ref. 8.2.39)
core thermal output	MW	160	3565
system pressure	psia	1850	2250
thermal design flow rate	Mlbm/hr	5	139.4
core average coolant mass velocity	Mlbm/hr-ft^2	0.5	2.41
core inlet coolant temperature	°F	500	556.8
core average rise in reactor core	°F	90	63.2
core average heat flux	MBtu/hr-ft^2	0.02	0.206
local peak heat flux	MBtu/hr-ft^2	0.03	0.515
minimum CHFR at nominal condition	ratio	2.3	2.47

8.0 References

8.1 Source Documents

8.1.1 American Society of Mechanical Engineers, *Quality Assurance Program Requirements for Nuclear Facility Applications*, NQA-1-2008, NQA-1a-2009 Addenda, New York, NY (endorsed by Regulatory Guide 1.28, Revision 4).

8.1.2 *U.S. Code of Federal Regulations*, "Quality Assurance Criteria for Nuclear Power Plants and Fuel Reprocessing Facilities," Appendix B, Part 50, Chapter 1, Title 10, "Energy," (10 CFR 50).

8.2 Referenced Documents

8.2.1 "Safety Evaluation by the Office of Nuclear Reactor Regulation Relating to VIPRE-01 Mod 02 for PWR and BWR Applications," EPRI-NP-2511-CCM-A, Revision 3, October 30, 1993.

8.2.2 Stewart, C.W., et al., NP-2551-CCM-A, Volume 1, Mathematical Modeling, Revision 4.5, "VIPRE-01 A Thermal-Hydraulic Code for Reactor Cores," Computer Code Manual, February 2014.

8.2.3 Stewart, C.W., et al., NP-2511-CCM-A, Volume 2, User's Manual, Revision 4.5, "VIPRE-01 A Thermal-Hydraulic Code for Reactor Cores," Computer Code Manual, February 2014.

8.2.4 Stewart, C.W., et al., NP-2511-CCM-A, Volume 3, Programmer's Manual, Revision 4.5, "VIPRE-01 A Thermal-Hydraulic Code for Reactor Cores," Computer Code Manual, February 2014.

8.2.5 Stewart, C.W., et al., NP-2511-CCM-A, Volume 4, Applications, Revision 4.5, "VIPRE-01 A Thermal-Hydraulic Code for Reactor Cores," Computer Code Manual, February 2014.

8.2.6 Stewart, C.W., and J.M. Cuta, NP-2511-CCM, Volume 5, Guidelines, "VIPRE-01: A Thermal-Hydraulic Code for Reactor Cores," Computer Code Manual, March 1988.

8.2.7 NuScale Power, LLC, "NuScale Power Critical Heat Flux Correlation NSP2," TR-0116-21012, Revision 0, October 2016.

8.2.8 NuScale Power, LLC, "Nuclear Analysis Codes and Methods Qualification," TR-0616-48793, Revision 0, August 2016 (ML16243A517).

8.2.9 NuScale Power, LLC, "Applicability of AREVA Fuel Methodology for the NuScale Design," TR-0116-20825, Revision 1, June 2016 (ML16187A017).

8.2.10 NuScale Power, LLC, “Non-LOCA Methodologies,” TR-0516-49416, Revision 0 (in development)

8.2.11 NuScale Power, LLC, “NuScale Rod Ejection Accident Methodology,” TR-0716-50350, Revision 0 (in development)

8.2.12 NuScale Power, LLC, “Accident Source Term Methodology,” TR-0915-17565, Revision 1, April 2016 (ML16099A394).

8.2.13 Dominion, “Reactor Core Thermal-Hydraulics Using the VIPRE-D Computer Code,” DOM-NAF-2, Rev. 0.0-A, August 2006 (ML062650184).

8.2.14 Westinghouse Electric Company, LLC, “VIPRE-01 Modeling and Qualification for Pressurized Water Reactor Non-LOCA Thermal-Hydraulic Safety Analysis,” WCAP-15306-NP-A, October 1999 (ML993160096).

8.2.15 Mitsubishi Heavy Industries, "Thermal Design Methodology,” MUAP-07009-NP-A, August 2013 (ML13284A069).

8.2.16 Duke Power Company, “Duke Power Company Oconee Nuclear Station Core Thermal-Hydraulics Using VIPRE-01,” DPC-NE-2003-P-A Rev.1, June 2000 (ML003752843).

8.2.17 AREVA NP Inc., “COBRA-FLX: A Thermal-Hydraulic Code,” ANP-10311NP, Revision 0, March 2010 (ML101550173).

8.2.18 U.S. Nuclear Regulatory Commission, “Safety Evaluation by the Office of Nuclear Reactor Regulation Related to Review of Topical Report COBRA-FLX: A Core Thermal-Hydraulic-Analysis Code,” ANP-10111P, Revision 0, TAC No. ME 3909, Attachment A (ML12193A680).

8.2.19 AREVA NP Inc., “Response to Request for Additional Information for the Review of A Core Thermal-Hydraulic Analysis Code,” ANP-10311Q1NP, Revision 0, January 2011 (ML13135A054).

8.2.20 Lahey, Jr., R. T., and F.J. Moody, “The Thermal Hydraulics of a Boiling Water Nuclear Reactor,” 2nd edition. ANS Monograph, New York, pp. 168–184, 1993.

8.2.21 Hwang, D. H., et al., “Assessment of the Interchannel Mixing Model with a Subchannel Analysis Code for BWR and PWR Conditions,” Nuclear Engineering and Design, 199, 257–272, 2000.

8.2.22 Beus, S.G., “A Two-Phase Turbulent Mixing Model for Flow in Rod Bundles,” Westinghouse Report, Bettis Atomic Power Laboratory, WAPD-T-2438, 1971.

8.2.23 Yoo, Y.J., et al., “Effect of Turbulent Mixing and Void Drift Models on Predictions of COBRA-IV-I,” KAERI, 1996.

8.2.24 Lahey, Jr., R. T., B.S. Shiralkar, and D.W. Radcliffe, “Two-Phase Flow and Heat Transfer in Multirod Geometries: Subchannel and Pressure Drop Measurements in a Nine- Rod Bundle for Diabatic and Adiabatic Conditions,” GEAP-13049, General Electric Company, San Jose, CA, March 1970.

8.2.25 Christensen, H., “Power-to-Void Transfer Functions,” ANL-6385, Argonne National Laboratory, Argonne, Il, 1961.

8.2.26 Martin, R., “Measurement of the Local Void Fraction at High Pressure in a Heating Channel,” Nuclear Science and Engineering, Vol. 48, pp. 125-138, 1972.

8.2.27 Nylund, O., et al., “FRIGG Loop Project: Hydrodynamic and Heat Transfer Measurements on a Full-Scale Simulated 36-Rod Marviken Fuel Element with Uniform Heat Flux Distribution,” FRIGG-2, R4 447/RTL-1007, ASEA and AB Atomenergi, Stockholm, Sweden, 1968.

8.2.28 Nylund, O., et al., “FRIGG Loop Project; Hydrodynamic and Heat Transfer Measurements on a Full Scale Simulated 36-rod Marviken Fuel Element with Nonuniform Heat Flux Distribution,” FRIGG-3, ASEA and AB Atomenergi, Stockholm, Sweden, 1968.

8.2.29 Nylund, O., et al., “FRIGG Loop Project: Hydrodynamic and Heat Transfer Measurements on a Full-Scale Simulated 36-Rod Marviken Fuel Element with Nonuniform Heat Flux Distribution,” FRIGG-4, ASEA and AB Atomenergi, Stockholm, Sweden, 1968.

8.2.30 Ferrell, J.K., and J. W. McGee, “Two-Phase Flow Through Abrupt Expansions and Contractions,” TID-23394 (Vol. 3), June 1966.

8.2.31 Marinelli, V., L. Pastori, and B. Kjellen, “Experimental Investigation on Mass Velocity Distribution and Velocity Profiles on LWR Rod Bundle,” European Two-Phase Flow Group Meeting, Rome, Italy, June 6-8, 1972.

8.2.32 Marshall, R.C., and R.P. Letendre, “Influence of Inlet Geometry on Flow in the Entrance Region of a Nuclear Reactor Rod Bundle,” American Society of Mechanical Engineers, New York, NY, August 1968.

8.2.33 Lahey, Jr., R.T., B.S. Shiralkar, and D.W. Radcliffe, “Two-Phase Flow and Heat Transfer in Multirod Geometries: Subchannel and Pressure Drop Measurements in a Nine-Rod Bundle for Diabatic and Adiabatic Conditions,” GEAP-13049, General Electric Company, San Jose, CA, March 1970.

8.2.34 Lahey, Jr., R.T., B.S. Shiralkar, D.W. Radcliffe, and E.E. Polomik, “Out-of-Pile Subchannel Measurements in a Nine-Rod Bundle for Water at 1000 psia,” Progress in Heat and Mass Transfer, Vol. 6, pp. 345-363, Pergamon, London, 1972.

8.2.35 Neykov, Aydogan, Hochreiter, Ivanov, Utsuno, Kasahara, Sartori, Martin, “NUPEC BWR Full-size Fine-mesh Bundle Test (BFBT) Benchmark,” ISBN 92064-01088-2, Nuclear Science, 2005.

8.2.36 Herkenrath. H., W. Hufschmidt, U. Jung, and F. Weckermann, “Experimental Investigation of the Enthalpy and Mass Flow Distribution in 16-Rod Clusters with BWR-PWR Geometries and Conditions,” Final Report EUR 7575 EN, Joint Research Center, Ispra, Italy, 1981.

8.2.37 Yun, B.J., G.C. Park, J. Enrique Julia, and T. Hibiki, “Flow Structure of Subcooled Boiling Water Flow in a Subchannel of 3x3 Rod Bundles,” Journal of Nuclear Science and Technology, Vol. 45, No. 5, pp. 402-422, 2008.

8.2.38 Gustafsson, B., R. Harju, and O. Imset, “Flow and Enthalpy Distribution in a 9-Rod Bundle,” European Two-Phase Flow Group Meeting, Harwell, England, June 3-7, 1974.

8.2.39 Vogtle Electric Generating Plant, “Updated Final Safety Analysis Report Revision 12,” November 5, 2004.

8.2.40 AREVA, Inc. “COPERNIC Fuel Rod Design Computer Code,” BAW-10231P-A, Revision 1, January 2004.

8.2.41 NuScale Power LLC, “NuScale Topical Report: Quality Assurance Program Description for the NuScale Power Plant,” NP-TR-1010-859-NP, Revision 3, April 2016.

8.2.42 “Safety Evaluation Report on EPRI NP-2511-CCM VIPRE-01,” May 1986.

Enclosure 3:

Affidavit of Thomas A. Bergman, AF-0217-53030

NuScale Power, LLC
1100 NE Circle Blvd., Suite 200 Corvallis, Oregon 97330 Office 541.360-0500 Fax 541.207.3928
www.nuscalepower.com

NuScale Power, LLC

AFFIDAVIT of Thomas A. Bergman

I, Thomas A. Bergman , state as follows:

(1) I am the Vice President of Regulatory Affairs of NuScale Power, LLC (NuScale), and as such, I have been specifically delegated the function of reviewing the information described in this Affidavit that NuScale seeks to have withheld from public disclosure, and am authorized to apply for its withholding on behalf of NuScale

(2) I am knowledgeable of the criteria and procedures used by NuScale in designating information as a trade secret, privileged, or as confidential commercial or financial information. This request to withhold information from public disclosure is driven by one or more of the following:

(a) The information requested to be withheld reveals distinguishing aspects of a process (or component, structure, tool, method, etc.) whose use by NuScale competitors, without a license from NuScale, would constitute a competitive economic disadvantage to NuScale.

(b) The information requested to be withheld consists of supporting data, including test data, relative to a process (or component, structure, tool, method, etc.), and the application of the data secures a competitive economic advantage, as described more fully in paragraph 3 of this Affidavit.

(c) Use by a competitor of the information requested to be withheld would reduce the competitor's expenditure of resources, or improve its competitive position, in the design, manufacture, shipment, installation, assurance of quality, or licensing of a similar product.

(d) The information requested to be withheld reveals cost or price information, production capabilities, budget levels, or commercial strategies of NuScale.

(e) The information requested to be withheld consists of patentable ideas.

(3) Public disclosure of the information sought to be withheld is likely to cause substantial harm to NuScale's competitive position and foreclose or reduce the availability of profit-making opportunities. The accompanying topical report reveals distinguishing aspects about the analytical method by which NuScale performs its subchannel analysis.

NuScale has performed significant research and evaluation to develop a basis for this methodology and has invested significant resources, including the expenditure of a considerable sum of money.

The precise financial value of the information is difficult to quantify, but it is a key element of the design basis for a NuScale plant and, therefore, has substantial value to NuScale.

If the information were disclosed to the public, NuScale's competitors would have access to the information without purchasing the right to use it or having been required to undertake a similar expenditure of resources. Such disclosure would constitute a misappropriation of NuScale's intellectual property, and would deprive NuScale of the opportunity to exercise its competitive advantage to seek an adequate return on its investment.

(4) The information sought to be withheld is in the enclosed licensing topical report entitled Subchannel Analysis Methodology.The enclosure contains the designation "Proprietary" at the top of each page containing proprietary information. The information considered by NuScale to be proprietary is identified within double braces, "{{ }}" in the document.

(5) The basis for proposing that the information be withheld is that NuScale treats the information as a trade secret, privileged, or as confidential commercial or financial information. NuScale relies

upon the exemption from disclosure set forth in the Freedom of Information Act ("FOIA"), 5 USC § 552(b)(4), as well as exemptions applicable to the NRC under 10 CFR §§ 2.390(a)(4) and 9.17(a)(4).

(6) Pursuant to the provisions set forth in 10 CFR § 2.390(b)(4), the following is provided for consideration by the Commission in determining whether the information sought to be withheld from public disclosure should be withheld:

(a) The information sought to be withheld is owned and has been held in confidence by NuScale.

(b) The information is of a sort customarily held in confidence by NuScale and, to the best of my knowledge and belief, consistently has been held in confidence by NuScale. The procedure for approval of external release of such information typically requires review by the staff manager, project manager, chief technology officer or other equivalent authority, or the manager of the cognizant marketing function (or his delegate), for technical content, competitive effect, and determination of the accuracy of the proprietary designation. Disclosures outside NuScale are limited to regulatory bodies, customers and potential customers and their agents, suppliers, licensees, and others with a legitimate need for the information, and then only in accordance with appropriate regulatory provisions or contractual agreements to maintain confidentiality.

(c) The information is being transmitted to and received by the NRC in confidence.

(d) No public disclosure of the information has been made, and it is not available in public sources. All disclosures to third parties, including any required transmittals to NRC, have been made, or must be made, pursuant to regulatory provisions or contractual agreements that provide for maintenance of the information in confidence.

(e) Public disclosure of the information is likely to cause substantial harm to the competitive position of NuScale, taking into account the value of the information to NuScale, the amount of effort and money expended by NuScale in developing the information, and the difficulty others would have in acquiring or duplicating the information. The information sought to be withheld is part of NuScale's technology that provides NuScale with a competitive advantage over other firms in the industry. NuScale has invested significant human and financial capital in developing this technology and NuScale believes it would difficult for others to duplicate the technology without access to the information sought to be withheld.

I declare under penalty of perjury that the foregoing is true and correct. Executed on February 15, 2017.

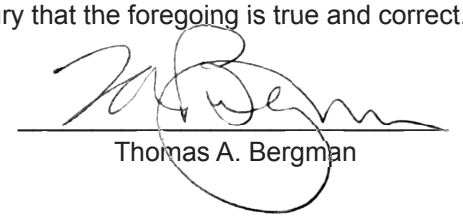

Thomas A. Bergman